2020

Diurnal dysfunction in control of sodium excretion in diet-induced obesity

Reham Soliman
University of Alabama at Birmingham

DIURNAL DYSFUNCTION IN CONTROL OF SODIUM EXCRETION IN DIET-INDUCED OBESITY

by

REHAM HAMDY SOLIMAN

DAVID M. POLLOCK, MENTOR
SHANNON M. BAILEY
ORLANDO M. GUTIERREZ
COURTNEY M. PETERSON
JENNIFER S. POLLOCK

A DISSERTATION

Submitted to the graduate faculty of The University of Alabama at Birmingham,
in partial fulfillment of the requirements for the degree of
Doctor of Philosophy

BIRMINGHAM, ALABAMA

2020

DIURNAL DYSFUNCTION IN CONTROL OF SODIUM EXCRETION IN DIET-INDUCED OBESITY

REHAM HAMDY SOLIMAN

PATHOBIOLOGY, PHARMACOLOGY & PHYSIOLOGY THEME

ABSTRACT

The renal endothelin system plays a key role in sodium excretion, particularly under high salt (HS) diet. HS stimulates renal endothelin-1 (ET-1), which binds and activates the endothelin receptor B (ET_B) to excrete the excess salt. Loss of ET_B receptor is linked to the development of hypertension under HS. Central clock genes are important in maintaining rhythmic patterns of sodium excretion and ET-1 is identified as a target for clock genes, including *Period* and *Bmal1*. ET-1 excretion follows a diurnal rhythm along with sodium excretion. Sexual dimorphism is evident in the diurnal regulation of endothelin-mediated natriuresis and its downstream targets.

Obesity enhances sodium reabsorption leading to the development of hypertension. However, the role of renal ET-1 diurnal rhythms in obesity is poorly understood. Recent studies showed that Dahl salt-sensitive (Dahl SS) rats on HF diet have impaired ET_B-mediated natriuresis. However, whether this impairment occurs in obesity in general is not known.

The overarching hypothesis of this dissertation is that diet-induced obesity impairs diurnal renal salt handling ability that is associated with renal ET-1 dysfunction in a sex-specific manner. After 8 weeks of high fat (HF) diet, male rats had significantly reduced natriuresis in response to an acute NaCl injection when given at the beginning of their active period. This was mirrored by lower ET-1 excretion and lower ET-1 mRNA expression in the kidneys of HF-treated rats. HF-treated males had higher blood pressure

and developed salt sensitivity on HS diet. Females fed a HF diet showed intact acute natriuretic response and ET-1 excretion rates similar to normal fat (NF) controls. While female rats developed hypertension on HF diet, they were not salt sensitive, which points out a clear sex difference in response to diet-induced obesity and suggests that obesity-associated hypertension is ET-1 independent in female rats. In addition, females fed regular chow had a lower natriuretic response to blockade of ET-1 downstream target channel, ENaC, by benzamil compared to males at different times of day.

In conclusion, our study demonstrates that HF diet modulates renal ET-1 system and highlights this impairment as a potential mechanism in the development of obesity-induced hypertension.

Keywords: kidney, endothelin-1, high fat, sodium excretion, diurnal, male and female

DEDICATION

To my parents Nahed & Hamdy. To my husband Ayman Farag.
To Lian, Basel, Adham & Asser.

ACKNOWLEDGEMENTS

First of all, I would like to deeply acknowledge my mentor, Dr. David Pollock for his guidance and support through this journey. From the first day I joined his lab, I was given the opportunity to work with a stellar group of scientists under his lead. He always encouraged me to think independently and advised me on my quest to achieve my potential in becoming the physician scientist I have always dreamt to be. He taught by example that great scientists are dedicated, persistent, supportive of others and have calm demeanor. Secondly, I would like to acknowledge my fellow graduate students and close friends, Crystal and Dingguo for helping me navigate the graduate school life. I would also like to extend my acknowledgement to the postdoctoral fellows and supporting staff in my lab. I would like to thank Chunhua Jin in particular for her help through her amazing surgical skills that made my project possible. I would also like to thank all members of my thesis committee for their mentoring, invaluable input and commitment through their busy schedules.

I would like to thank my parents, to whom I am indebted for life, for believing in me more than I believed in myself and for their unlimited love and support throughout this journey that took me thousands of miles away from home. They have been the best cheering squad alongside with my siblings, Rehab, Mennah and Ahmed. Most importantly, I would like to thank my husband and best friend, Ayman Farag, for being the most amazing partner, for his unconditional love and encouragement and for lifting me up whenever I was in doubt. I am eternally grateful to him for supporting me realize my capabilities, and it's only because of him I was able to finish graduate school in three years.

TABLE OF CONTENTS

Page

LIST OF TABLES

LIST OF FIGURES

Figure ***Page***

LIST OF ABBREVIATIONS

ACE	Angiotensin-converting enzyme
AGT	Angiotensinogen
Ang II	Angiotensin II
AT1	Angiotensin receptor type 1
AT2	Angiotensin receptor type 2
Bmal1	Brain and muscle ARNT-like protein 1
BMI	Body mass index
BP	Blood pressure
CCD	Cortical collecting duct
CD	Collecting duct
CK1δ/ε	Casein kinase isoforms 1δ and 1ε
CKD	Chronic Kidney Disease
CLOCK	Circadian locomotor output cycles kaput
CRY	Cryptochrome
DBP	Diastolic blood pressure
DCT	Distal convoluted tubule
Dahl SS	Dahl salt sensitive
ENaC	Epithelial sodium channel
ERRβ	Estrogen-related receptor β
ET	Endothelin

ET-1	Endothelin-1
ET_A	Endothelin receptor type A
ET_B	Endothelin receptor type B
ET_B-def	ET_B deficient
GFR	Glomerular filtration rate
GILZ	Glucocorticoid-induced leucine zipper
GPER	G protein-coupled estrogen receptor
HETE	Hydroxyeicosatetraenoic acid
HF	High fat
Hif-1α	Hypoxia-inducible factor 1-alpha
HRE	Hormone response element
HS	High salt
IM	Inner medulla
IMCD	Inner medullary collecting duct
KO	Knockout
MAP	Mean arterial pressure
MBF	Medullary blood flow
mIMCD-3	Mouse inner medullary collecting duct cells-3
MpkCCD	mouse kidney cortical collecting duct cells
NaCl	Sodium chloride
NCC	Sodium-chloride co-transporter
NF	Normal fat
NF-κB	Nuclear factor kappa B

NHE3	Sodium-hydrogen exchanger 3
NKCC2	Sodium-potassium-2chloride co-transporter 2
NO	Nitric oxide
NOS	Nitric oxide synthase
NS	Normal salt
OM	Outer medulla
OMCD	Outer medullary collecting duct
OVx	Ovariectomy
PER	Period
RAAS	Renin-angiotensin-aldosterone system
Ren-2	Renin gene
REV-ERBα	Reverse erythroblastosis alpha
SCN	Suprachiasmatic nucleus
SGK1	Glucocorticoid-induced kinase 1
SGLT	Sodium-glucose co-transporter
TAL	Thick ascending limb
TGF-β	Transforming growth factor β
TTFL	Transcriptional-translational feedback loop
UKV	Urinary potassium excretion
UNaV	Urinary sodium excretion
UV	Urine flow rate
Vezf1	Vascular endothelial zinc finger 1
ZT	Zeitgeber time

CHAPTER 1

STATEMENT OF THE PROBLEM

Obesity is a major metabolic health disorder that adversely influences most organ systems, significantly increasing risk for cardiovascular and chronic kidney disease (15, 72, 113). Population-based studies show an increase in the number of obese (BMI > 30) women from 69 million in 1975 to 390 million in 2016 and from 31 million to 281 million obese men (24), of those more than 60% live in high-income countries (66). Age-adjusted prevalence of obesity was 42% in the United States with no sex-difference (63). Obesity is associated with enhanced renal sodium reabsorption due, in part, to activation of the renin-angiotensin-aldosterone system (RAAS) and sympathetic overactivity, with the subsequent development of hypertension. However, our understanding is incomplete especially with important natriuretic factors necessary for eliminating a high salt (HS) diet such as endothelin-1 (ET-1).

ET-1 is 23-amino acid polypeptide that is expressed in vascular endothelial as well as renal tubular cells and functions in an autocrine and paracrine manner through binding to two G-protein coupled receptors, ET receptor A (ET_A) and ET receptor B (ET_B). While considered the most potent vasoconstricting factor through its binding to the ET_A receptor, ET-1/ET_B binding promotes sodium excretion through nitric oxide (NO)-mediated epithelial sodium channel (ENaC) inhibition (18, 28).

Under conditions of HS diet, renal ET-1 responds to increased tubular sodium and through binding to the ET_B receptor, it promotes sodium excretion (104) such that ET_B-mediated natriuresis is critical for blood pressure control (51). Loss of ET_B function leads to the development of hypertension under HS conditions (12, 51). Mice lacking ET-1 in their collecting ducts develop salt sensitive hypertension (3), reflecting the critical role of the renal endothelin system in body fluid and blood pressure regulation. Our lab has shown that ET_B-mediated natriuresis varies over the course of the day, with impaired acute natriuretic response in ET_B-deficient rats (88) in addition to a phase shift in *Bmal1* gene expression under HS diet (181). Global knockout of the core clock gene, *Bmal1* in rats results in loss of diurnal control of sodium excretion (87). It is important to note that ET_B-dependent natriuresis is different in females compared to male rats. Loss of ET_B receptors had no significant effect on the acute natriuretic response at different times of day in females. ET_A contributed to the natriuretic response in ET_B-deficient females and studies have shown higher protein abundance of the ET-1 downstream target sodium channel, ENaC, in female *vs* male rats. This evidence reflects the critical role of the renal endothelin system on the kidney clock and the diurnal regulation of sodium excretion and highlights sex differences in renal sodium handling and ET-dependent natriuresis.

A recent study showed reduced ET_B-dependent natriuresis in Dahl SS rats under high fat diet (97). However, the effect of diet on ET-1/ET_B system and their contribution to the diurnal regulation of sodium excretion and the development of hypertension and salt sensitivity under obese conditions is not understood.

Circadian rhythms are endogenously generated 24-hour cycles that are found in all living organisms including plants, bacteria and mammals. Physiological functions in the

body are timed to match metabolic requirements at different times of day. This is achieved through coordination between central and peripheral clocks. The central clock is located in the suprachiasmatic nucleus (SCN) in the hypothalamus, responds to time cues, such as light-dark and rest-activity and orchestrates rhythmicity of function throughout the body (85). The peripheral clock conducts its function through a complexity of interacting loops of transcription factors that oscillate at different times of day. CLOCK/BMAL1 represent the positive transcription arm of the loop, while Period/Cryptochrome heterodimer is the repressor arm, that feeds back to suppress CLOCK/BMAL1 transcription (159).

Studies have shown that obesity impairs circadian rhythms of clock genes and oscillating metabolites (39, 106). Studies in obese mice showed disruption of the circadian pattern of expression of *Clock*, *Bmal1 and Per2* in the liver and adipose tissues (106). Mice deficient in *Bmal1* have impaired lipid metabolism and have accelerated obesity-induced organ dysfunctions (23, 47). While studies have shown that obesity leads to attenuation of temporal rhythms of expression of core clock genes, no evidence exists on the effect of obesity on the diurnal patterns of expression and function of the endothelin system in the kidney.

Overall, absence and/or dysfunction of the ET_B receptor results in salt-sensitive hypertension. Loss of ET_B receptor leads to disruption of time-of-day sodium excretion. Sexual dimorphism is evident in diurnal ET-dependent natriuresis and in ENaC expression. Obesity-induced ET-1/ET_B dysfunction and its subsequent effects on temporal and sex-dependent patterns of sodium excretion is yet to be explored. Therefore, the goal of my studies is to determine if diet-induced obesity causes impairment of renal sodium handling

in a time-of-day dependent manner through diurnal renal endothelin system dysfunction, and whether it is sex-dependent through the following objectives:

Aim 1: To test the hypothesis that diet-induced obesity impairs diurnal rhythms of sodium excretion, that is associated with diurnal dysfunction in ET-1.

Aim 2: To test the hypothesis that diet-induced obesity impairs ET-1 and ET_B receptor expression and activity, leading to diminished renal capacity to maintain diurnal rhythms in natriuresis.

Aim 3: To test the hypothesis that diet-induced obesity leads to the development of salt sensitivity that is associated with endothelin-1 dysfunction in the kidney.

Aim 4: To test the hypothesis that sex differences in renal sodium handling will lead to a dimorphic pattern in the diurnal response to pharmacological intervention with benzamil.

CHAPTER 2

INTRODUCTION

Under physiological steady-state conditions, renal excretion of sodium and water is equal to intake. This leads to stable blood pressure levels in response to fluctuations in sodium and water intakes. The increased extracellular fluid volume secondary to increased salt intake leads to a temporary increase in arterial blood pressure. This increase is sensed mainly by the kidney, that responds through the renin-angiotensin system (RAS), the sympathetic nervous system and endothelin-1 (ET-1) leading to suppression of sodium reabsorption along the nephron and normalization of arterial blood pressure.

Obesity dysregulates a wide array of physiological responses that includes but not limited to kidney-specific blood pressure regulatory mechanisms leading to sodium retention, and consequently chronic elevation of arterial blood pressure. This introduction will provide information on the role of the kidney in regulating sodium handling at different times of day, with a focus on the renal endothelin-1 (ET-1) system as the center of my studies. This section will include evidence supporting circadian regulation of ET-1 function and sodium excretion. A brief review of circadian dysfunctions in obesity will link renal pathophysiological processes to the development of essential hypertension. Finally, this introduction will discuss sex differences in renal sodium handling and the sexual dimorphism in response to hypertension therapy.

Essential hypertension is defined as elevated blood pressure that cannot be attributed to secondary causes and is currently defined by systolic blood pressure >130

mmHg and diastolic > 80 mmHg (200). There is plenty of evidence supporting the role of diet-induced obesity in the pathogenesis of hypertension, with a plethora of studies investigating mechanistic links between obesity and the renin-angiotensin-aldosterone system (RAAS), the sympathetic nervous system (SNS) and vascular dysfunction. The renal ET-1 system is a potent natriuretic pathway that is highly expressed along the renal tubules, particularly in the renal medulla and leads to excretion of high salt diet, contributing to long term blood pressure regulation. However, characterization of the renal tubular ET-1 expression and function under obesity represents a gap in knowledge that I seek to investigate in this study. In addition to assessing its potential contribution in the development of obesity-induced hypertension.

Endothelin-1 in Health and Disease

Endothelin-1 was first identified as an "endothelium-derived" peptide with potent vasoconstriction properties, in fact it is the most potent with long lasting contractile effects (27, 206). ET-1 was isolated and cloned from cultured porcine aortic endothelial cells in 1988 (206), with the characterization of ET-1 considered a revolutionary step in cardiovascular physiology. ET-1 is expressed in all vascular endothelial cells and promotes vasoconstriction in response to a wide variety of stimuli, including hypoxia, thrombin, pressure and mechanical stretch (206). Studies then followed to reveal that ET-1 is not exclusive to endothelial cells, but is expressed and secreted from epithelial cells such as renal tubular cells and contributes to sodium homeostasis and blood pressure regulation

(27). Vascular smooth muscle cells (32), macrophages (169), fibroblasts (168) and some neuronal cells also produce ET-1 (27).

Endothelin Structure and Isoforms

The *EDN1* gene is located on the short arm of chromosome 6 (8) and its transcript encodes a preproprotein that through post-translational modifications and proteolytic cleavages yields the active 21 amino acid peptide, ET-1. The mRNA transcript encodes a 212-amino acid Preporo-ET-1, that is converted to the pro-ET-1 and then through the proteolytic action of furins yields the big ET-1. Big ET-1 is converted to the most active form, ET-1 at the cell surface, upon release from the secretory granules mainly through the action of the endothelin converting enzyme 1 (ECE-1) (94, 112). Though ECE-1 is the rate-limiting enzyme for post-translational modifications of ET-1, studies have shown that *edn1* gene transcription is the most essential regulatory mechanism of ET-1-mediated responses (112, 185). This is supported by the fact that the *EDN1* gene promoter has response elements to a wide variety of transcription factors, as will be discussed later. ET-1 is the most abundant isoform of the endothelin family, to which, ET-2, ET-3 belong. The *EDN* gene is highly conserved among mammals with high structural and functional homology to the sarafatoxin family of toxins that was first extracted from the venom of a snake Atractaspis engaddensis (67). Sarafatoxin is now the most widely used pharmacological isoform to ET-1 in basic research. ET-2 and ET-3 isoforms closely resemble ET-1 transcriptional and translational multi-step process, however, they are differentially expressed in tissues with variable receptor sensitivity. The human *EDN2* gene is located on the short arm of chromosome 1, while *EDN3* is on the long arm of chromosome 20 (8,

42). While ET-1 is expressed in almost all tissues of the body, ET-2 is expressed mainly in the heart, kidney, intestine, ovaries and placental tissues (27, 42). ET-3 was first detected in the rat brain and human pituitary glands where it showed higher levels than ET-1 in this area of the brain (27). Circulating ET-3 was detected in the plasma, with no clear evidence of endothelial production. ET-3 was detected in other tissues including the heart and endometrium. These three isoforms have similar affinity to the ET_B receptor, and ET-3 at physiological levels doesn't bind the ET_A receptor, to which ET-2 and ET-1 bind with equal affinities (27, 42).

Transcriptional Regulation and Post-Transcriptional Modifications of the EDN1 Gene

EDN1 hosts binding motifs for many transcription factors. These binding motifs are differentially expressed in tissues, some transcription factors are required for maintenance of ET-1 basal functions, while others are responsive to metabolic/environmental stressors including hypoxia (*HIF-1*), hyperinsulinemia (*Vezf1*), inflammation (SMAD, NFκB and AP-1) and high salt (HRE1/2). With renal ET-1 and blood pressure regulation being the scope of this literature review, we will discuss functionally-relevant promoter elements.

- *The vascular endothelial zinc finger 1 (Vezf1). Vef1* is exclusively expressed in the vascular endothelium as well as hematopoietic cells. It positively regulates *EDN1* gene expression at basal conditions (185).
- *Hormone response elements (HRE).* Aldosterone stimulates *EDN1* gene transcription through binding of aldosterone-mineralocorticoid receptor (MR) complex to an HRE embedded in *EDN1* promotor region as shown by Stow et al

(184). Isolated rat collecting duct cells showed upregulation of ET-1 transcription in response to increasing doses of aldosterone and pharmacological inhibition of aldosterone action prevented this response. While aldosterone and ET-1 have opposing actions on epithelial sodium channel (ENaC), Stow et al proposed a feedback loop between ET-1 and aldosterone that contribute to sodium balance under physiological conditions (184). However, the status of aldosterone-induced ET-1 secretion in response to HS, obesity or in hypertension is not clear.

- *E-box*. The promoter region of ET-1 gene expresses an E-box element. This motif has gained special importance because of its role in the circadian regulation of ET-1 expression. *Per1* binds to the E-box element of *EDN1* gene and suppresses the expression of ET-1 (160), which contributes to the temporal pattern of ET-1 expression and function (157, 186).

EDN1 gene transcription is also a target of epigenetic modification. CpG islands have been identified in intron1 and evidence suggests that tissue-specific silencing of the *ET-1* gene occur in response to CpG methylation (194), in addition to an emerging role of histone modifications in *EDN1* epigenetic regulation (185, 202).

Endothelin-1 Receptors

ET-1 functions in an autocrine and paracrine manner. For example, ET-1 synthesized by the vascular endothelium is secreted to act on the secreting and neighboring endothelial cells. ET-1 circulates in the plasma to target distant endothelial cells, vascular smooth muscle cells and circulating monocytes (27). Its function is mediated through two transmembrane G-protein-coupled receptors on cell membranes of target cells, named ET_A

and ET_B receptors. The physiological responses of ET-1 depend on the receptor it interacts with and type of tissue, initiating variable and sometimes opposing downstream signaling cascades. ET-1/ET_A interaction mediates vasoconstriction, inflammation and fibrosis (28), while the ET-1/ET_B complex promotes natriuresis in the kidney as well as promoting vasodilation (107). Overall, ET_B activation is considered beneficial, as in the renal tubules, but this is not always the case, as ET_B receptor activation of bronchial smooth muscles in the lung leads to bronchoconstriction and is implicated in the pathogenesis of airway disease (42). The functions of ET_A and ET_B receptors will be discussed later in details as related to different organ systems, with a focus on their role in the vasculature, kidney and circadian physiology and pathophysiology.

Physiology of Vascular Endothelin System

As previously mentioned, ET-1 was pioneered as a vasoactive agent, leading to studies of its vascular properties and its role in controlling vascular tone and blood pressure the heavily studied aspect of the endothelin system for more than a decade. The greatest abundance of ET_A receptor is expressed on vascular smooth muscle cells (27). ET-1 released from endothelial cells as well as from smooth muscle cells functions in a paracrine and autocrine manner respectively to activate the ET_A receptor and through multiple types of G-proteins, that initiate downstream signaling cascades resulting in Ca^{2+} release and cellular cytoskeletal contraction (57). This will lead to increased vascular tone, peripheral resistance and eventually increased blood pressure. Stimulation of ET_B receptors on the smooth muscles of some vascular beds will lead to similar effects, while activation of endothelial ET_B receptors promotes vasodilation through nitric oxide (NO)-dependent

pathway, abrogating the ET_A-induced constrictive response (199). It is important to note that under steady states conditions, a balance is maintained between the two arms of the ET system, to maintain blood pressure and vascular tone within physiological limits. Pathology manifests only when this balance is lost. For example, increased intravascular fluid volume secondary to chronic HS intake, will promote ET_A-induced increase in vascular tone and peripheral resistance leading to elevation blood pressure (103). Persistent smooth muscle contractility under HS conditions will eventually lead to arterial stiffness and hypertension. Hyperlipidemia accompanying HF diet promotes the development of atheromatous plaques with its underlying inflammation. Release of ET-1 from macrophages and lymphocytes within the atherosclerotic plaque, promotes vascular modulation (43). Immune-mediated release of ET-1 will not only lead to vasoconstriction, but will further stimulate the release of inflammatory cytokines and fibroblast proliferation inducing vascular damage (41). Studies providing evidence of bi-directional stimulatory loop between ET-1 and transforming growth factor-β (TGF-β) (168), and T-cell-induced stimulation of ET-1 production (169) highlighted the deleterious effects of upregulated ET-1 on the vascular system and the development of cardiovascular disease.

Physiology of the Renal Endothelin System

The functions of renal ET-1 extends beyond sodium transport regulation, to the regulation of renal blood flow, GFR, acid-base balance and renin release (104). Vascular endothelial and smooth muscle cells within the kidney express ET-1 that function in a similar way to the systemic vasculature. Karet and Davenport showed localization of mature ET-1 by immunostaining within the interlobular and arcuate arteries and veins (89).

They also showed evidence of ET-1 expression on renal arterioles, with lack of capillary staining. They however disregarded evidence suggesting tubular expression of ET-1 (89). Stimulation of the ET_A receptor on the endothelium leads to reduction of renal blood flow, with subsequent stimulation of the renin-angiotensin system.

The first report suggesting intrarenal production of ET-1 dates back to 1989 (95). Kitamura et al. assayed pigs kidneys to determine the regional distribution of the peptide and found that the renal inner medulla had the highest ET-1 concentration and was lowest in the cortex (95). Similar results were observed in rats (1, 96) and later in human kidneys (136). However, the source of ET-1 and whether renal tubular cells produce ET-1 was still unclear. Over the past few decades studies provided strong evidence of local renal ET-1 production by almost every cell type in the kidney (28, 103, 179). It is now evident that glomerular epithelial cells, tubular and interstitial cells variably synthesize and secrete ET-1 and express the two receptor subtypes (28). Glomerular endothelial cells are the main source of ET-1 in the glomerulus and its role has been mainly implicated in glomerular injury and renal disease (28). The glomerular endothelium exclusively expresses ET_B, and through its binding to ET-1 promotes NO production (11). However, glomerular endothelial ET-1 can modulate basement membrane structure and has been attributed to the development of focal segmental glomerulosclerosis (147). Podocytes express ET_A receptors and ET-1 was found to promote podocyte injury, apoptosis and shedding in different models of glomerular injury (11, 38, 116).

ET_B receptors show higher levels of expression in the renal medulla, mainly on inner medullary collecting ducts, as well as cortical collecting duct cells, while ET_A receptors predominate the vascular endothelial and interstitial cells of the kidney (103).

The endothelin system is a key modulator of sodium reabsorption along the nephron (Figure 1) and dysfunction of the ET-1/ET_B function leads to sodium retention and the development of hypertension (51, 105). Tubular ET-1 through its binding to ET_B receptor and the subsequent release of NO, inhibit the epithelial sodium channel (ENaC) open probability in the cortical collecting duct (CCD) with subsequent natriuresis (55). It is important to note that distal nephron sodium channels are critical for fine-tuning the amount of sodium excreted, with subsequent regulation of extracellular fluid volume and blood pressure. This process is tightly regulated and the involvement of endothelin as a key regulator at this stage reflects its crucial role in fluid homeostasis blood pressure regulation. Loss of ET-1 from mice collecting duct cells led to the development of hypertension and salt sensitivity that was ameliorated with pharmacological inhibition of ENaC (3). ET-1 directly inhibits NHE3 channel in the proximal tubules (40) and Na^+/K^+ ATPase activity (3). While the natriuretic effect of ET-1 is mainly achieved through the ET_B receptor, ET_A has been implicated in promoting natriuresis through ENaC inhibition in mice cortical CD (125) and in the inner medullary collecting ducts (IMCD) of female rats (138).

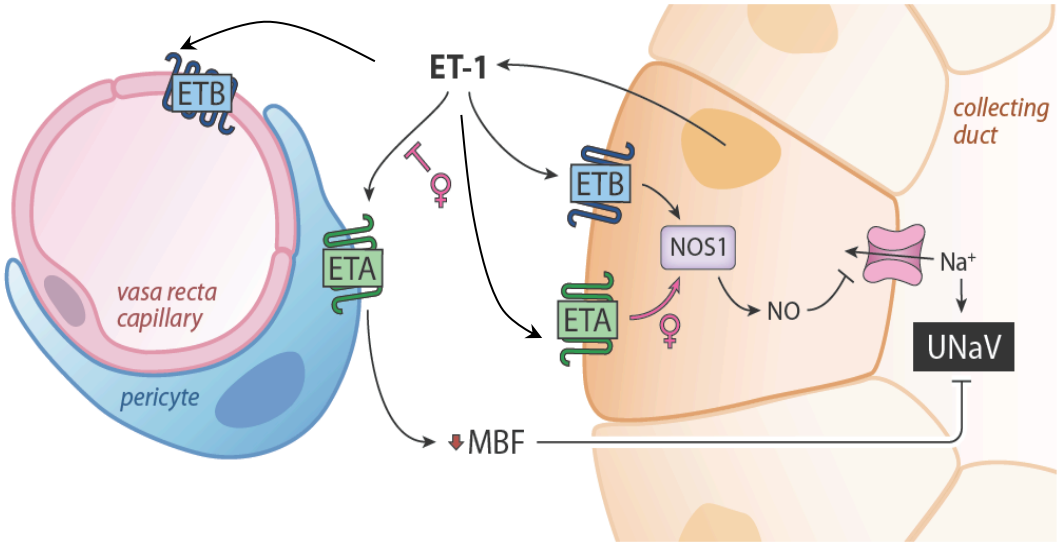

Figure 1: The biological actions of ET-1 are mediated through ET_A and ET_B receptors. ET-1 binds to ET_A receptor on the pericytes leading to reduced medullary blood flow (MBF). In females ET-1 binding to ET_A receptor has no influence on MBF. ET-1 binds to ET_B receptor on the renal tubular cell of the collecting duct, mediating NO-induced suppression of epithelial sodium channel (ENaC). Tubular ET_A receptor activation promotes natriuresis in females. ET_B receptor activation on the vascular endothelium leads to vasoconstriction (100).

Sex Differences in the Renal Endothelin System

Sexual dimorphism in cardiovascular and CKD have been a driving force for research on cardio- and reno-protective mechanisms in pre-menopausal women. Studies of renal ET-1 have shown that many ET-mediated functions are sex-dependent. Studies have shown that loss of ET_B receptor function produces a more severe hypertension phenotype

in female compared to male rats under HS diet (99). However, females utilize ET_A receptor to promote sodium excretion in the absence of ET_B (99). This observation is a potential mechanism for the maintained acute natriuretic response observed in ET_B-deficient female rats compared to the delayed natriuresis in the male counterparts (88). Female rats excreted an acute salt load more rapidly than males (196) and investigating sodium channels protein expression along the nephron revealed that phosphorylated NCC and the cleaved α- and γ-ENaC subunits are more abundant in female rat kidneys, suggesting higher channel activity in the distal part of the nephron (196).

Regulation of Blood Pressure Rhythms, Role of the Kidney

Molecular Basis of Circadian Rhythms

The suprachiasmatic nucleus (SCN) in the hypothalamus is the home for the central clock, that acts as the conductor, coordinating the rhythmicity of different organs (86). This is achieved through a transcriptional-translation feedback loop (TTFL). The central clock responds to external cues, including light signals that reach the SCN through the retinal-hypothalamic tract, which leads to a series of downstream signals yielding the generation CLOCK and Bmal1 gene transcripts (Figure 2). Circadian locomotor output cycles Kaput (*CLOCK*) and Brain and muscle Arnt-like protein-1 (*Bmal1*) genes are transcription factors that form a heterodimer and represent the positive arm of the loop. They bind to the E-box response elements in the promoter region of *Cryptochrome* (*Cry*) and *Period* (*Per*) genes stimulating their transcription. *Per* and *Cry* transcripts form the suppressor arm of the loop, they undergo Casein Kinase (CK1δ/ε)-mediated phosphorylation which facilitates their

nuclear entrance and feedback to inhibit CLOCK/BMAL1 activity (45, 86, 159). Dephosphorylation of Per1 through the action of Protein phosphatase-1 (PP-1), releases the inhibitory dimer from its nuclear binding site and is recycled back to the cytoplasm (159). Each arm of the loop peaks during certain times of day, with Bmal1 peaking at the beginning of the inactive period (nighttime in humans and daytime in nocturnal animals), with a corresponding trough in *Per1* expression.

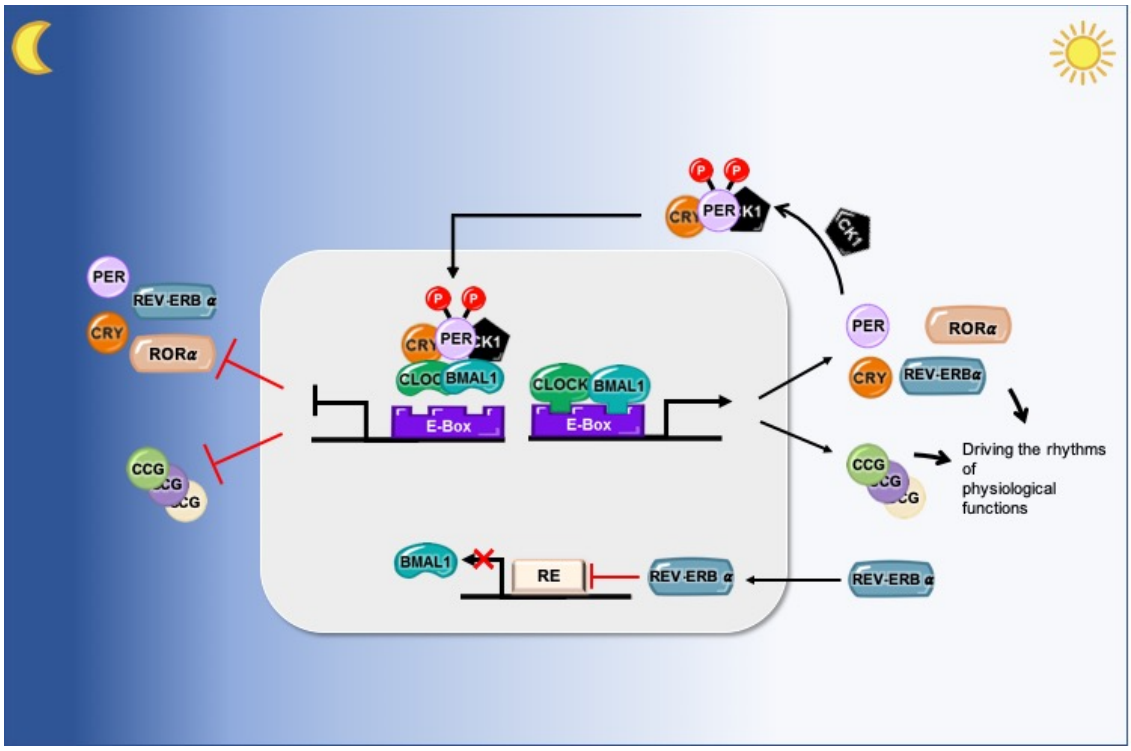

Figure 2: The transcription translation feedback loop. CLOCK:BMAL1 heterodimer binds to the E-box element of the promotor regions of *Period (Per)* and Cryptochrome (*Cry)* genes, driving their transcription. They also drive the transcription of many clock-controlled genes (CCG) in different organs, promoting rhythmicity of physiological functions. Cry and Per transcripts heterodimerize and through phosphorylation of Per by the action of CK1δ/ε, they enter the nucleus to inhibit CLOCK:BMAL1 binding to the E-box element. CLOCK:BMAL1 binding promotes the transcription of REV-ERB*α*, which binds to the response element (RE) of *Bmal1* promotor and inhibits its transcription.

Peripheral clocks are imbedded within the genome of all peripheral tissues with variable rates of expression. While the liver has the highest percentage of oscillating genes in the body, only 3% of protein-encoding transcripts oscillate in the hypothalamus (210). The central clock in the SCN influences peripheral tissues metabolic functions through

neural and hormonal factors. However, rapidly growing convincing evidence showed that cells have autonomous molecular clocks that function independently of SCN influence.

In the beginning of the last century, studies showed that urine output has a day-night difference regardless of time of water or food intakes (52, 132), which was then described as "night water retention" (52). Subsequent studies found that the majority of kidney functions display diurnal rhythms, including GFR, urine osmolarity, urine electrolyte excretion (45), endothelin-1 excretion (181) and autonomic nervous system activity (13).

In this section, we present evidence in support of the intrinsic mechanisms regulating time of sodium excretion along the nephron and the influence of environmental time cues, as timing of salt intake on rhythms of sodium excretion and the subsequent effect on blood pressure.

Sodium Channels along the Nephron and Kidney Clock

Sodium channels are abundantly expressed along the nephron, with the ascending limb of the loop of Henle being the only part of the nephron devoid of sodium channels (148). The multi-stop journey of sodium along the nephron is tightly regulated by hormonal, neuronal and paracrine factors, reflecting the importance of sodium balance on body fluid homeostasis and as will be discussed in this section, the diurnal regulation of blood pressure. More than 99% of the filtered sodium is reabsorbed along the nephron. The complex machinery of transporters along the renal tubule is responsible for micro-adjustment of the remaining 1% to achieve extracellular fluid balance and cellular homeostasis (148).

The proximal tubule (PT) reabsorbs approximately two-thirds of filtered sodium, which is highly permeable to ions and rich in mitochondria to provide the driving energy for sodium reabsorption. This is driven by the Na^+/K^+ ATPase on the basolateral border pumping sodium out of the cell into the interstitial space thus providing the gradient necessary for sodium transport (204). Reabsorption from the tubular fluid is then achieved largely through the function of sodium-hydrogen exchanger 3 (NHE3) and an array of symporters, that include, but not limited to sodium-glucose co-transporter 1 and 2 (SGLT1/2) (121) at the apical border of the cell membrane. NHE3 is expressed in the thick ascending loop of Henle (TALH) and together with $Na^+/K^+/2Cl^-$ cotransporter (NKCC2), 25% of sodium is reabsorbed in this part of the nephron (86). The distal convoluted tubule (DCT) is divided into proximal (DCT1) and distal (DCT2) segments that lead to the collecting duct (CD) through the connecting tubule (148). Sodium reabsorption along this part of the nephron is highly regulated and critical for extracellular fluid homeostasis. It is also the target of pharmacological agents in the treatment of hypertension that DCT1 is often referred to as the thiazide sensitive segment and DCT2 and CD epithelial sodium channel (ENaC) is described as the amiloride sensitive sodium channel. The DCT reabsorbs 6-10% of the total filtered sodium and only 1% of sodium now reaches the CD. While it may sound counterintuitive, precise matching sodium intake to excretion occurs primarily through physiological adjustments in the CD and not the proximal that reabsorbs nearly two thirds of filtered sodium (148).

Interactions between clock genes and the wide array of sodium channels have been the focus of a growing area of research (86, 211), however, this research is in its early stages and so we have yet to establish clear mechanistic pathways of circadian regulation

of renal sodium handling. In this section, we will focus on clock-mediated regulation of sodium transport along the nephron (Figure 3).

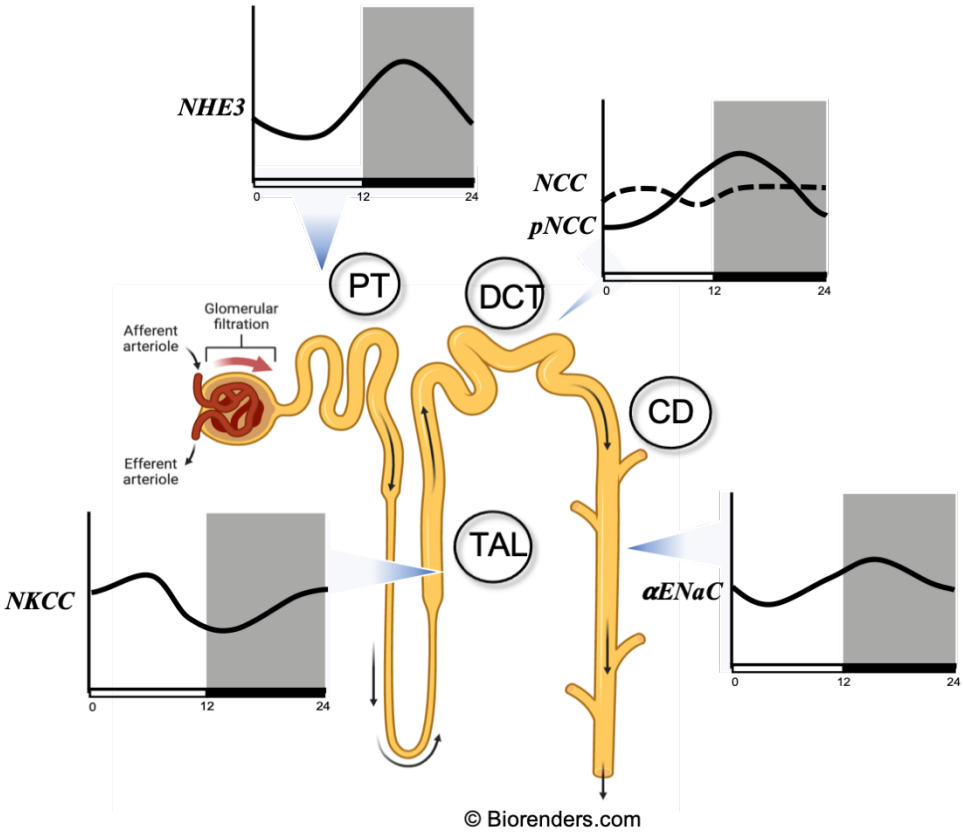

Figure 3: Distribution of the major oscillating sodium channels along the nephron with approximation of their circadian rhythms. Na^+/H^+ exchanger 3 (NHE3) (163), $Na^+/K^+/2Cl^-$ cotransporter (NKCC) (152), Na^+/Cl^- cotransporter (NCC) (188) and epithelial sodium channel (ENaC) (152, 181) in the proximal tubule (PT), thick ascending limb (TAL), distal convoluted tubule (DCT) and collecting duct (CD) respectively.

Sodium-Hydrogen Exchanger 3 (NHE3)

Na^+/H^+ exchanger 3 is critical for sodium reabsorption and acid base balance along the nephron (5) especially in the proximal tubule(5, 7, 163). In situ hybridization studies and laser capture microdissection techniques showed evidence of circadian oscillation of NHE3 in the thick and thin ascending limbs of the nephron, with a ZT12 peak (142). However, proximal tubular cells were not assessed in this study. Rohman et al provided the first report of circadian rhythmicity in NHE3 gene expression in rodent kidneys, that is directly regulated by Clock:Bmal1 heterodimer (163). Cry1/2 null mice showed loss of circadian oscillation of NHE3, *Bmal1* and *Per2* mRNA in the kidney, and transfecting opossum kidney (OK) cells with *mPer2* and *mCry2* downregulated NHE3 expression as measured by luciferase activity. They further utilized OK cells and luciferase reporter plasmids with *NHE3 5*' flanking regions of variable lengths to determine the promotor region essential for gene transcription, and in this fragment, the consensus sequence for Clock:Bmal1 E-box element was identified. Mutations in NHE3 promotor led to failure of Clock and Bmal1 transactivation, while OK cells expressing intact NHE3 promotor responded by fivefold increase in transcriptional activity upon treatment with both Clock and Bmal1. This study provides evidence that circadian rhythms in sodium homeostasis are driven by the autonomous kidney clock. The study also showed evidence for NHE3 and Per2 co-localization in the brush border of the proximal convoluted tubules. Blood pressure was not measured in the Cry1/2 null mice, however, we know from other studies that these mice are normotensive with preserved blood pressure rhythm under normal salt conditions (143), suggesting that circadian regulation of NHE3 is not the key determinant of blood pressure phenotype. This is supported by studies showing that knockout of NHE3

from the proximal tubule had no effect on systolic blood pressure (119). It is also of note that the application of computational methods predicted *Bmal1* and *Clock* modulation of NHE3 circadian rhythmicity, and a loss of this circadian variation, but not sodium reabsorption, in the absence of either clock gene (198). Similarly, Per1 was detected at the promotor region of NHE3 (175). Per1 cannot enter the nucleus without phosphorylation by the casein kinase isoform δ/ε (CK1δ/ε) (20, 159). Injection of a CK1δ/ε inhibitor into 129/sv WT mice resulted in suppression of NHE3 mRNA expression in mouse cortex collected at midnight. This observation was further confirmed by suppression on NHE3 expression and transcriptional activity in pharmacologically-induced blockade of Per1 nuclear entry and siRNA-induced knockdown in HK-2 cells (175).

Taken together, these studies show that NHE3 is a direct target for circadian clock gens, with Clock:Bmal1 and Per1 acting as positive direct regulators, while Cry1/2 as well as Per2 are suppressors of channel expression. Further characterization of NHE3 expression and activities in different animal models of clock gene dysfunction, will further establish the role of the critically important proximal tubule channel in modulating sodium reabsorption in response to changes in timing of sodium intake.

Sodium-Glucose Co-transporter (SGLT)

Glucose is exclusively reabsorbed in the proximal tubule coupled with sodium reabsorption and is achieved via the apical sodium-glucose transporter1 (SGLT1) and SGLT2. Coupled reabsorption of sodium and glucose through this channel is driven by the basolateral Na^+/K^+ ATPase activity and intracellular glucose accumulation drives GLUT2-mediated glucose pump back to the plasma (53).

Evidence of circadian regulation of SGLT1 comes from studies of the gut. SGLT1 was identified as a circadian target in the small intestine, with loss of temporal pattern of SGLT1 expression in *Clock* mutant mice (150). Interfering with *Bmal1* in vitro resulted in upregulation of SGLT1 expression in differentiated Caco-2 cells through a PAX-4 mediated transcriptional suppression (189). However, in the kidney, evidence of circadian control of SGLT1/2 expression and activity is limited. Solocinski et al. identified Per1 as a positive regulator of SGLT1 in a mechanism that is similar to NHE3 (175). Studies on the role of SGLT1/2 in circadian regulation of renal sodium and glucose homeostasis are needed, particularly with the recently presented evidence showing association between loss of SGLT1 and higher systolic blood pressure in Atika mice (177). In addition to glucose, sodium reabsorption is also coupled with amino acids, lactate and P_i with no available data on circadian regulation.

Sodium-Potassium-Chloride Co-transporter (NKCC2)

While the loop of Henle accounts for roughly 25% of tubular NaCl reabsorption (86), little is known about a role for clock genes in this part of the nephron. Apart from the circadian expression of NKCC2 in the kidney (152), studies discussed here only show evidence of indirect circadian regulation of the Na^+/K^+ channel. Krid et al studied circadian oscillation of the estrogen-related receptor β (ERRβ) in the thick ascending limb (110). ERRβ showed a temporal pattern of expression with a light phase peak (ZT4), coinciding with NKCC2 peak of expression (152, 173). In fact, mice treated with the pan-ERR inhibitor, diethylstilbestrol, suffered sodium wasting and inability to concentrate urine manifested in marked increase in urine volume and significantly reduced osmolarity. Krid

et al suggested that this phenotype is an ERRβ-mediated NKCC2 dysregulation based on their observations that 1) ERRβ expression is highest in the thick ascending limb, 2) increased Na^+/K^+ excretion ratio in the urine, 3) decreased NKCC2 mRNA expression and activity secondary to ERR inhibition, with no effect on NCC expression and 4) Mouse thick ascending limb (MKTAL) cell line treated with selective ERRβ agonist showed a 2-fold increase in the relative expression of NKCC2 (110). However, whether pharmacological manipulation of ERRβ was associated with changes in core clock gene profiles was not assessed. Male mice lacking the circadian transcription factor Per1 showed a non-dipping hypertension phenotype under combined HS diet and short-term mineralocorticoid treatment (174). While WT mice suppressed the expression of renin in response to treatment, *Per1KO* mice showed no renin suppression as well as no change in NKCC2 channel expression in the renal cortex relative to normal salt conditions (37, 174). However, the temporal pattern of expression of NKCC2 was not investigated in this study, and whether loss of *Per1* will lead to a complete loss or phase shift in NKCC2 expression and activity under HS is yet to be determined.

Sodium-Chloride Co-transporter (NCC)

The sodium chloride cotransporter (NCC) is the main apical sodium channel in the first part of the DCT with reduced expression in the late part of the DCT (148) and is characterized by its sensitivity to thiazide diuretics and response to changes in plasma K^+ concentration (80). As mentioned before, sodium reabsorption is tightly regulated in this part of the nephron and this is evident in NCC multi-step signal cascade and the necessity of phosphorylation for channel activity (80). However, mice lacking NCC showed no

changes in sodium excretion or blood pressure under normal conditions (80, 165), possibly through downstream ENaC-mediated compensation (17). Many studies have shown circadian regulation of NCC through multiple mechanistic pathways, reflecting a role for NCC in time-of-day sodium regulation. A newly published study by Bailey and colleagues showed a different NCC response dependent on the class of steroid hormones (80). Glucocorticoid receptor activation increased channel activity through promoting phosphorylation, while mineralocorticoids increased the total NCC pool without affecting phosphorylation. Acute GR-induced phosphorylation was associated with increased expression of *Bmal1, Per1, Per2* and *Cry1* in the kidneys of C57BL6 mice (80). Previous studies have shown a peak of the phosphorylation level of NCC at the beginning of the active period, but limited oscillation of the inactive form of the channel protein (188). Bailey's group reported the same observation, with attenuation of the diurnal rhythmicity of pNCC and *Per1* with chronic GR blockade (80). A report of upregulated NCC relative expression in a Cre-model of distal nephron-specific *Per1KO* mouse (37) supported the hypothesis of clock-mediated regulation of sodium transport in the DCT. NCC is important in blood pressure regulation and its activation follows a diurnal rhythm (22, 81). Inactive phase upregulation of pNCC through chronic corticosterone infusion leads to rise in day-time blood pressure and development of non-dipping phenotype in C57BL6 mice (81) The blood pressure phenotype was associated with impaired circadian rhythm of mRNA expression of *Bmal1, Per1* and glucocorticoid-induced kinase 1 (*Sgk1)*. SGK1 functions as a regulator of a number of tubular sodium transporters (140). Few studies have attempted to identify direct and indirect clock-mediated mechanisms in the regulation of channel expression and activity. However, there has been one report showing that *Per1* regulates

NCC through the WNK pathways (158) but whether corticosterone-induced upregulation of Sgk1 and glucocorticoid-induced leucine zipper (GILZ), an oscillating transcriptional regulator responding to glucocorticoids, are potential pathways for clock-induced NCC regulation is to be determined. This is particularly important, since little is known about molecular mechanisms integrating NCC rhythmicity and the kidney clock transcription-translation feedback loop.

Epithelial Sodium Channel (ENaC)

The epithelial sodium channel (ENaC) has a hetero-multimeric structure of α-, β-, and γ-subunits and the functionality of the channel depends on αENaC proteolytic cleavage (90, 172). ENaC is localized to the DCT2, CNT and the collecting ducts (CD) (61). This amiloride sensitive channel is critical for final control of sodium homeostasis, responding to changes in tubular sodium delivery, ET-1, aldosterone, NO as well as growing evidence of clock gene regulation to tightly regulate sodium excretion to match the intake and to achieve fluid-electrolyte balance (148, 172). Studies by our group have shown rhythmic oscillations of αENaC in rat inner medulla, with an active period peak and more than 50% reduction in the amplitude in response to HS diet (181). Testing this observation through benzamil blockade at different times of day, showed no difference in natriuresis in response to drug administration at ZT0 vs ZT12 (172). This reflects a disconnect between mRNA expression and function and calls for further studies on channel conductivity at different times of day at baseline vs high salt conditions.

Given the critical role of ENaC in the regulation of blood pressure, studies have focused on investigating circadian regulation of ENaC under different dietary salt

conditions. Data provided from *in vitro* studies supported the hypothesis that Per1 positively regulates αENaC expression and directly promotes channel activity. Mouse inner medullary collecting duct (IMCD-3) cells were treated with siRNA directed against Per1, showed 80% reduction in *Per1* mRNA expression and marked reduction in αENaC expression that was not responsive to aldosterone (60). Using both luciferase activity and protein abundance assays, cortical collecting duct cells ($mpkCCD_{c14}$) transfected with dominant negative Per1 vector or Per-1-specific siRNA respectively, showed reduction in αENaC promotor activity and expression (58). Similarly, targeting *Per1* in Xenopus 2F3 distal nephron cells with siRNA, showed a reduction in channel density and open probability (6).

The first reported global *Per1KO* mouse, on a 129/sv background (10), showed a lower blood pressure phenotype (186) and studies by Gumz et al. reported downregulation of αENaC expression in the cortex of the KO mice (58). However, the C57BL/6J *Per1KO* mouse model showed no blood pressure phenotype and similar ENaC expression profile compared to WT controls under normal dietary conditions (174). Likewise, the loss of *Per1* from the distal part of the mouse nephron was associated with upregulation of alpha αENaC expression in the cortex (37). An interesting observation of the C57BL/6J *Per1KO* mouse model was that a combination of high salt and deoxycorticosterone pivalate (HS/DOCP) treatment stimulated the expression of αENaC that was correlated with the serine/threonine kinase SGK1 expression in this group, promoting salt sensitivity and non-dipping hypertension. Whereas, the higher SGK1 in the WT mice, was not associated with changes in αENaC expression, suggesting that missing *Per1* is contributing to the inappropriately higher αENaC (37).

Collectively, these studies highlight a disconnect between the *in vitro* and *in vivo* models as well as strain-specific phenotypes. This calls for the utilization of other models of circadian and blood pressure dysfunction, both in humans and rodents, to provide a better understanding of circadian regulation of renal salt handling and blood pressure homeostasis.

Circadian Regulation of Renal ET-1

There is growing evidence of clock-mediated regulation of the endothelin axis, and dysfunction of ET-1 system is deleterious to diurnal sodium handling, cardiovascular health, and associated with chronic kidney disease. *ET-1* gene promotor hosts binding motifs for many transcription factors, of which are the hormone response element (184) and E-box element (160) that contribute to circadian regulation of ET-1 transcription.

Circadian regulation of ET-1 has gained special interest after the identification of preproendothelin and period homolog as early aldosterone-responsive genes in mice by the Gumz group (59). Subsequently, this group studied the role of the circadian clock gene *Period 1* (*Per1)* in the regulation of ET-1 function and blood pressure homeostasis (36, 158, 186). Transfecting mpk cortical collecting duct cells (mpkCCD) with *Per1- 8 siRNA* was associated with *ET-1* mRNA induction and increased ET-1 concentration in the culture media (186). In their model of *129/sv Per1KO* mouse, *ET-1* mRNA expression was higher in the cortex and medulla of kidneys collected at noon and at midnight compared to WT controls (186). *Per1* heterozygous mice showed elevated ET-1 levels in their inner medulla, with no effect on the mRNA expression of ET_B or ET_A receptors, that were expressed in a diurnal, but opposite rhythms in both WT and *Per1* heterozygous mice

(160). These studies show that Per1 is a direct negative regulator of ET-1, but not its receptors and supports the hypothesis that ET-1 is involved in circadian regulation of renal rhythms and blood pressure regulation.

ET-1 is essential in excreting HS loads and studies have found that HS diet induced a phase shift in *Bmal1* mRNA expression in rat's inner medulla (181), which proposed a role for the core clock transcription factor *Bmal1* in the diurnal regulation of the ET-1 system and circadian rhythms of sodium excretion. This was recently confirmed with the observed loss of diurnal rhythms of sodium excretion in global *Bmal1 KO* rat (87). ET-1-induced suppression of *Bmal1* mRNA expression in mouse inner medullary collecting duct cells (mIMCD-3) (181). Johnston et al. reported delayed natriuretic response in ET_B-deficient rats in response to an acute salt load given either at the beginning of the inactive or active periods, supporting the role of ET1/ET_B interaction in the diurnal regulation of sodium excretion (88). ET_B-deficient rats on HS diet, showed suppression of *Cry1* and *Per2* expression in their kidneys with no effect on *Bmal1* in contrast to transgenic controls that showed HS-induced phase shift of Bmal1 as previously mentioned (181). This suggests that HS-induced circadian disruption of *Bmal1* requires an intact endothelin axis, with potential compensatory mechanisms promoting *Cry* and *Per* genes in the rat kidney.

Clinical studies showed evidence of ET system overactivity and involvement in diurnal regulation of blood pressure in chronic kidney disease (CKD) patients (31, 197). Patients with CKD had higher midnight plasma ET-1 compared to healthy controls, with loss of day – night difference, in addition to loss of night-time dip in systolic and diastolic blood pressure (31, 134). Subjecting 27 CKD normotensive patients to ET_A receptor antagonist, sitaxentan, as part of a reno-protective protocol for six weeks, promoted a

reduction in night-time blood pressure with more than 8% dip in SBP compared to baseline (week 0) (31). This study further builds on the evidence of ET system involvement in diurnal regulation of blood pressure.

Our knowledge of clock-mediated regulation of the endothelin system is growing, however, studies elucidating mechanisms that govern clock-mediated responses of the endothelin system and its subsequent effect on cardiovascular and renal health are still lacking.

Circadian Rhythms in Obesity-induced Hypertension

Mechanisms of Obesity-hypertension: Circadian Links

Obesity is the most important risk factor for hypertension. Obesity is defined as excessive accumulation of adipose tissue in the body and individuals having a BMI of 30 or more are considered obese (137). More than 70% of patients with essential hypertension are obese. Adiposity mediates sodium retention, a hallmark of essential hypertension, in pathways that directly or indirectly involve the kidney. In addition to increased salt intake that characterizes high fat diets, obesity promotes increased renal sodium reabsorption through hormonal, neural, and local mechanistic pathways. Most, if not all of these pathways involve the kidney, which has been recognized by Guyton as the center for blood pressure regulation (66). In the following section, we will discuss pathways involved in obesity-induced dysfunctions in renal sodium handling and their contribution to the development of hypertension. We will then discuss circadian disruptions in obesity and obesity-hypertension.

The Renin Angiotensin Aldosterone System

The renin-angiotensin-aldosterone system (RAAS) when activated promotes sodium reabsorption, extracellular fluid volume expansion and blood pressure increase. It also influences renal hemodynamics as a vasoconstrictor. The cascade of RAAS activation involves many co-stimulatory and inhibitory signals that can act independently or in synchrony with RAAS components. This multi-step signaling cascade allows for tight control of extracellular fluid and blood pressure in response to changes in dietary salt intake. Stimulation of the RAAS is an important driving factor to the development of hypertension in obesity.

The liver is the primary source of angiotensinogen (AGT), but studies have shown that adipose tissue can be a source for AGT, with a tendency for higher adipose-tissue dependent production under states of obesity (62, 195). Human and rodent adipose tissues variably express RAS components (166). A study on subcutaneous abdominal adipose tissue biopsies from 46 overweight (BMI = 29 +1) human subjects, provided evidence of positive correlation between BMI and adipose tissue AGT mRNA expression (207). However, all subjects were normotensive and with a small window of BMI variation. So, whether that contributes to the overall increased RAAS system activity in obesity-hypertension is not entirely clear. This is particularly important since another study on 10 overweight and 12 lean subjects failed to show a difference in AGT expression between the two groups (54). The kidney's proximal tubules, in addition to the heart, lung, blood vessels, (77) brain and adrenal gland produce AGT (178).

Renin converts angiotensinogen into angiotensin I, which is then converted through the action of angiotensin converting enzyme (ACE), produced from the lung, into

angiotensin II (Ang II) (164). Ang II is known for its sodium absorption-promoting effects, both directly and through stimulating the release of aldosterone form the adrenal gland. Renal tubules express angiotensin type 1(AT1) and type 2 (AT2) receptors, and studies showed that the anti-natriuretic effect of Ang II is mediated through AT1 receptor (209), supported by evidence showing that mice lacking AT1 receptor in the kidney are protected from Ang II-induced hypertension (25) and that the loss of AT_{1a} receptor in the distal nephron reduced NCC and ENaC abundance in kidney homogenates (14, 16, 209).

The kidney is in possession of an intrarenal RAS system, that functions independently of the systemic RAS. Intrarenal RAS activation has been associated with the development of salt sensitive hypertension and sodium retention, through a pathological feed-forward tubular Ang II-induced stimulation of renin release and direct upregulation of distal nephron sodium transporters (102, 209). Urinary AGT/Creatinine ratios were higher in patients with hypertension compared to normotensive subjects (101). The presence and activation of intrarenal RAS in response to high salt and in hypertensive states, could explain the deleterious effects of Ang II in these conditions, despite mild elevation of circulating RAS components (66).

Higher levels of circulating Ang II have been associated with obesity. Obese zucker rats show increased expression of renal AT1 receptor, that promotes Ang II -mediated sodium retention (166). Ang II constricts glomerular efferent arterioles, dysregulate the glomerulotubular feedback and stimulates sodium transporters along the nephron, either directly or through aldosterone. These effects mediate sodium imbalance in obesity and promote the rise in blood pressure seen in individuals with higher BMI (66, 166).

The distal convoluted tubule, mainly its late segment, as well as the cortical collecting duct are sensitive to the mineralocorticoid, aldosterone (148), which through influencing clock genes in this part of the nephron, promotes sodium reabsorption. Similar to Ang II, plasma and urinary aldosterone follow diurnal rhythms with an early morning peak in healthy humans and at the corresponding active phase in rodents (158, 161). The interaction between the transcription-translation feedback loop of the circadian clock and aldosterone has recently been the center of attention in terms of aldosterone-dependent hypertension (Figure 4). For example, *Per1* was found to be upregulated by aldosterone, both in vivo and in vitro (59, 60, 158). Aldosterone injection into male Sprague-Dawley rats induced more than 3-fold increase in *Per1* mRNA and considering the stimulatory effect of aldosterone on αENaC, treating mIMCD-3, OMCD and mpkCCD cell lines with aldosterone resulted in significant increase in αENaC expression that was proceeded with *Per1* induction and suppressed when cells are treated with Per-specific siRNA (60). Aldosterone regulation of *Per1* occurs at the transcriptional level, and so does Per1 stimulating αENaC transcription. These results likely explain the sodium-wasting and hypotensive phenotype of the *Per1*-deficient mice.

Clock-null mice showed disrupted circadian rhythms of plasma aldosterone, with no effect on 24-hour mean values (140). Circadian profiling of the whole kidney transcriptome along with real time PCR showed a significant reduction in the number of oscillating genes in *Clock*$^{-/-}$ mice, as well as disruption of many transcript-encoding genes irrespective of circadian rhythmicity (140). This includes transcripts encoding for cytochrome p450 enzymes, leading to impaired 20-Hydroxyeicosatetraenoic acid (20-HETE) synthesis and excretion, as well as an observed acrophase shift in kidney

microsomes of the KO animals. 20-HETE, in addition to its vasopressor action, exhibits a bimodal role in sodium balance. It inhibits luminal sodium channels as well as the Na^+/K^+ ATPase activity in the TAL, promoting sodium excretion (140, 208). This is in addition to promoting the production of aldosterone through induction of ACE (171, 203). Aldosterone is tightly linked to clock genes, and many genetic models of clock gene dysfunction exhibit disrupted aldosterone balance. *Cry-null* mice, with complete loss of *Cry1* and *2*, have high circulating plasma aldosterone and low renin activity (143). Studies have also shown accelerated renal damage and proteinuria as a secondary effect to hyperaldosteronism (19).

Aldosterone is also secreted from adipose tissues and studies have correlated BMI with circulating aldosterone levels in obesity-hypertension (166) which contributes to the salt-retaining phenotype characteristic of obesity and further potentiates the adverse effect on blood pressure.

Circadian Rhythms in the RAAS

Diurnal rhythms in urinary sodium excretion and blood pressure have driven studies exploring the circadian rhythms in systemic and intrarenal RAS as a regulator of body fluid and blood pressure homeostasis. Evidence on circadian rhythms in RAS has been extensively reviewed in the literature (85, 93, 144) and to summarize, researchers have found that plasma renin activity, as well as circulating Ang II were higher in early morning in human subjects (144). No diurnal rhythm of excretion was observed in urinary AGT in normal subjects (79, 141). However, patients with CKD, not only showed higher AGT in their urines compared to normal subjects, but also showed a night-time dip in excretion

rates, that was positively correlated with blood pressure measurements (144). In an animal model of renin-dependent hypertension, *mRen2.Lewis* rats, that show a disrupted rhythm of blood pressure, with day-time peak, administration of AT1 receptor blocker, valsartan, for 2 weeks led to restoration of blood pressure rhythm (135). This was driven mainly by reduction of day-time blood pressure, while the addition of the renin inhibitor, Aliskiren, potentiated a more robust antihypertensive effect, that was associated with reduced plasma and kidney Ang II (135). This study shows that inappropriate intrarenal RAS contributes to circadian disruption in hypertension.

Studies on the role of aldosterone in promoting the circadian rhythms of sodium and blood pressure have been more comprehensively characterized. *Per1* and aldosterone exhibit a bi-directional feedback loop (Figure 4). Aldosterone stimulates *Per1* expression in cultured collecting duct cells and mice lacking the transcription factor *Per1* are hypotensive, but show maintained diurnal rhythms of blood pressure. Loss of *Per1* gene has reported no effect on circadian rhythmicity of blood pressure (186). On the other hand, *Cry-null* mice are salt sensitive and hypertensive, with marked elevation in their circulating aldosterone, mirroring an increase in production by the adrenal gland and increased β-hydroxysteroid dehydrogenase-isomerase (3β-HSD) enzyme activity (35).

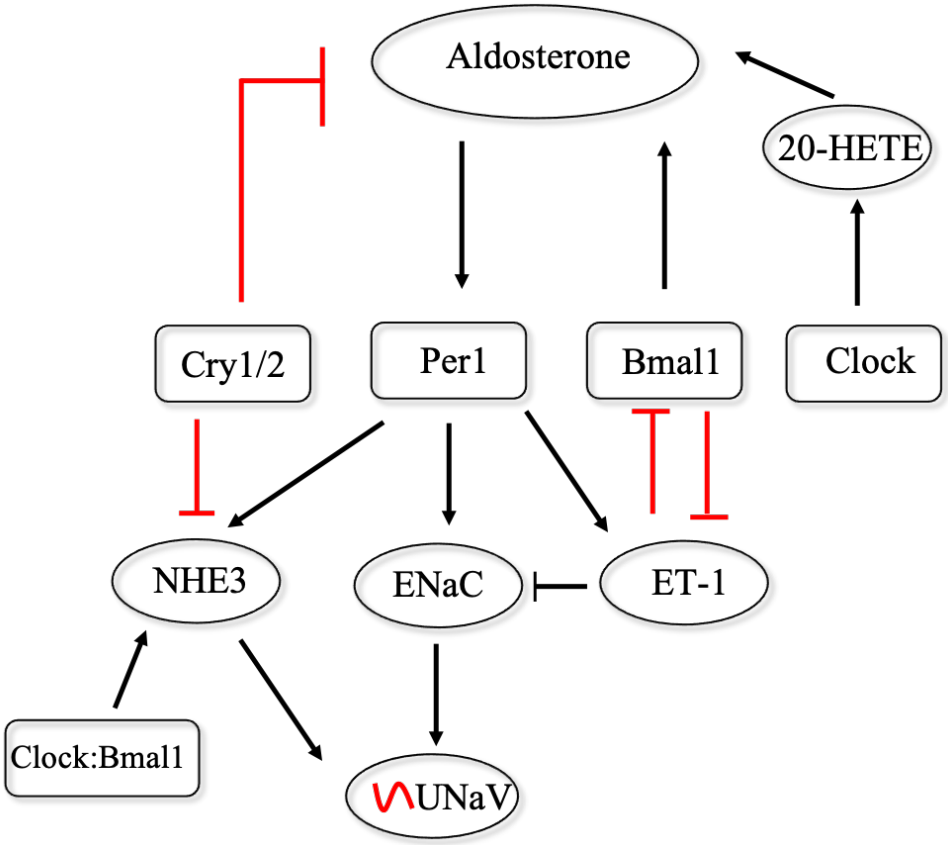

Figure 4: Proposed interaction between clock genes, aldosterone and endothelin-1 (ET-1) in the regulation of diurnal rhythms of sodium excretion, through the function of ENaC. Abbreviations: UNaV, urinary sodium excretion; ENaC, epithelial sodium channel; ET-1, endothelin-1; 20-HETE, 20-Hydroxyeicosatetraenoic acid.

Sympathetic Nervous System Activation

Increased sympathetic nerve activity is a consistent finding in obese individuals that affects most organs, including the kidney (109). Obese hypertensive individuals treated with combined alpha and beta-adrenergic blockers showed significantly lower blood pressure recordings compared to lean hypertensive controls, showing that blockade of

sympathetic nerve activity in obesity is a beneficial therapeutic target (201). Renal sympathetic nerve activity (RSNA) increased within one week of the onset of HFD in rabbits and proceeded the peak of arterial blood pressure by 2 weeks (9), suggesting that increased RSNA is contributing to the development of obesity-induced hypertension. Increased RSNA potentiates renin release, RAS activation and tubular sodium reabsorption (66, 109).

Obesity is also associated with baroreflex dysfunction, manifested by blunted increase in heart rate following baroreflex stimulation and reduced heart rate variability (170). Impaired baroreflexes were observed early on with the introduction of high-fat feeding in experimental animals, and activation of the baroreflex through carotid sinus stimulation in obese hypertensive dogs, normalized their blood pressure and decreased circulating noradrenaline levels (66). In long standing obesity, the development of vascular stiffness, further contributes to baroreflex dysfunction through limiting arterial wall distension in response to changes in intravascular pressure (66).

Local Factors

Mechanical compression of the kidney has been described as a potential contributing factor to the increased renal sodium reabsorption observed in obesity. Framingham Heart Study showed that increased renal sinus fat was associated with more than 2-fold increase in the risk of hypertension and development of chronic kidney disease (46). Hall et al. discussed potential consequences of kidney compression on renal sodium handling (66). Compression of the thin loop of Henle and vasa recta by sinus fat leads to reduced tubular flow rate in the ascending limb, potentiating sodium reabsorption in this

part of the nephron. This is followed by reduction in sodium delivered to the macula densa, which initiates dilation of glomerular afferent arterioles, increased renal blood flow and GFR through the tubuloglomerular feedback, as well as increased renin release from the juxtaglomerular cells (66). The accumulated sinus and peri-renal fat could potentiate local pro-inflammatory cytokine release, to further disrupt renal functions and contribute to CKD (66).

Circadian Disruption in Obesity

Loss or dysfunction of central and peripheral clock components result in loss of metabolic homeostasis and predisposes to obesity, metabolic and cardiovascular disease. Concurrently, a growing field of circadian research is showing evidence that high-fat feeding induces circadian misalignment, leading to disruption of peripheral circadian clocks and impaired signaling with the central clock in the hypothalamus. Mice lacking the core clock gene, *Bmal1*, have higher fasting blood glucose levels as well as hyperinsulinemia compared to their wild type controls (167). *Bmal1KO* mice fed high fat diet for 2 months showed higher body fat percentage, despite similar food intake between groups. In addition, high fat feeding led to marked suppression of locomotor activity in *Bmal1KO* mice. Inciting circadian misalignment in WT mice through constant lighting conditions led to a similar phenotype to the observed in the KO rats. Under LL conditions, WT mice on HF diet increased their fat mass and showed reduced locomotor activity (167). This study highlights the metabolism-regulating role of the clock and provides evidence that inherit and environmental factors of circadian dysfunction, predispose to metabolic diseases and exacerbates the deleterious effects of obesity. *Clock-mutant* mice are

hyperphagic and more susceptible to obesity, showing ~ 50% increase in their body weights with HF feeding (193). On regular chow, *Clock-mutant* mice had hyperlipidemia, hyperglycemia and low circulating insulin levels. However, blood pressure phenotype was not defined in these animal models under obese conditions.

In human studies, evidence associating obesity to clock disruption is limited to small observational studies. Genetic polymorphisms of *CLOCK* and *REV-ERB*α were associated with obesity (130). Circadian misalignment inflicted by shift-work increased cardiovascular disease risk up to 3-fold (131) and is associated with obesity and diabetes (48). Reverse-dipper pattern of blood pressure was positively correlated with metabolic syndrome in male hypertensive subjects (205). Disrupted diurnal rhythms of blood pressure is associated with metabolic disorders (190). A study on 181 patients with hypertension, showed that 43% of patients had higher systolic blood pressure in the morning. This phenotype of morning hypertension was significantly associated with metabolic syndrome (190). Taken together, these studies provide evidence that circadian regulation of blood pressure is dependent on metabolic signaling, yet molecular mechanisms are yet to be defined.

CHAPTER 3

MATERIALS AND METHODS

Experimental Animals

The study protocols and experimental procedures were approved by the University of Alabama at Birmingham Institutional Animal Care and Use Committee (UAB – IACUC) in compliance with the National Institute of Health (NIH) Guide for the Care and Use of Laboratory Animals. The study included both male and female Sprague-Dawley rats supplied by Envigo (Harlan Laboratories, Indianapolis, IN) as our animal model of interest.

Experiments for aim 1 through aim 3 were performed on Sprague-Dawley rats under the following experimental protocol:

Age-matched animals were randomly divided into 2 groups at 6 weeks of age and were put on either high-fat (45 Kcal% fat, D12451, HF) or normal-fat (10 Kcal% fat, D12450K, NF) diet as a control diet (Research Diets Inc., New Brunswick, NJ) for 8 weeks. Rats were given free access to the diets with free access to drinking water. Rats were housed conventionally (2 rats/cage) in a temperature and humidity-controlled environment and under a 12:12 hours light-dark cycle. Lights were turned on at 7:00 AM (ZT0) and turned off at 7:00 PM (ZT12). Rats were weighed and tail-marked at the beginning of the

feeding protocol and every 2 weeks. At the end of the study and before euthanization, rats were weighed and a body composition analysis scan was performed using quantitative magnetic resonance (QMR) technology provided by UAB Small Animal Phenotyping Core.

Experiments for aim 4 were performed on Sprague-Dawley rats under the following experimental protocol:

Both male and female Sprague-Dawley rats (12-16 wks. old) used for these experiments were obtained from Envigo (Harlan Laboratories, Indianapolis, IN) and housed conventionally (2rats/cage) in temperature and humidity-controlled conditions under a 12:12 hour light-dark cycle with ad-libitum access to water and regular chow (0.49% NaCl).

Acute Salt Loading Protocol

At the beginning of the last week (week 8) of HF and NF feeding protocol, both HF and NF rats were put in metabolic cages for 2 days of acclimation (Figure 5). On day 3, 12-hour baseline recordings of food and water intake as well as urine collections started. Recordings were obtained at ZT0 and ZT12 for 2 days. On day 5, HF and NF rats were given an acute intraperitoneal injection (i.p) of a 900 μEq NaCl bolus in 1 mL H2O, either at the beginning of their inactive (ZT0) or active (ZT12) time periods. Urine was collected in 12-hour windows over the following day as well as food and water intakes readings. Food and water were weighed every 12 hours and topped according to rat requirements. Rats were then returned to their regular cages for 5 days of recovery and then the

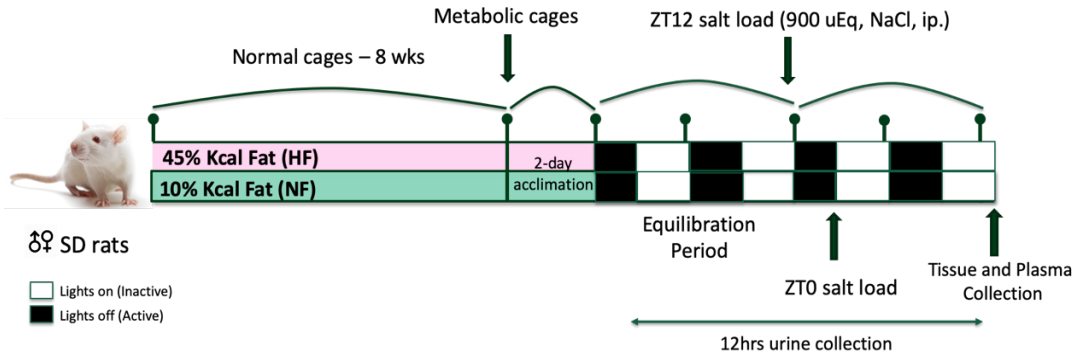

Figure 5: Experiment protocol and timeline for acute salt loading of male and female Sprague-Dawley rats fed either NF or HF diets.

experiment was repeated with switching the time-of-day of the acute salt load, meaning that a rat that received a ZT0 sodium challenge, will now be given the same bolus at ZT12. Rats were then euthanized for tissue and plasma collections.

Chronic salt Loading and Telemetry Blood Pressure Measurements

Midway through the feeding protocol, both HF and NF rats were implanted with telemetry transmitters (HD-S10, Data Sciences International, St. Paul, MN). The transmitter is connected to a catheter which is implanted into the abdominal aorta, after brief proximal occlusion. The body of the transmitter is then sutured to the abdominal wall. Rats are anesthetized with 2% isoflurane throughout the surgical procedure. The rats were allowed 7 days of recovery post-operative before telemeters were turned on (Figure 6). Recordings were obtained for 2-minute periods every 10 minutes at 1000 samples/second. Data collected included arterial blood pressure, heart rate, activity and temperature. Data were collected for 5 days under normal salt conditions (0.3% NaCl for HF diet and 0.2% NaCl for NF). Following baseline data collection, rats were further divided into 2

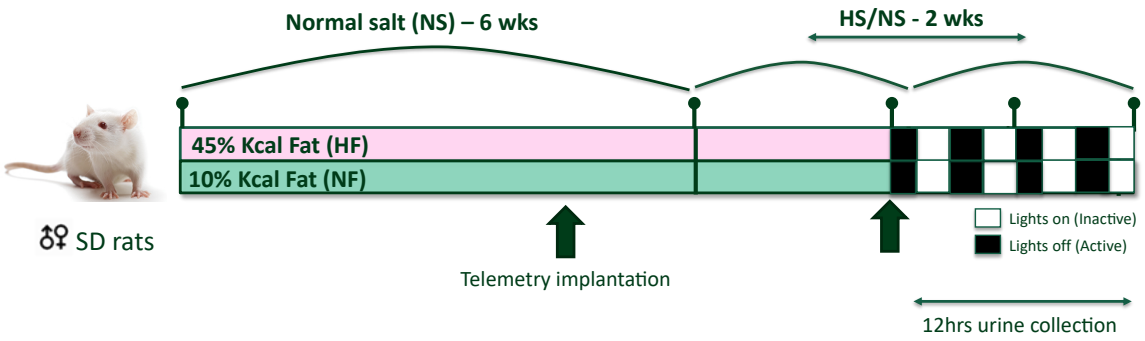

Figure 6: Experiment protocol and timeline for chronic salt diet and telemetry measurements of male and female Sprague-Dawley rats fed either NF or HF diets.

subgroups, to receive either a HS version (4% NaCl) of each diet or continue on the NS form for additional 2 weeks. Rats were then put in metabolic cages for the last 4 days of the protocol for urine collection and food and water intake monitoring.

Benzamil Administration Protocol

The experimental protocol began with rats placed in metabolic cages with free access to water and normal salt diet (Teklad custom diet TD.96208, 0.49% NaCl from Envigo, Indianapolis, IN). Animals were allowed to acclimatize to the new cages for two days and afterwards, baseline data were collected, where 12-hour urine collections were obtained to measure baseline urine flow rate (UV) and sodium (UNaV) and potassium excretion as well as water and food intake (Figure 7). On the third day after baseline collections, benzamil (Sigma-Aldrich, St. Louis, MO) was given at a dose of 1 mg/kg (i.p.) either at the beginning of their inactive period/lights on (Zeitgeber Time 0, ZT0, 7am) or their active period/lights off (ZT12, 7pm). At low doses, benzamil selectively blocks luminal ENaC in the aldosterone-sensitive collecting duct (2, 4). Following treatment,

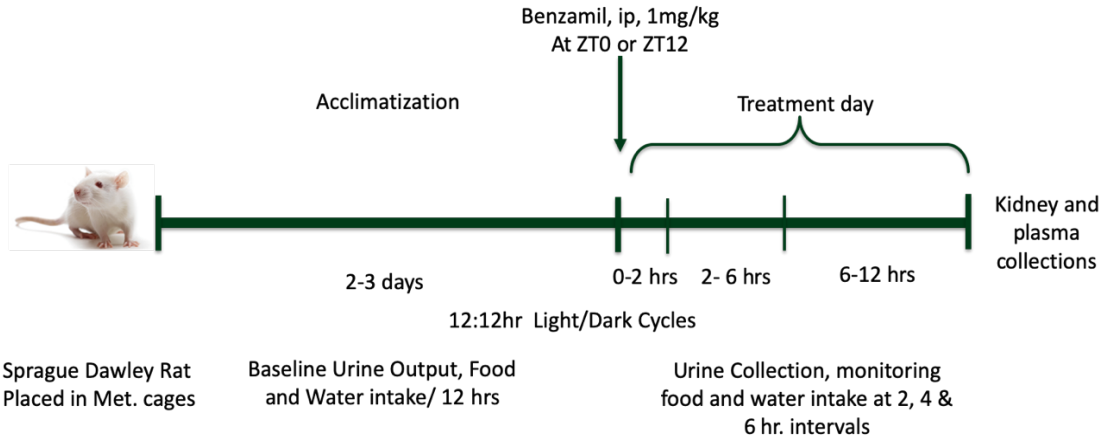

Figure 7: Experimental protocol of benzamil administration to male and female Sprague-Dawley rats under normal salt diet.

urine was collected at 2, 6 and 12 hours. Rats were then returned to their regular cages to allow them to recover for 5-7 days, after which, the protocol was repeated with reversal of benzamil injection time.

Ovariectomy Protocol

Female Sprague-Dawley rats (11-12 wks. old) were divided into ovariectomy (OVx) and sham (control) groups. Female rats in the OVx group were subjected to bilateral ovariectomy through bilateral dorsal incisions, the ovaries were located, ligated and then removed. The muscle layer was sutured back by simple continuous sutures, while the overlying skin was closed by wound clips (56). The same procedure was performed on the sham group; however, the ovaries were simply exposed with no ligation or removal. Isoflurane (2%) was used for anesthesia. Rats were given pain control medication on the surgical table (buprenorphine, 0.05 mg/kg, subcutaneous injection and topical application

of bupivacaine HCl (0.5%) on the closed surgical wound). Rats were allowed to recover for 3 weeks to ensure complete withdrawal of ovarian hormones before metabolic cage experiments were repeated as previously mentioned.

Quantitative Real Time PCR

Tissues were collected from rats euthanized at either ZT0 or ZT12 at the end of the 8-week feeding protocols. Kidneys were dissected into cortex, outer medulla and inner medulla upon euthanization, snap frozen in liquid nitrogen and then kept at - 80°C. Pieces of tissue (20 – 40 mg) were homogenized and mRNA was extracted using Purelink miniRNA extraction kit (12183018A, ThermoFisher Scientific, Grand Island, New York) according to manufacturer's instructions. The extracted RNA was then treated with DNA-free DNA removal kit (AM1906) from the same manufacturer. RNA purity and concentration were then determined using a Nanodrop spectrophotometer (ND-1000, Thermo Scientific, Waltham, MA). 1 μg RNA was reverse transcribed into cDNA using the iScript cDNA synthesis kit (1708891, BioRad Laboratories, Hercules, CA). The resulting cDNA was used for the relative quantification of mRNA using reverse transcription (RT) polymerase chain reaction (CFX96 Real-Time System, BioRad Laboratories, Hercules, CA). We used TaqMan primers for rat *EDN-1* (Rn00561129_m1), *EDNRA* (Rn00561137_m1), *EDNRB* (Rn00569139_m1) and *β-Actin* (Rn00667869_m1) genes supplied by Life Technologies Corporation (Grand Island, NY). Gene expression of each target gene was normalized relative to *β-actin* and calculated using the $2^{-\Delta\Delta Ct}$ method.

Western Blotting

Renal cortical tissues collected from male and female Sprague-Dawley rats at either ZT0 or ZT12 were dissected on ice and homogenized in hypotonic sucrose buffer (250 mmol/L sucrose, 30 mmol/L Tris, and 1 mmol/L EDTA at pH 7.5) and protease inhibitors (10 μmol/L leupeptin, 2 μmol/L pepstatin A, 1 mmol/L phenylmethylsulfonyl fluoride). Homogenates were centrifuged at 5000xg for 5 mins at 4°C. The pellet was discarded and the supernatant was used to measure total protein concentration with Bradford assay (Quick Start, Bio-Rad Inc., Hercules, CA). Twenty micrograms of protein was loaded and separated by SDS-PAGE and transferred onto polyvinylidene fluoride membranes (76). Each membrane was probed with the antibody for a single ENaC subunit (Table 1) and incubated overnight shaking at 4°C. Secondary antibody was added at dilutions shown in Table 1. Antibody against β-ENaC was custom produced by ProSci (Poway, CA) against rat amino acid sequence 617-638 C-TERM (NH2-CNYDSLRLQPLDTMESDSEVEAI-COOH). α and γENaC antibodies were purchased from StressMarq Biosciences, Inc. Then, the membranes were visualized with the LI-COR Infrared Odyssey Imaging System (Lincoln, NE). Signal intensity units were measured using LI-COR image studio software and densitometry units were normalized to the male group set as the control at either ZT0 or ZT12. Membranes were probed for actin and then stained with Coomassie blue and quantified to ensure equal loading. Blots for ENaC subunits in addition to representative blots of actin and Coomassie are shown in figure 38.

Table 1

Antibodies used in immunoblotting.

Antibody target	Primary Ab supplier	Ab host	Dilution	Secondary Ab supplier	Ab host	Dilution
ENaC-α	StressMarq (SPC-403D)	Rabbit	1:1000	Invitrogen (SA5-10036)	Goat	1:1000
ENaC-β	ProSci (Poway, Ca) (83, 129)	Rabbit	1:2000	Invitrogen (SA5-10036)	Goat	1:1000
ENaC-γ	StressMarq (SPC-405)	Rabbit	1:1000	Invitrogen (SA5-10036)	Goat	1:1000
Actin	Sigma (A1978)	Mouse	1:20000	Invitrogen (A21057)	Goat	1:10000

Analytical and Statistical Methods

Urine collected during metabolic cage experiments were assayed for electrolytes using the EasyLyte analyzer (Medica Corporation, Bedford, MA). Urine ET-1 was measured by immunoassay (QuantiGlo; R&D Systems, Minneapolis, MN) according to manufacturer's instructions. Urine and plasma aldosterone concentrations were measured by immunoassay developed and validated by Gomez-Sanchez et al (127).

Statistical analysis was performed using GraphPad Prism software version 8 for macOS (GraphPad Software LLC, San Diego, CA). Data are presented as means ± SEM with $P < 0.05$ was considered statistically significant. Statistical tests used for analysis of each dataset are indicated in the figure legends.

Footnote: The UAB Small Animal Phenotyping Core is supported by the NIH Nutrition & Obesity Research Center *P30DK056336*, Diabetes Research Center *P30DK079626* and the UAB Nathan Shock Center *PAG050886A*.

CHAPTER 4

RESULTS

AIM 1: TO TEST THE HYPOTHESIS THAT DIET-INDUCED OBESITY IMPAIRS DIURNAL RHYTHMS OF SODIUM EXCRETION, THAT IS ASSOCIATED WITH DIURNAL DYSFUNCTION IN RENAL ET-1.

Diet-induced Obesity Model

To characterize the phenotype of our animal model of diet-induced obesity, we first measured body weights as well as food and water intake (Table 2) for male and female rats that were randomly assigned into either HF or NF groups.

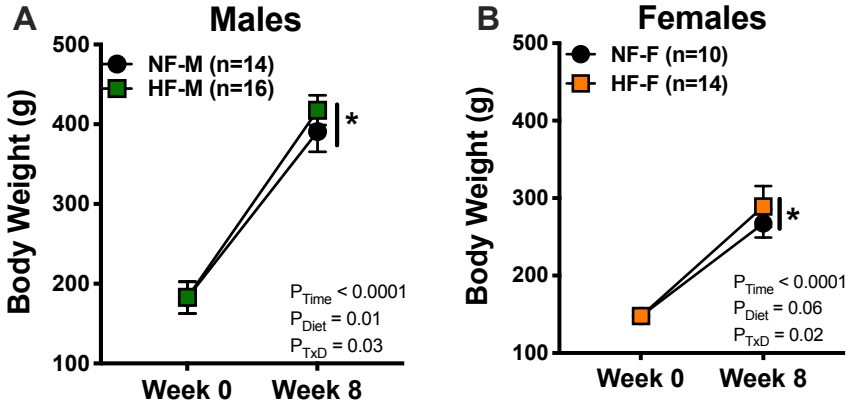

Figure 8: All rats had age-related increases in body weight after 8 weeks of either NF or HF diets. However, this increase was significantly larger in rats of both sexes when fed HF diet. Repeated measures two-way ANOVA (A: P_{Diet} =0.01, P_{Time} <0.0001, P_{DxT} = 0.03. B: P_{Diet} =0.06, P_{Time} <0.0001, P_{DxT} = 0.02), *$p < 0.05$ *vs* corresponding NF control as determined by Sidak's post-hoc test.

HF and NF male rats at the start of the experiment (week 0) had similar body weights (Figure 8A) that averaged 182 ± 5 grams. Female rats mean body weight was 148 ± 2 grams for both groups (Figure 8B). At week 8 of the feeding protocol, HF males had higher body weights compared to NF controls ($p = 0.002$; Figure 8A) and so did female rats on HF diet ($p = 0.007$; Figure 8B).

Body composition analysis with QMR showed a significant increase in total body fat in HF compared to NF-treated males (Figure 9A). Female rats under HF diet also had a significant increase in body fat from 10% under NF up to a mean of 15% (Figure 9A). There was a corresponding reduction in lean body mass and water content in both sexes (Figure 9B, 9C).

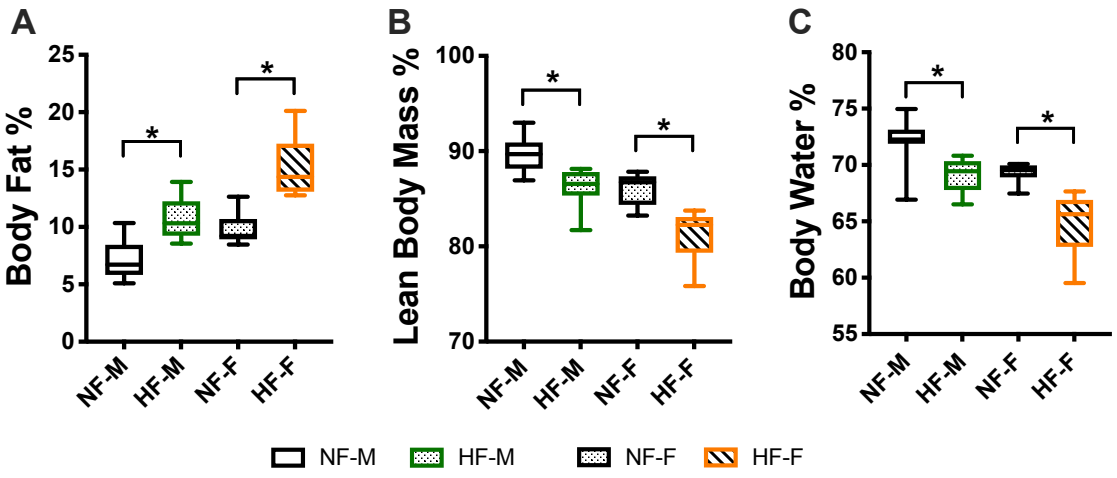

Figure 9: Body composition analysis of male and female Sprague-Dawley rats after 8 weeks on either NF or HF diets, as measured by QMR. Ordinary one-way ANOVA, *$p < 0.05$ *vs* corresponding NF control as determined by Sidak's post-hoc test.

Food and water intakes showed a clear diurnal rhythm in both male and female rats regardless of the type of diet (Table 2). Twenty-four hours food intake was lower in males on HF diet, compared to lean controls, as evident by an overall effect of diet ($p = 0.01$) but was not significantly different when determined at either day or night specifically. However, females on HF diet consumed significantly larger amounts of food over the 24-hour period, compared to their lean controls and the difference was significant during the active period ($p = 0.02$). Water intake had the same diurnal rhythm, with a significant effect of the diet to increase intake, only in HF females ($p = 0.0003$).

Despite the slight differences in food intake in male rats on HF diet, no significant difference in total NaCl intake calculated from food intake was observed between HF and NF male rats. This was due to the slightly higher NaCl content in the HF diet (0.3%) *vs* 0.2% NaCl in NF diet. In contrast, females on HF diet had active time NaCl intake that was significantly higher compared to lean controls.

Table 2

Diurnal parameters from metabolic cage studies in NF and HF-treated male and female rats.

	Males		***Females***	
	Normal Fat	*High Fat*	*Normal Fat*	*High Fat*
	Normal Salt Diet			
***Food Intake**, g/12 hrs.*				
Inactive Period	3.8 ± 0.5	2.8 ± 0.4	1.2 ± 0.3	2.5 ± 0.4
Active Period	11.6 ± 0.4	10.6 ± 0.7	10.8 ± 0.8	13.1 ± 0.7*
***NaCl Intake**, mg/12 hrs.*				
Inactive Period	9.1 ± 1.3	8.8 ± 1.3	4.8 ± 0.8	7.6 ± 1.3
Active Period	29.2 ± 1.1	31.8 ± 2.1	27.5 ± 2.3	39.6 ± 2.0*
***Water Intake**, ml/12 hrs.*				
Inactive Period	5.6 ± 0.4	4.9 ± 0.3	3.6 ± 0.3	4.5 ± 0.5
Active Period	14.1 ± 0.6	15.1 ± 0.7	12.3 ± 0.9	16.5 ± 0.7*
	High Salt Diet			
***Food Intake**, g/12 hrs.*				
Inactive Period	2.3 ± 0.7	2.6 ± 0.5	1.0 ± 0.2	2.4 ± 0.4
Active Period	11.8 ± 1.7	13.0 ± 0.8	12.4 ± 0.7	11.6 ± 0.5
***NaCl Intake,** mg/12 hrs.*				
Inactive Period	91.7 ± 28.7	104.3 ± 19.3	41.3 ± 7.5	94.5 ± 17.0
Active Period	471.3 ± 68.4	518.3 ± 30.3	497.3 ± 27.3	464.3 ± 20.9
***Water Intake,** ml/12hrs.*				
Inactive Period	6.8 ± 1.7	6.4 ± 0.9	4.9 ± 0.9	5.9 ± 0.3
Active Period	27.4 ± 3.0	27.0 ± 1.3	29.6 ± 3.1	25.1 ± 1.6

Data presented as mean ± SE. *$P < 0.05$ vs corresponding NF control, repeated measures, two-way ANOVA, with Sidak's post-hoc test.

Blood Pressure Phenotype of Diet-induced Obesity

We investigated if HF diet has an influence on blood pressure in male and female Sprague-Dawley rats. After 6 weeks on HF diet, male rats showed a significantly higher mean arterial pressure (MAP) compared to their lean controls, with active period mean of

120 ± 1 vs. 114 ± 2 mmHg, respectively (Figure 10A, 10B). Systolic blood pressure (SBP) (Figure 10C, 10D) and diastolic blood pressure (DBP) (Figure 10E, 10F) were similarly higher in HF-treated males, with maintenance of diurnal rhythm of blood pressure. There was no difference between the two groups in heart rate (HR) or body temperature with maintained circadian rhythms in either HF and NF groups (Figure 11A – 11D). However, HF diet led to relative suppression of diurnal rhythm of activity, as evident by an overall reduced activity counts compared to lean controls (Figure 11E, 11F).

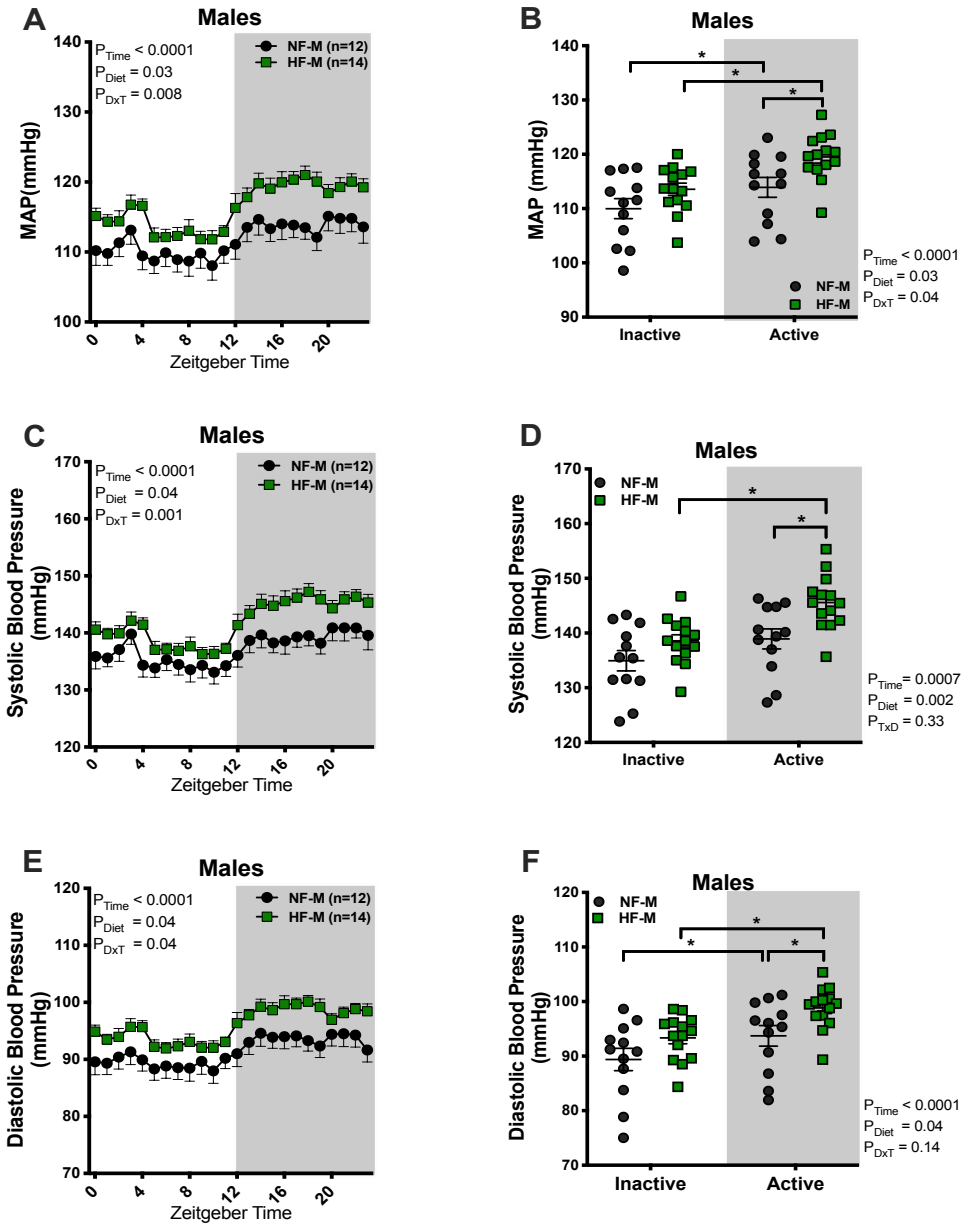

Figure 10: High fat diet induced an increase in mean (MAP), systolic (SBP) and diastolic (DBP) blood pressure in male Sprague-Dawley rats. Blood pressure was measured by radiotelemeters after 6 weeks on either NF or HF diet protocol. Data represent 2-day average of continuous 24-hour recordings (A, C and E) and 12-hour averages (B, D and F) in both groups ± SEM. Data were analyzed by repeated measures 2-way ANOVA, *denotes $p < 0.05$ vs corresponding NF control or corresponding inactive period as determined by Sidak's post-hoc test.

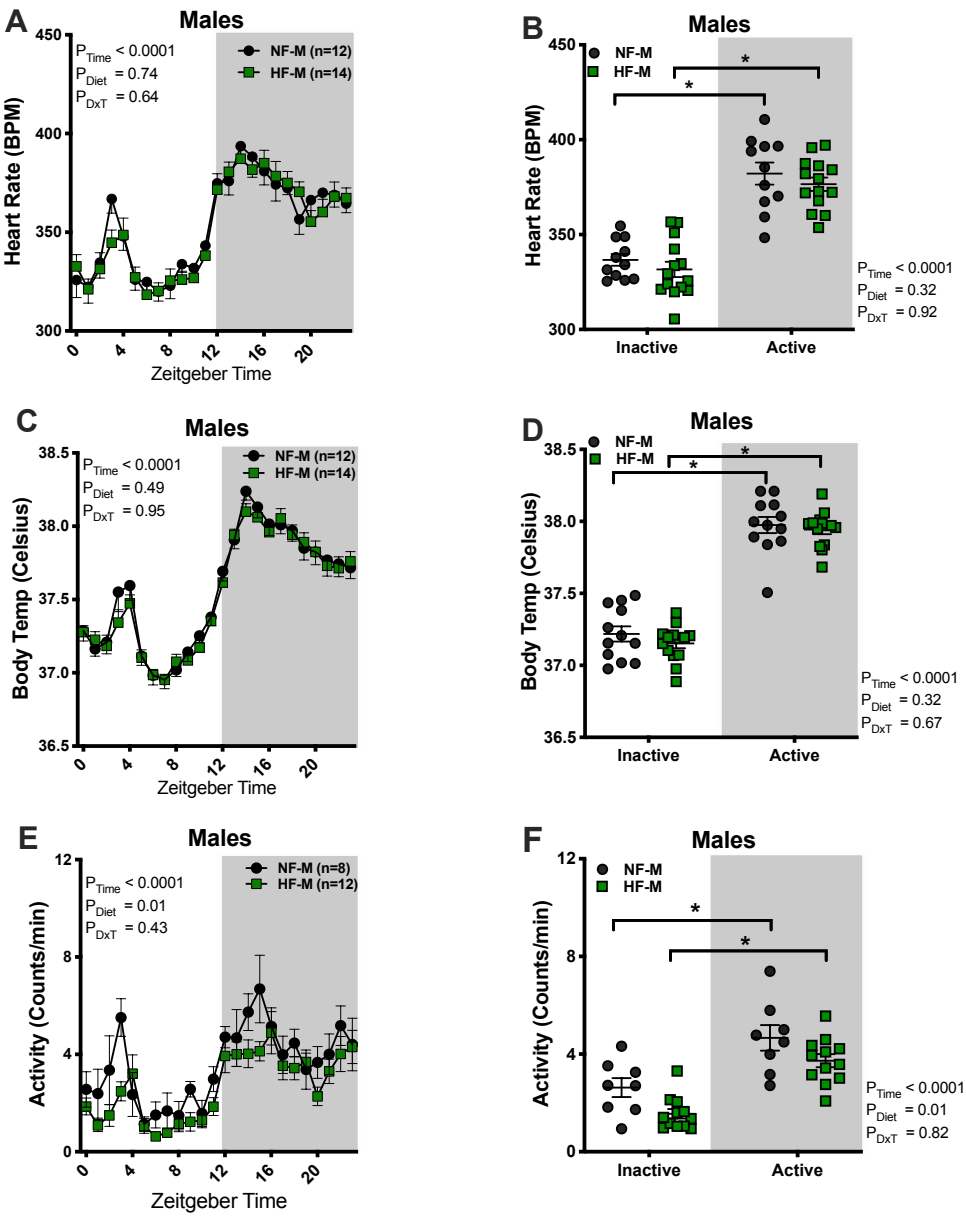

Figure 11: High fat diet had no effect on heart rate (A, B) and body temperature (C, D), with suppression of activity rhythms of male Sprague-Dawley rats under HF diet. Heart rate, body temperature and activity were measured by radiotelemeters after 6 weeks on either NF or HF diet protocol. Data represent 2-day average of continuous 24-hour recordings (A, C and E) and 12-hour averages (B, D and F) in both groups ± SEM. Data were analyzed by repeated measures 2-way ANOVA, *denotes $p < 0.05$ *vs* corresponding NF control or corresponding inactive period as determined by Sidak's post-hoc test.

The blood pressure phenotype in female rats followed a similar pattern as males. MAP was higher in females after 6 weeks on the HF diet (Figure 12A). MAP maintained a normal circadian rhythm with a peak of 112 ± 1 mmHg during the active period in HF-treated females compared to 106 ± 2 mmHg in the NF group (Figure 12B). SBP was higher with HF diet (Figure 12C, 12D), but the diet didn't have a significant impact on DBP in female rats, with maintained circadian rhythm (Figure 12E, 12F).

Activity, heart rate and body temperature showed a circadian rhythm, with active period peak and a trough during the inactive period in the two groups (Figure 13). Our results show no sex difference in the blood pressure response to HF diet, with a tendency towards a milder phenotype in females. Female rats on HF diet showed higher SBP and MAP, but DBP was not significantly higher compared to their NF controls (Figure 12).

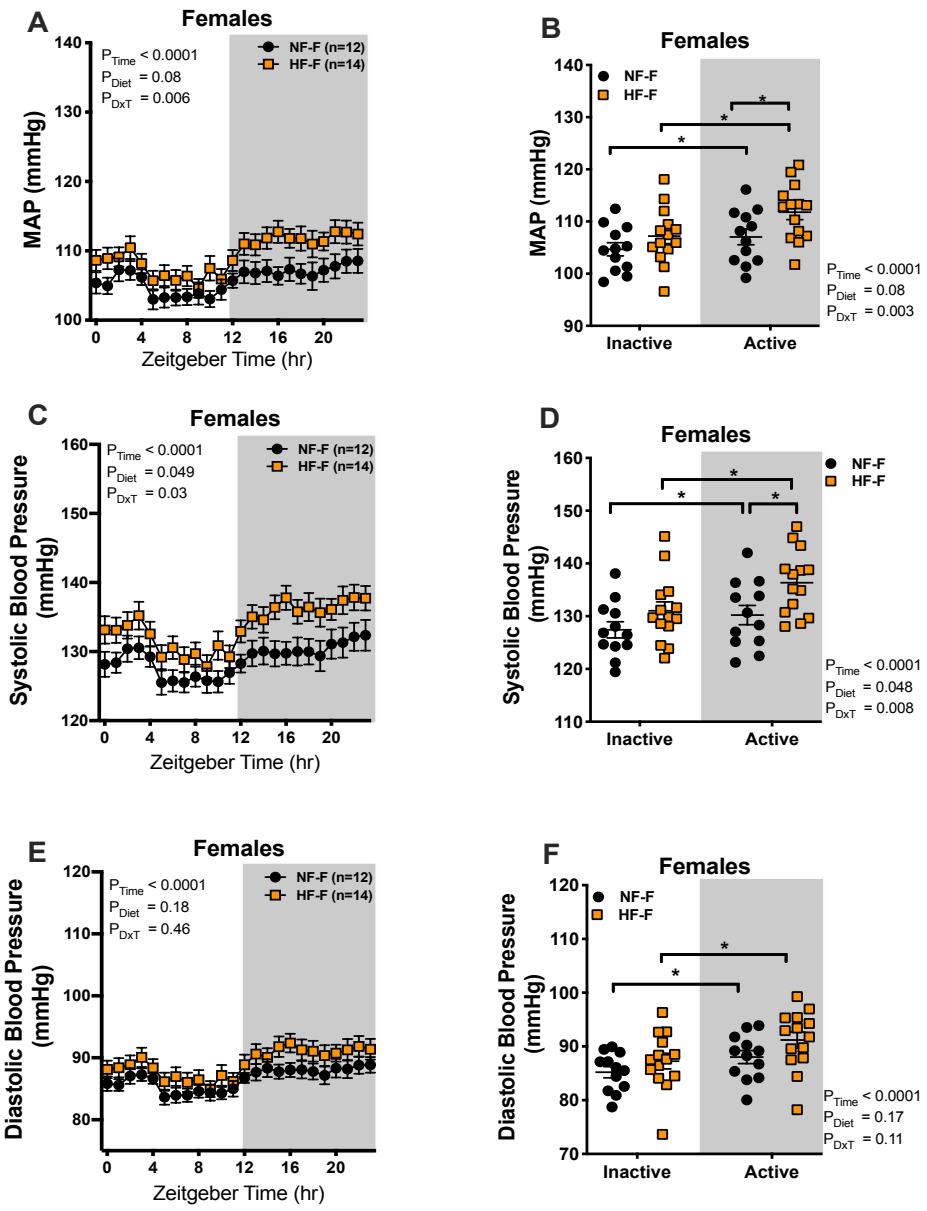

Figure 12: **High fat diet induced an increase in mean (MAP), systolic (SBP), but not diastolic (DBP) blood pressure in female Sprague-Dawley rats.** Blood pressure was measured by radiotelemeters after 6 weeks on either NF or HF diet protocol. Data represent 2-day average of continuous 24-hour recordings (A, C and E) and 12-hour averages (B, D and F) in both groups ± SEM. Data were analyzed by repeated measures 2-way ANOVA, * denotes $p < 0.05$ *vs* corresponding NF control or corresponding inactive period as determined by Sidak's post-hoc test.

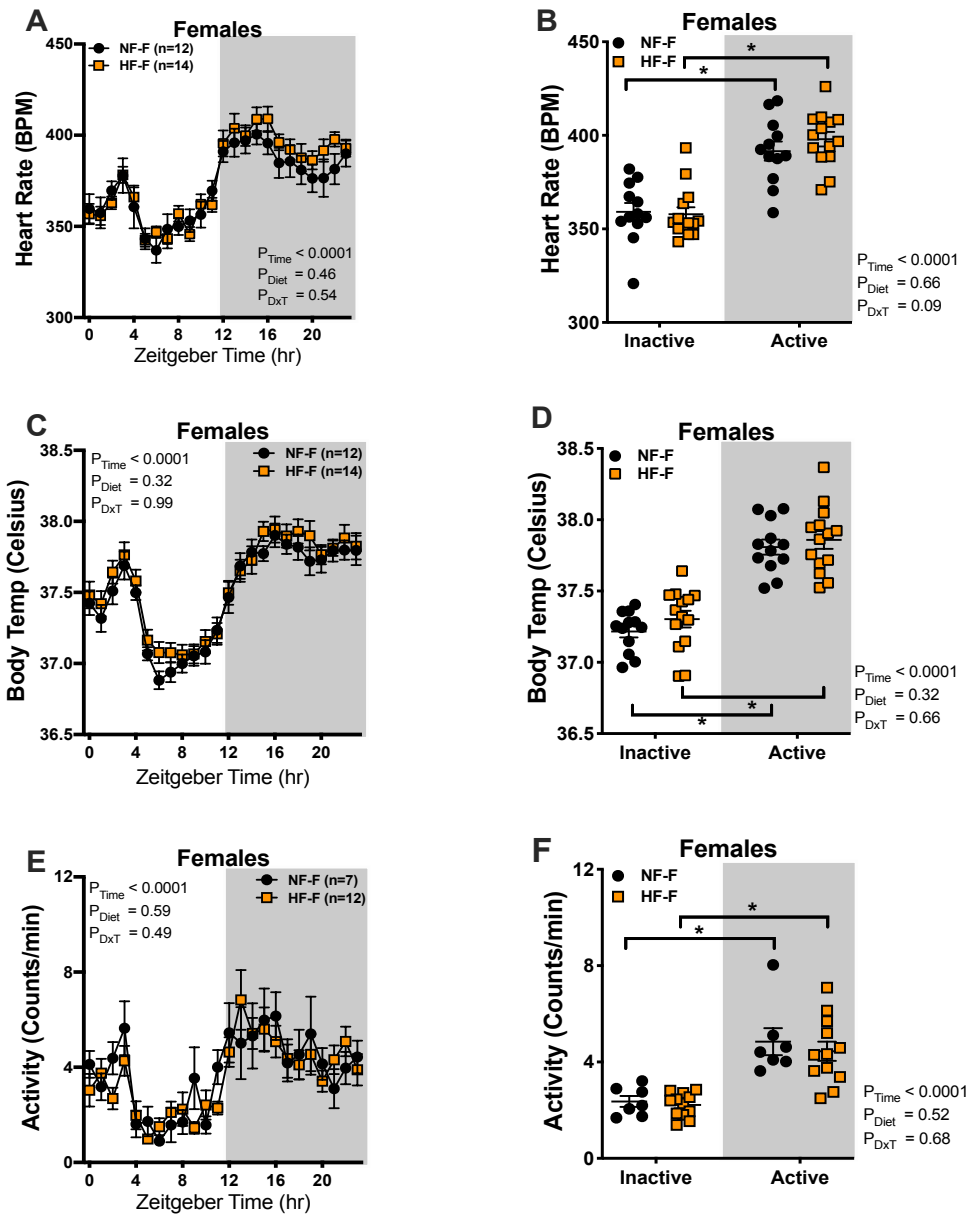

Figure 13: High fat diet had no effect on the diurnal rhythms of heart rate (A, B), body temperature (C, D) and activity (E, F) of female Sprague-Dawley rats. Heart rate, temperature and activity were measured by radiotelemeters after 6 weeks on either NF or HF diet protocol. Data represent 2-day average of continuous 24-hour recordings (A, C and E) and 12-hour averages (B, D and F) in both groups ± SEM. Data were analyzed by repeated measures 2-way ANOVA, *denotes $p < 0.05$ *vs* corresponding inactive period as determined by Sidak's post-hoc test.

Impaired Acute Natriuretic Response during HF Feeding

To determine if HF diet impacts the ability of the kidney to excrete an acute salt load, male and female Sprague-Dawley rats given HF and NF diets, were put in metabolic cages in the last week of the feeding protocol.

Figure 14 shows the diurnal rhythms of urine, sodium and potassium excretions for 2 days before and after salt challenge (Red arrow) in male Sprague-Dawley rats. UV and UNaV showed no effect of diet at baseline in the male group (Figure 14 and 15), while UKV was significantly higher in the HF group driven by higher excretion rates at baseline prior to ZT12 NaCl challenge (Figure 15E). We calculated the absolute change in urine flow rate (ΔUV) as well as urinary sodium (ΔUNaV) and potassium (ΔUKV) after NaCl load at ZT0, relative to the corresponding 12-hour baseline excretion rates. Rats challenged with 900 μEq NaCl at ZT0 excreted nearly half of the salt load in the first 12-hours post-load. There was no significant difference in ΔUV, ΔUNaV or ΔUKV between the HF and NF-treated rats (Figure 14A – 14F).

However, when the salt load was given at ZT12, rats on HF diet excreted significantly less urine compared to NF, with lower ΔUNaV in the first 12-hours post ZT12 salt (Figure 15). Rats on NF diet excreted the majority of their sodium load in the first 12 hours post injection (Figure 15B, 15D). There was no significant difference between the 2 groups in ΔUV or ΔUNaV in the second 12 hours post load (subsequent inactive period), suggesting that males on HF diet are retaining the salt for a longer period than their lean controls. There was no significant difference in ΔUKV between the two groups in response to acute NaCl load (Figure 15E, 15F).

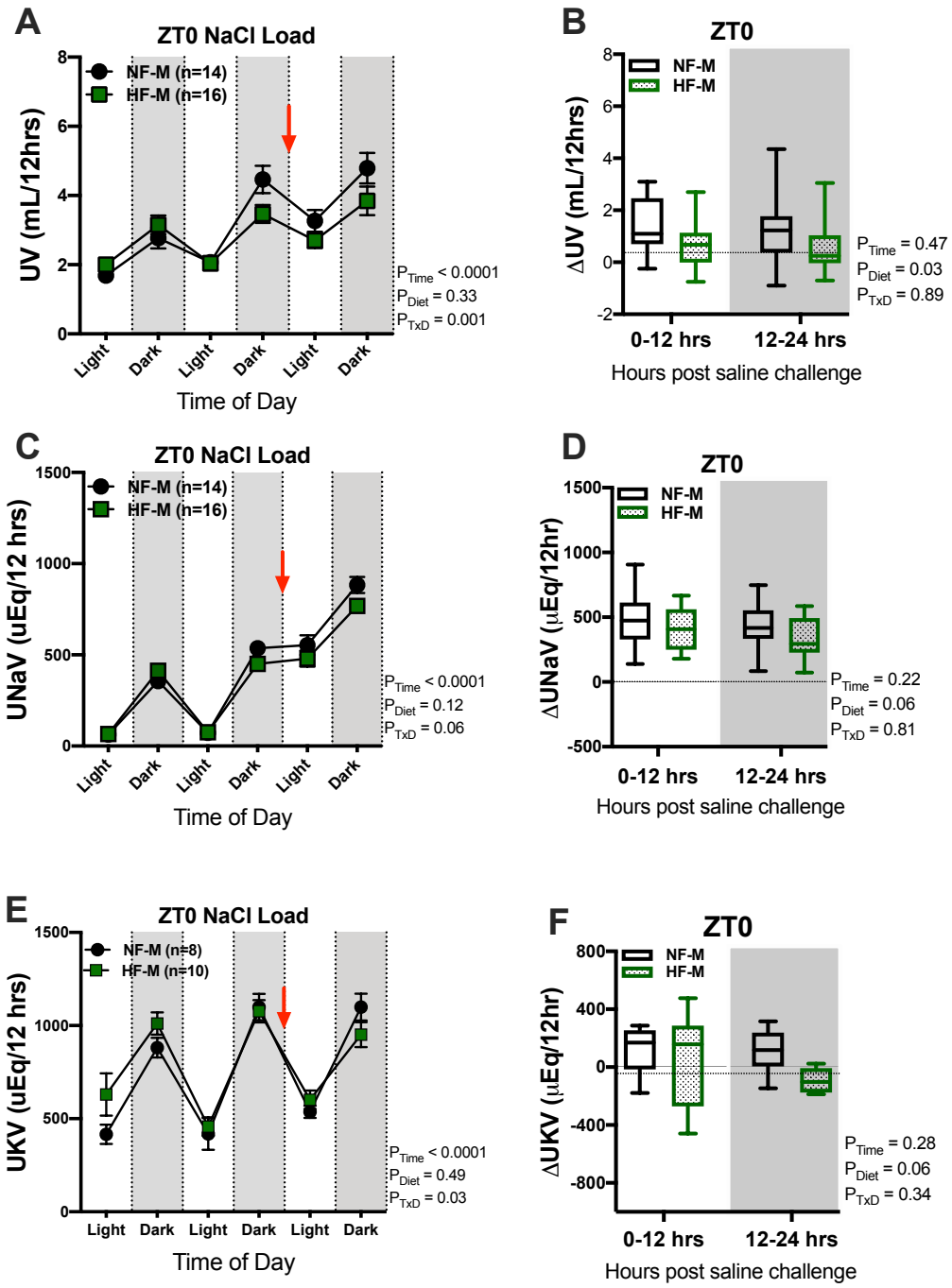

Figure 14: Acute natriuretic response to an i.p. injection of NaCl at ZT0 in male Sprague-Dawley rats on either NF or HF diets. Diurnal rhythms of UV (A), UNaV (B) and UKV (C) and the change (Δ) in UV (B), UNaV (D) and UKV (F) from baseline following acute NaCl load at ZT0. Repeated measures, 2-way ANOVA, and Sidak's post-hoc test. Arrow indicates time of salt load. Arrow indicates time of NaCl injection.

Figure 16 shows data for the 12 hour means for urine, sodium and potassium excretion along with the response to the acute salt-loading challenge in female rats on NF or HF diets. Females on HF diet excreted more amounts of urine, UNaV and UKV at baseline prior to salt challenge, which would appear to be driven by higher water and food intake in this group (Table 2). After ZT0 injection (Red arrow), HF and NF-treated female rats showed a robust increase in UV, UNaV and UKV that was not different between HF and NF groups (Figure 16A, 16C and 16E).

A similar natriuretic response was observed following a ZT12 NaCl load (Figure 17). Both HF and NF rats excreted the majority of their sodium load in the first 12-hours post-load (Figure 16D, 17D) regardless of time of salt challenge. Overall (Figure 16 and 17) there was no effect of HF diet on ΔUV, ΔUNaV or ΔUKV between the 2 groups and HF-treated female rats excreted the load as efficiently as their lean controls.

It is of note that a diurnal rhythm in baseline urine and electrolyte excretion was observed in all groups, with consistently higher levels during the active period.

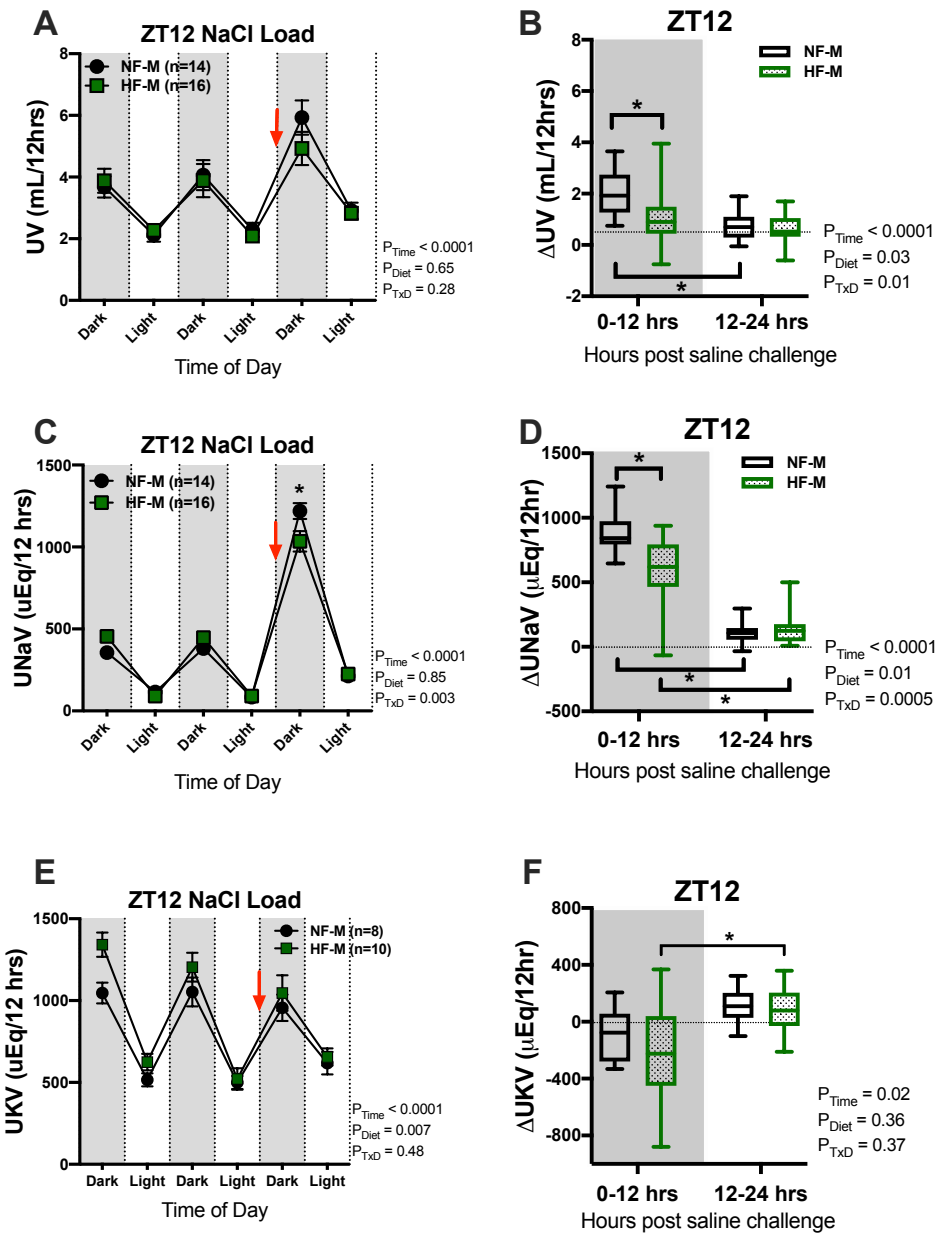

Figure 15: Acute natriuretic response to an i.p. injection of NaCl at ZT12 in male Sprague-Dawley rats on either NF or HF diets. Diurnal rhythms of UV (A), UNaV (B) and UKV (C) and the change (Δ) in UV (B), UNaV (D) and UKV (F) from baseline following acute NaCl load at ZT12. Data were analyzed by repeated measures 2-way ANOVA, *denotes $p < 0.05$ *vs* corresponding NF control or corresponding inactive period as determined by Sidak's post-hoc test. Arrow indicates time of NaCl injection.

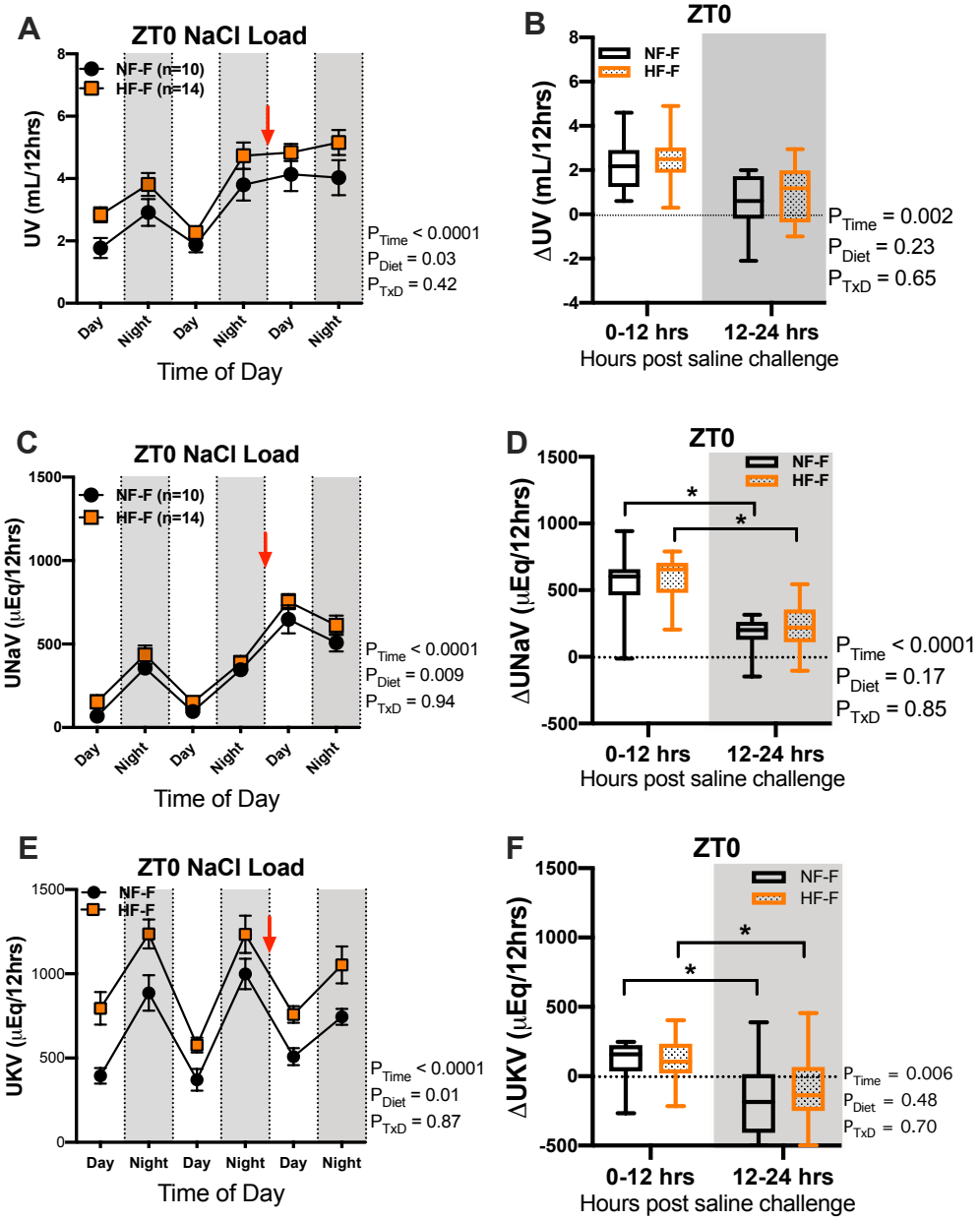

Figure 16: Acute natriuretic response to an i.p. injection of NaCl at ZT0 in female Sprague-Dawley rats on either NF or HF diet. Diurnal rhythms of UV (A), UNaV (B) and UKV (C) and the change (Δ) in UV (B), UNaV (D) and UKV (F) from baseline following acute NaCl load at ZT0. Data were analyzed by repeated measures 2-way ANOVA, * denotes $p < 0.05$ *vs* corresponding inactive period as determined by Sidak's post-hoc test. Arrow indicates time of NaCl injection.

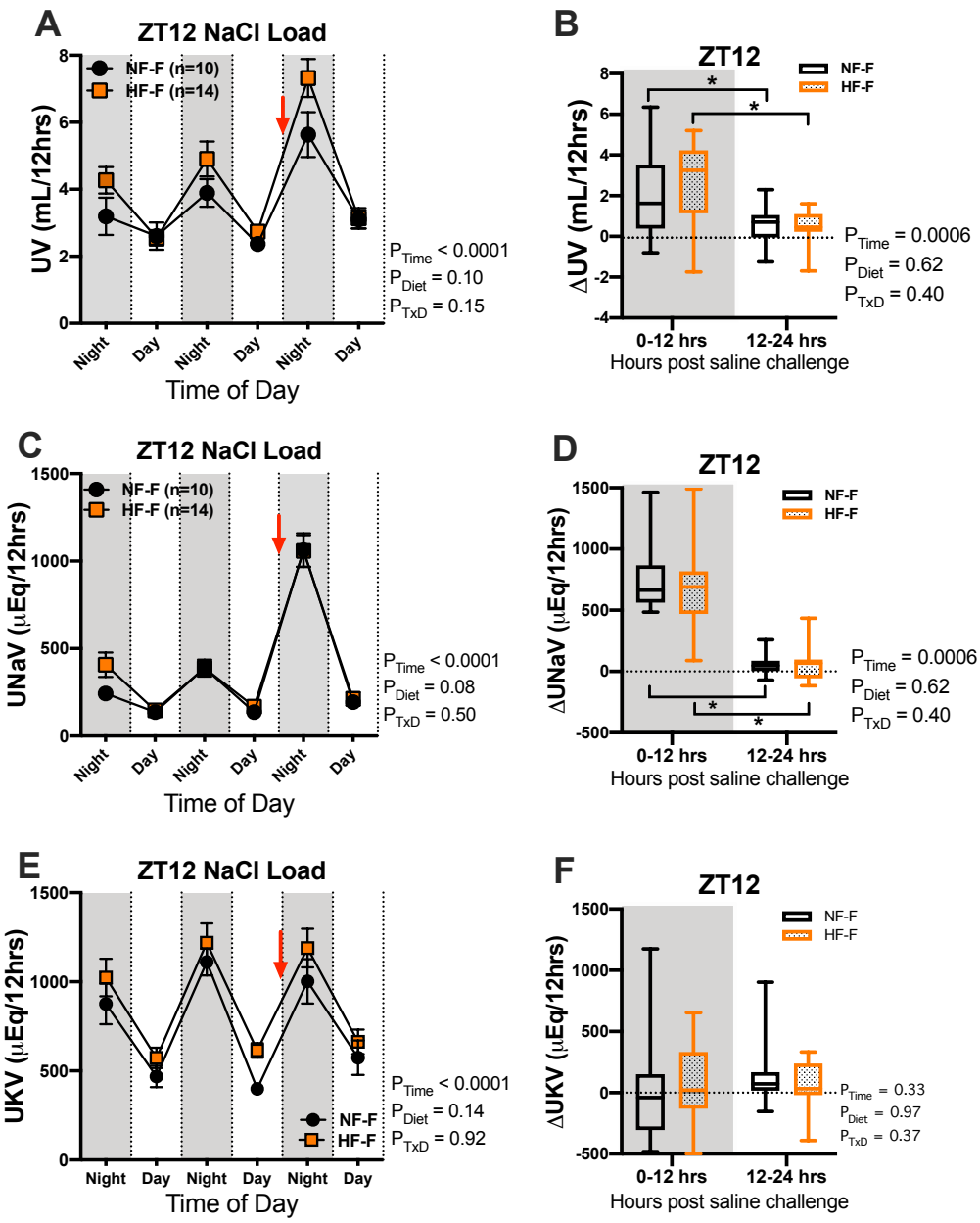

Figure 17: Acute natriuretic response to an i.p. injection of NaCl at ZT12 in female Sprague-Dawley rats on either NF or HF diets. Diurnal rhythms of UV (A), UNaV (B) and UKV (C) and the change (Δ) in UV (B), UNaV (D) and UKV (F) from baseline following acute NaCl load at ZT12. Data were analyzed by repeated measures 2-way ANOVA, * denotes $p < 0.05$ *vs* corresponding inactive period as determined by Sidak's post-hoc test. Arrow indicates time of NaCl injection.

High-fat Diet Impairs the Renal Endothelin System

Endothelin-1 produced within the kidney is an important natriuretic peptide and contributes to the renal response to high salt intake (181). Since urine ET-1 reflects intrarenal production, we measured urinary ET-1 excretion to assess the effect of HF diet on the renal endothelin system. HF and NF-fed male rats expressed a diurnal rhythm of ET-1 excretion, with higher levels during the active period (Figure 18) coinciding with higher food intake and subsequently higher salt intake. However, male rats on HF diet

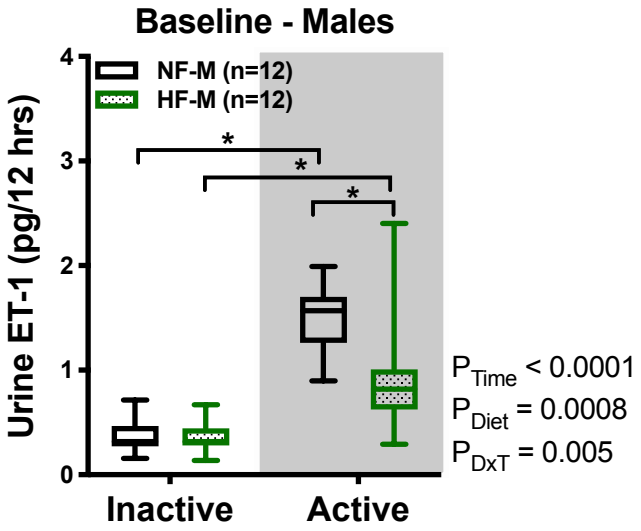

Figure 18: High fat diet impairs active period urine ET-1 excretion in male Sprague-Dawley rats. ET-1 was measured in urine samples collected at either ZT0 or ZT12 from rats fed either NF or HF diets. Data were analyzed by repeated measures 2-way ANOVA, *denotes $p < 0.05$ *vs* NF control or corresponding inactive period as determined by Sidak's post-hoc test.

excreted an average of 0.9 ± 0.2 pg during the active period, which was significantly lower than the average excretion in lean rats of 1.5 ± 0.1 pg during the same time period (p = 0.0008). ET-1 excretion during the inactive period was not significantly different between the two diet groups.

Following an acute NaCl load at ZT0, male rats on both NF and HF diet had similar ET-1 excretion rates as during baseline and were not significantly different between diets (Figure 19A). During the subsequent 12-24 hrs after the ZT0 salt load, rats on HF diet, again showed a significantly lower ET-1 excretion compared to NF during the active period (Figure 19A). When NaCl was given at ZT12, the impairment in ET-1 excretion in rats on HF diet was again significant during the first 12 hours post-load, with a return to similar lower values at 12-24 hours post-load (Figure 19B). These data show impaired renal ET-1 excretion in rats on HF diet that is limited to the active period when the renal ET-1 system is most active.

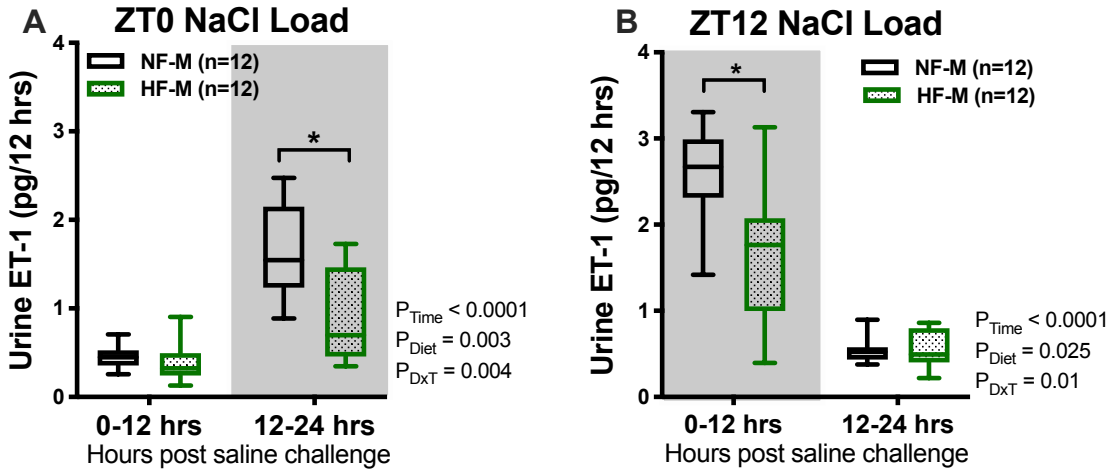

Figure 19: Male Sprague-Dawley rats on HF diet have impaired active time urine ET-1 excretion following acute NaCl load at either ZT0 (A) or ZT12 (B). Data were analyzed by repeated measures 2-way ANOVA, *denotes $p < 0.05$ *vs* corresponding NF control as determined by Sidak's post-hoc test.

We performed a similar analysis of urinary ET-1 excretion in females on HF and NF diet. Similar to male rats, we observed a significant diurnal rhythm in ET-1 excretion regardless of the type of diet (Figure 20). ET-1 excretion during the active period was 1.0 ± 0.1 pg and 1.2 ± 0.1 pg for each group respectively (*p= 0.29*). There was a tendency for ET-1 excretion to be lower in the HF group during the active period as indicated by the significant interaction between time of day and diet (*p= 0.049*) although post hoc comparisons of individual means did not reveal a significant difference.

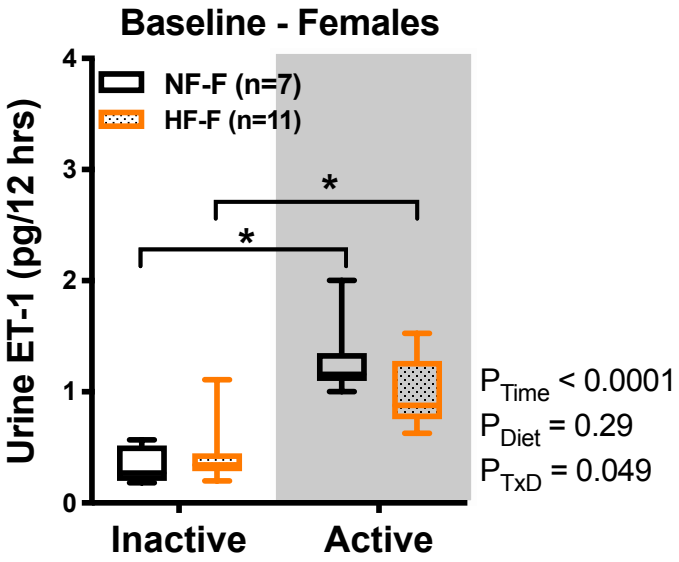

Figure 20: Urine ET-1 excretion rates in female Sprague-Dawley rats on NF or HF diet. ET-1 was measured in urine samples collected at either ZT0 or ZT12 from rats fed either NF or HF diets. Data were analyzed by repeated measures 2-way ANOVA, *denotes $p < 0.05$ *vs* corresponding inactive period as determined by Sidak's post-hoc test.

Following NaCl challenge at ZT0, ET-1 excretion was similar between diet groups during both the first and second 12 hours post-load (Figure 21A). ET-1 excretion in the first 12 hours after ZT0 load was significantly higher in the HF group, compared to the corresponding light period baseline. However, it did not reach statistical significance in the NF group. Likewise, ET-1 excretion after the ZT12 salt challenge was not significantly different between diet groups (Figure 21B). However, ET-1 excretion showed no significant increase from baseline in both groups.

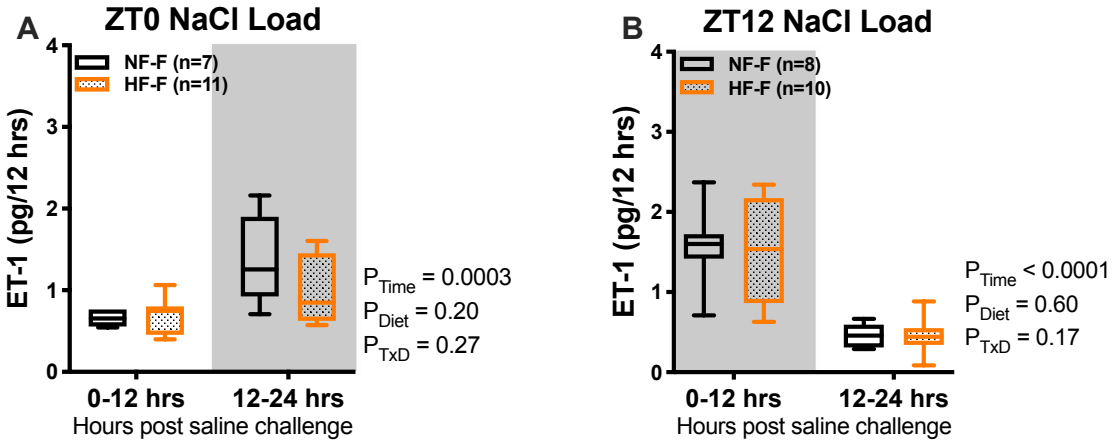

Figure 21: Urine ET-1 excretion rates following acute NaCl i.p injection at either ZT0 (A) or ZT12 (B) in female Sprague-Dawley rats. Data were analyzed by repeated measures 2-way ANOVA and Sidak's post-hoc test.

Aim 2: TO TEST THE HYPOTHESIS THAT DIET-INDUCED OBESITY IMPAIRS ET-1 AND ET_B RECEPTOR EXPRESSION AND ACTIVITY, LEADING TO DIMINISHED RENAL CAPACITY TO MAINTAIN DIURNAL RHYTHMS IN NATRIURESIS.

To assess whether the reduced ET-1 excretion might be due to decreased production or perhaps increased clearance through the ET_B receptor, we measured mRNA expression of ET-1 gene and its receptors (ET_A and ET_B) in kidney tissues collected at either ZT0 or ZT12 for both NF and HF groups.

ET-1 gene expression in the renal cortex and outer medulla was significantly lower in HF-treated animals compared to their lean controls (Figure 22A, 22B), which was evident in tissues collected at the beginning of the active period (ZT12). However, ET-1 mRNA expression in the inner medulla was not significantly different between the NF and HF groups (Figure 22C).

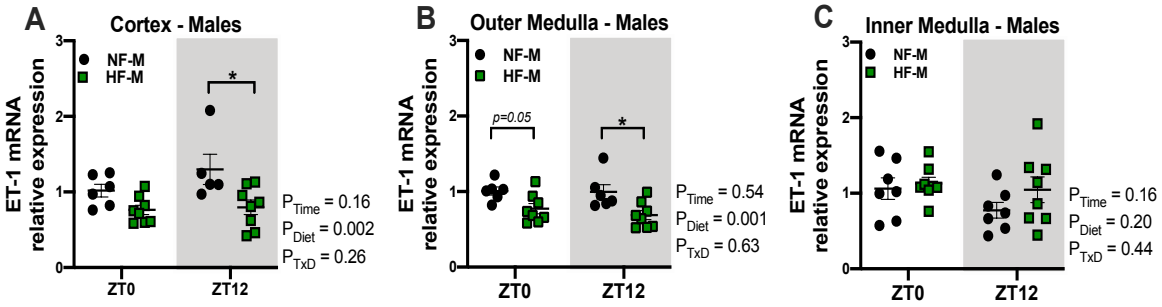

Figure 22: ET-1 mRNA expression in the renal cortex (A), outer medulla (B) and inner medulla (C) of male rats fed either HF or NF diet. mRNA expression was normalized to β-actin and relative to NF group at ZT0. Data were analyzed by 2-way ANOVA, * denotes $p < 0.05$ *vs* corresponding NF control as determined by Sidak's post-hoc test.

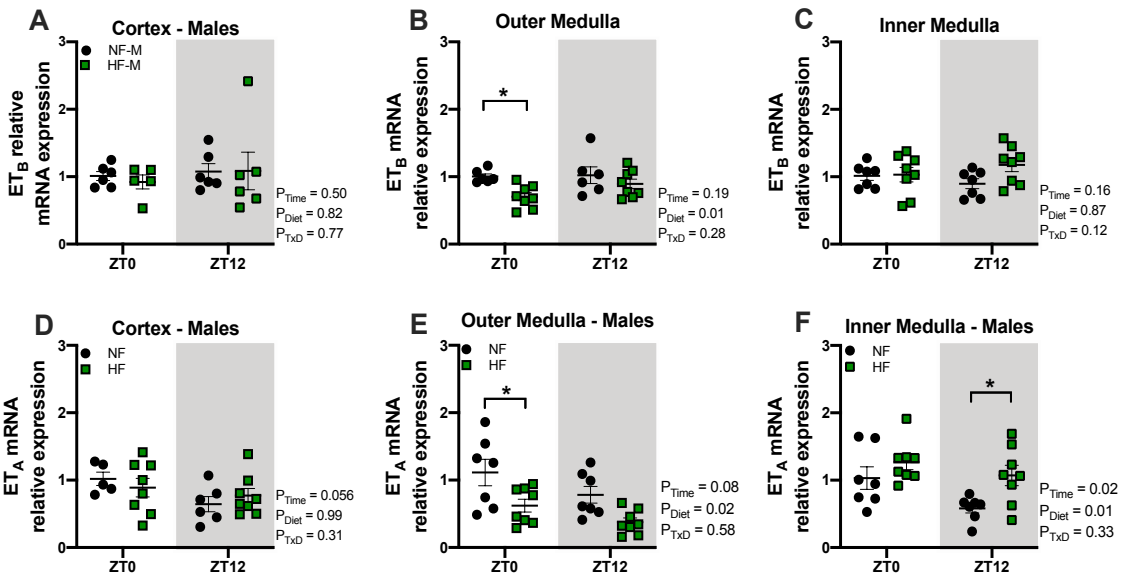

Figure 23: ET_B and ET_A receptors mRNA expression in the renal cortex (A, D), outer medulla (B, E) and inner medulla (C, F) of male Sprague-Dawley rats fed either HF or NF diet. mRNA expression was normalized to β-actin and relative to NF group at ZT0. Data were analyzed by 2-way ANOVA, *denotes $p< 0.05$ *vs* corresponding NF control as determined by Sidak's post-hoc test.

ET_B receptor expression in the cortex and inner medulla was not significantly different between the two diet groups at ZT0 and ZT12 (Figure 23A, 23C). However, ET_B mRNA relative expression was lower in the outer medulla of male rats on HF diet, particularly in tissues collected at the beginning of the inactive period, ZT0 (Figure 23B). ET_A receptor expression in the cortex showed no difference between HF and NF male rats (Figure 23D). Relative ET_A expression was lower in HF outer medullas and higher in their inner medulla compared to NF rats (Figure 23E, 23F). Our data showed that ET-1, ET_A and ET_B genes expression in different parts of the kidney was not significantly different

between ZT0 and ZT12 in either NF or HF groups (Figure 22 and 23), with the exception of ET_A expression in the inner medulla (Figure 23F).

Kidneys collected from female rats did not show any differences in ET-1, ET_A and ET_B mRNA expression in kidney samples collected at ZT0 compared to ZT12, with few exceptions (Figure 24 and 25). Furthermore, there was no significant effect of HF diet on ET-1 mRNA relative expression, in all parts of the kidney from female rats (Figure 24). ET_B receptor expression was also similar between females on NF and HF in the cortex and outer medulla (Figure 25A, 25B). However, tissues collected from the inner medulla showed an overall lower relative ET_B mRNA expression in the HF group (Figure 25C). ET_A receptors showed similar pattern of expression as the ET_B receptor, with lower expression levels only in the inner medulla of females under HF diet (Figure 25F).

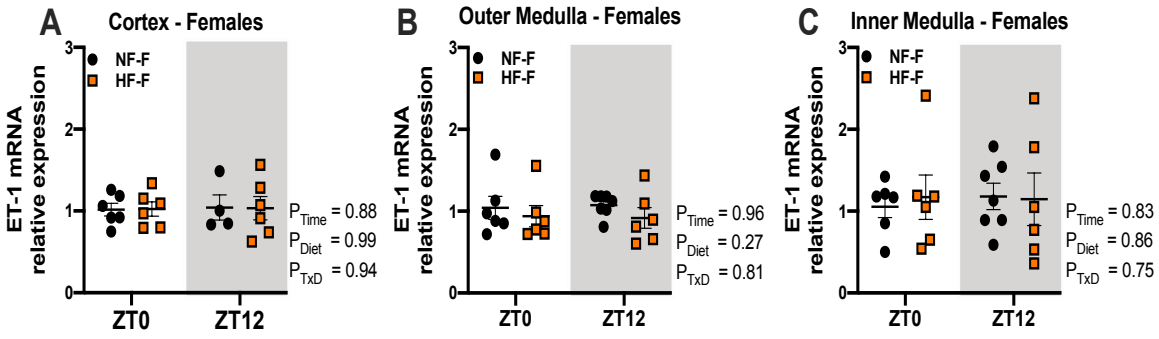

Figure 24: ET-1 mRNA expression in the renal cortex (A), outer medulla (B) and inner medulla (C) of female rats fed either HF or NF diet. mRNA expression was normalized to β-actin and relative to NF group at ZT0. Data were analyzed by 2-way ANOVA and Sidak's post-hoc test.

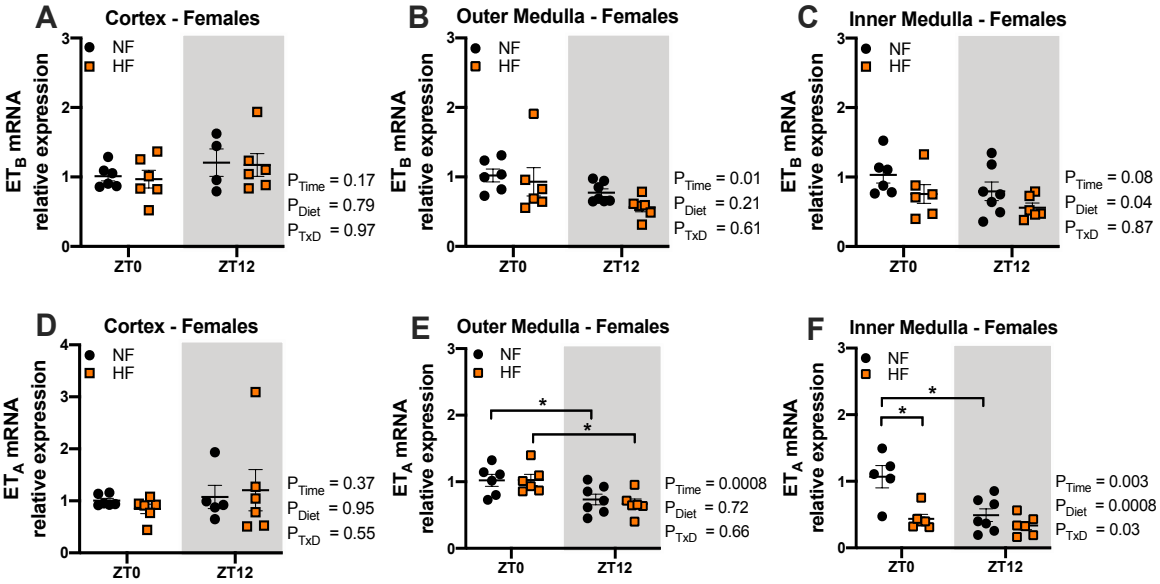

Figure 25: ET_B and ET_A receptors mRNA expression in the renal cortex (A, D), outer medulla (B, E) and inner medulla (C, F) of female rats fed either HF or NF diet. mRNA expression was normalized to β-actin and relative to NF group at ZT0. Data were analyzed by 2-way ANOVA, * denotes $p < 0.05$ vs corresponding NF control or corresponding inactive period as determined by Sidak's post-hoc test.

Diet-induced Obesity Promotes Aldosterone Excretion

Aldosterone production and activity is typically increased in obesity and is thought to be a major contributing factor in the pathophysiology of hypertension (109). Therefore, we measured aldosterone in the urine both at baseline and after acute sodium loading. At baseline, aldosterone exhibited diurnal rhythm of excretion ($P_{Time} = 0.05$, Figure 26A), despite not being statistically significant at certain time points. Males on HF diet tended to have higher aldosterone excretion compared to NF but was not statistically significant ($P_{Diet} = 0.07$; Figure 26A). Following an acute salt load at ZT0, aldosterone excretion was significantly higher in male Sprague-Dawley rats on HF diet compared NF (Figure 26B). This was also observed following ZT12 salt challenge (Figure 26C). Since both baseline and post-challenge urine samples were collected from the same rats, we assessed the ability of acute salt challenge to suppress urinary aldosterone excretion. We found that the higher post-load urinary aldosterone in the HF group at ZT0 (Figure 26B) was mainly driven by a failure of the obese males to suppress their post-load aldosterone in response to NaCl injection ($p= 0.12$, *repeated measures 2-way ANOVA)* in the first 12 hours compared to baseline aldosterone, while the NF group had a normal physiological response to NaCl injection ($p= 0.0005$, *repeated measures 2-way ANOVA*) versus corresponding inactive period baseline.

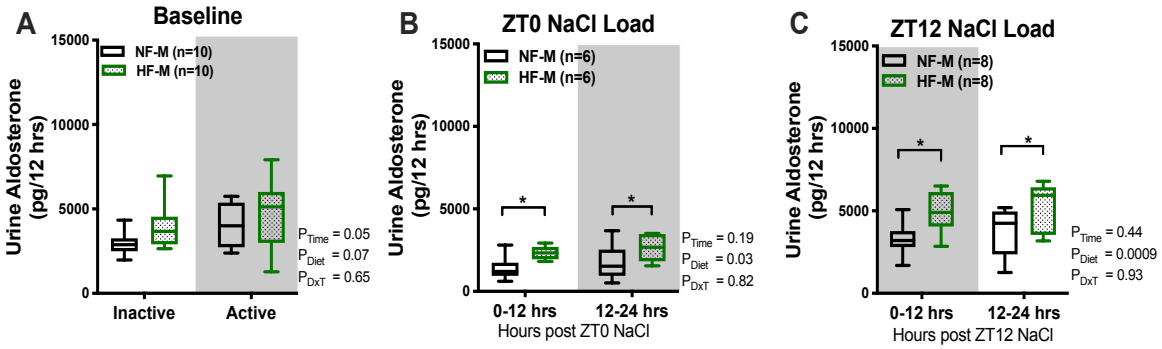

Figure 26: Urine aldosterone excretion was inappropriately elevated in male Sprague-Dawley rats under HF diet either at baseline (A), or after NaCl load at ZT0 (B) and ZT12 (C). Aldosterone was measured in urine samples collected at either ZT0 or ZT12 from rats fed either NF or HF diets. Data were analyzed by repeated measures 2-way ANOVA, * denotes $p < 0.05$ *vs* corresponding NF control as determined by Sidak's post-hoc test.

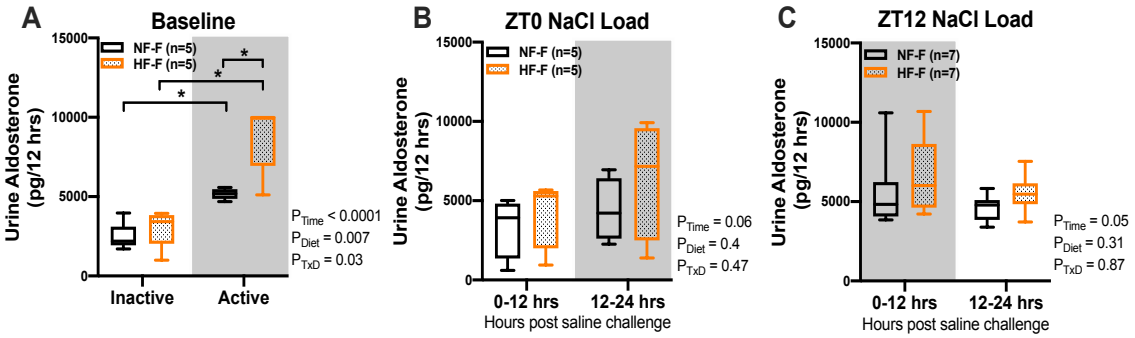

Figure 27: Urine aldosterone excretion was inappropriately elevated in female Sprague-Dawley rats under HF diet at baseline (A), with no significant difference between groups after NaCl load at ZT0 (B) and ZT12 (C). Aldosterone was measured in urine samples collected at either ZT0 or ZT12 from rats fed either NF or HF diets. Data were analyzed by repeated measures 2-way ANOVA, * denotes $p < 0.05$ *vs* corresponding NF control or corresponding inactive period as determined by Sidak's post-hoc test.

Both HF and NF females showed a diurnal rhythm in baseline urine aldosterone, with higher excretion rates during the active period in both groups. Female rats on HF diet had significantly higher aldosterone excretion compared to the NF control group (Figure 27A). Post-hoc analysis revealed this was primarily due to the higher active period excretion (p= 0.04, vs NF). Following the acute salt load at either ZT0 or ZT12, aldosterone excretion in the HF group was similar to lean controls (Figure 27B, 27C).

We also measured aldosterone levels in the plasma of male and female rats at ZT0 or ZT12. We observed an overall significant effect of HF diet to increase plasma aldosterone in male rats, that was consistent between the two times of day. However, the diet effect in female rats was not significant, yet there was a significant interaction with time of day due to the higher plasma aldosterone at ZT0 in female rats on HF diet compared to their corresponding NF controls (Figure 28).

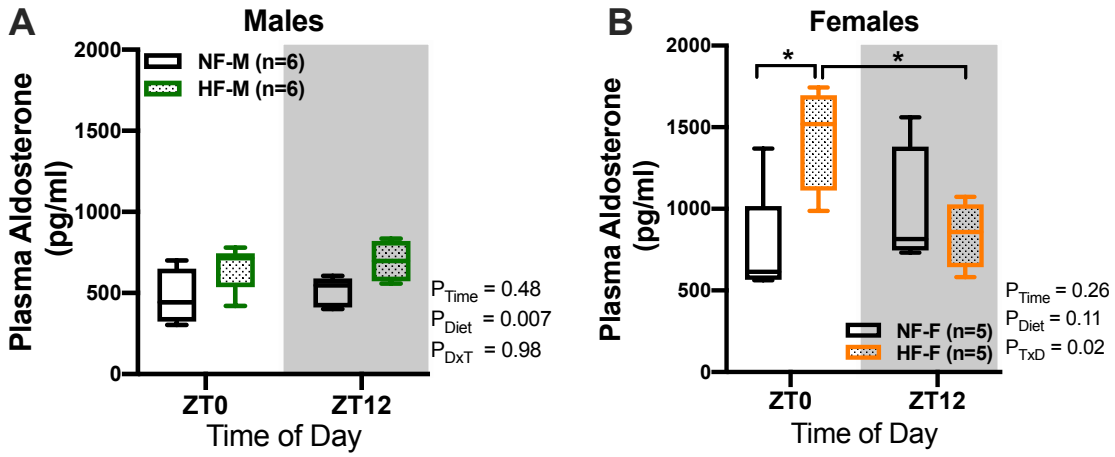

Figure 28: Plasma aldosterone concentration in male (A) and female (B) Sprague-Dawley rats, euthanized at either ZT0 or ZT12 after 8 weeks of NF and HF diets. Data were analyzed by 2-way ANOVA, *denotes $p < 0.05$ *vs* corresponding NF control as determined by Sidak's post-hoc test.

AIM 3: TO TEST THE HYPOTHESIS THAT DIET-INDUCED OBESITY LEADS TO THE DEVELOPMENT OF SALT SENSITIVITY THAT IS ASSOCIATED WITH ENDOTHELIN-1 DYSFUNCTION IN THE KIDNEY.

High Salt Diet Promotes Salt Sensitivity in HF-treated Rats.

In a separate cohort, high salt (4% NaCl) was added to the diets of male and female rats fed either NF or HF diet at the beginning of week 7 of the feeding protocol and for 2 weeks. In males and females, the addition of HS to the diets, had no significant effect on food intake in either NF or HF groups. Further, these rats all had similar diurnal patterns of food intake (Table 2). Water intake significantly increased with HS diet in both NF and HF groups.

HS diet led to a further increase in MAP in males on HF, but not NF diet (Figure 29A, 29D). A trend towards higher SBP and DBP was observed in the HF group (Figure 29B, 29C), yet not reaching statistical significance. NF males maintained their MAP, SBP and DBP values and rhythms with no apparent salt sensitivity (Figure 29D – 29F). The addition of salt to the diets of female rats had no significant effect on blood pressure parameters in either NF or HF groups (Figure 30). None of the dietary interventions had a significant effect on HR, body temperature, or locomotor activity in either males or female rats (Figure 31 and 32). These data show that the effect of HS diet to increase blood pressure is limited to male rats on HF diet.

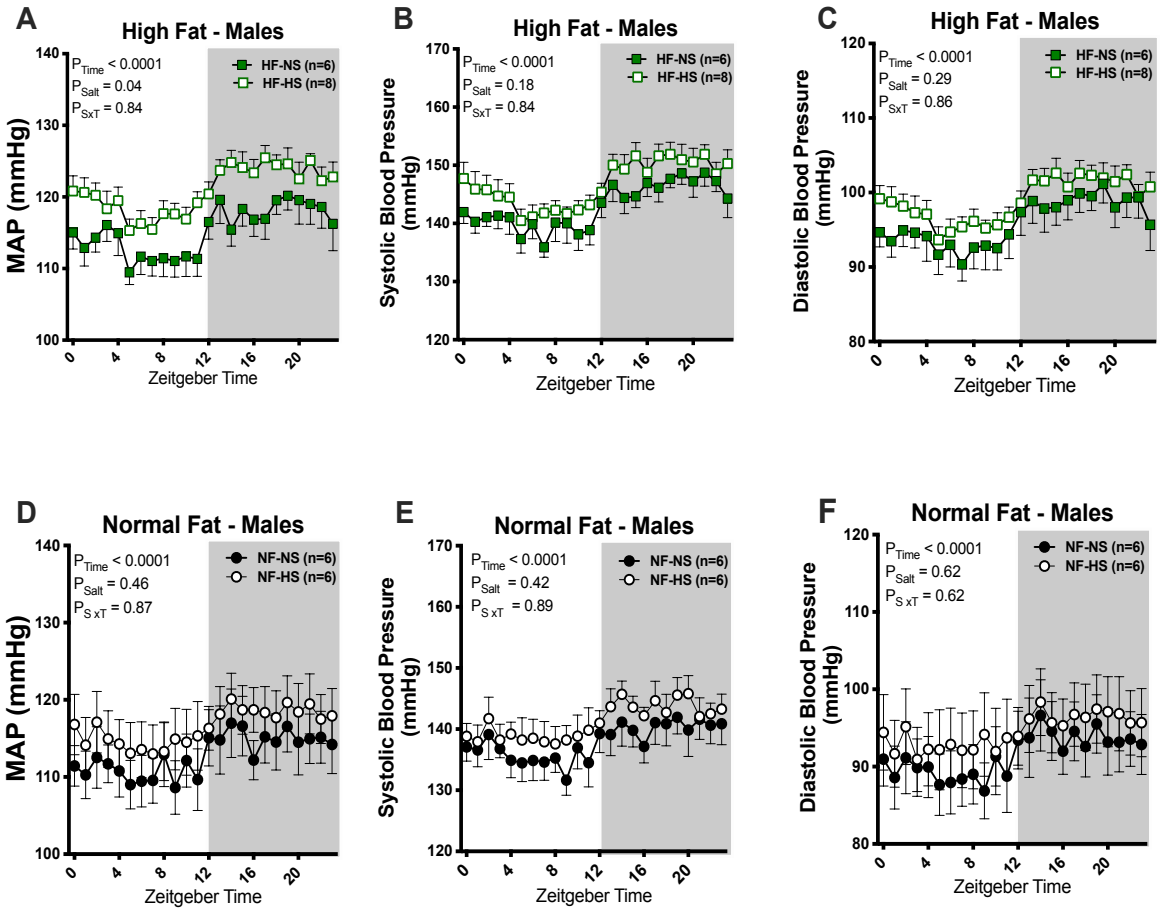

Figure 29: Chronic HS diet increased MAP (A, D), but not SBP (B, E) and DBP (C, F) of male Sprague-Dawley rats under HF. Blood pressure was measured by radiotelemeters after 2 weeks on either NS or HS diets that supplemented the original NF and HF dietary protocol. Data represent 2-day average of 24-hour recordings in both groups ± SEM. Repeated measures, 2-way ANOVA.

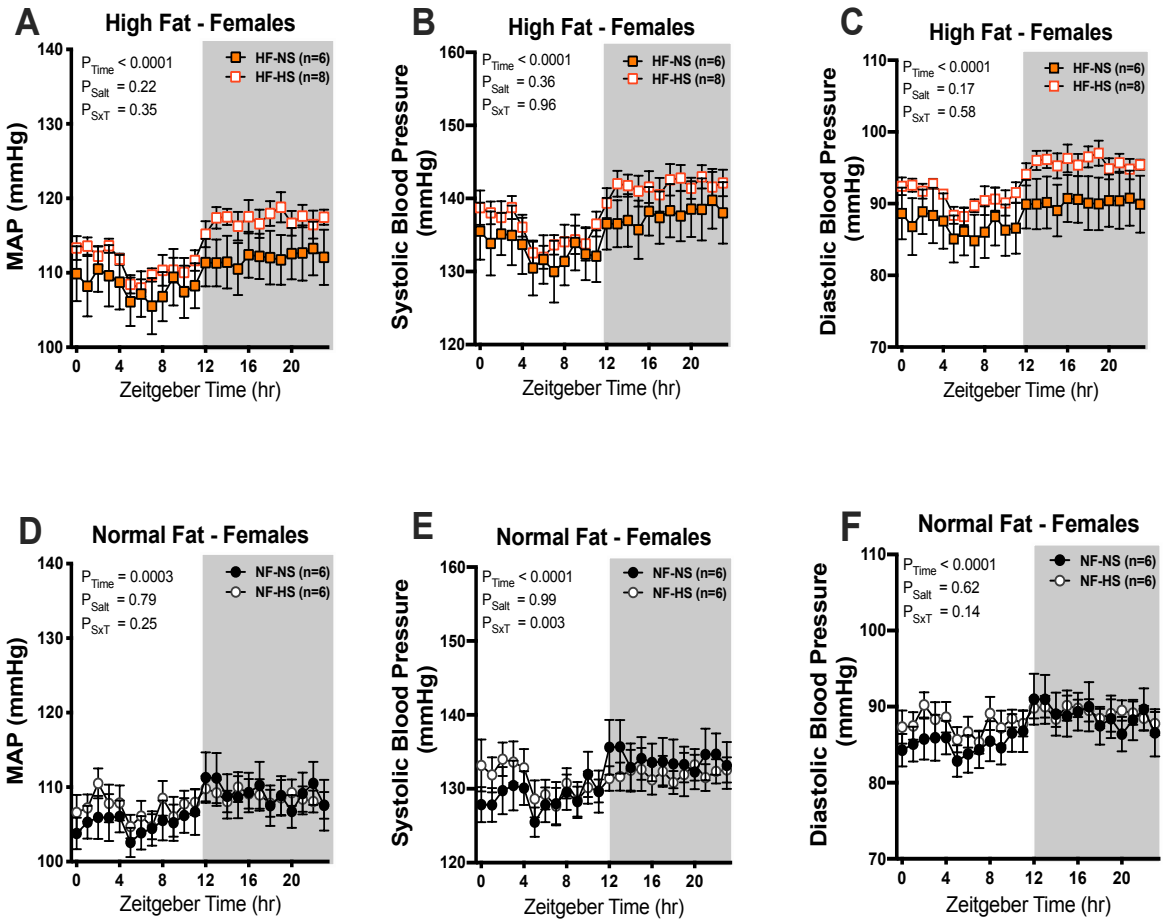

Figure 30: Chronic HS diet had no significant effect on MAP (A, D), SBP (B, E) and DBP (C, F) of female Sprague-Dawley rats under either HF or NF diet. Blood pressure was measured by radiotelemeters after 2 weeks on either NS or HS diets that supplemented the original NF and HF dietary protocol. Data represent 2-day average of 24-hour recordings in both groups ± SEM. Repeated measures, 2-way ANOVA.

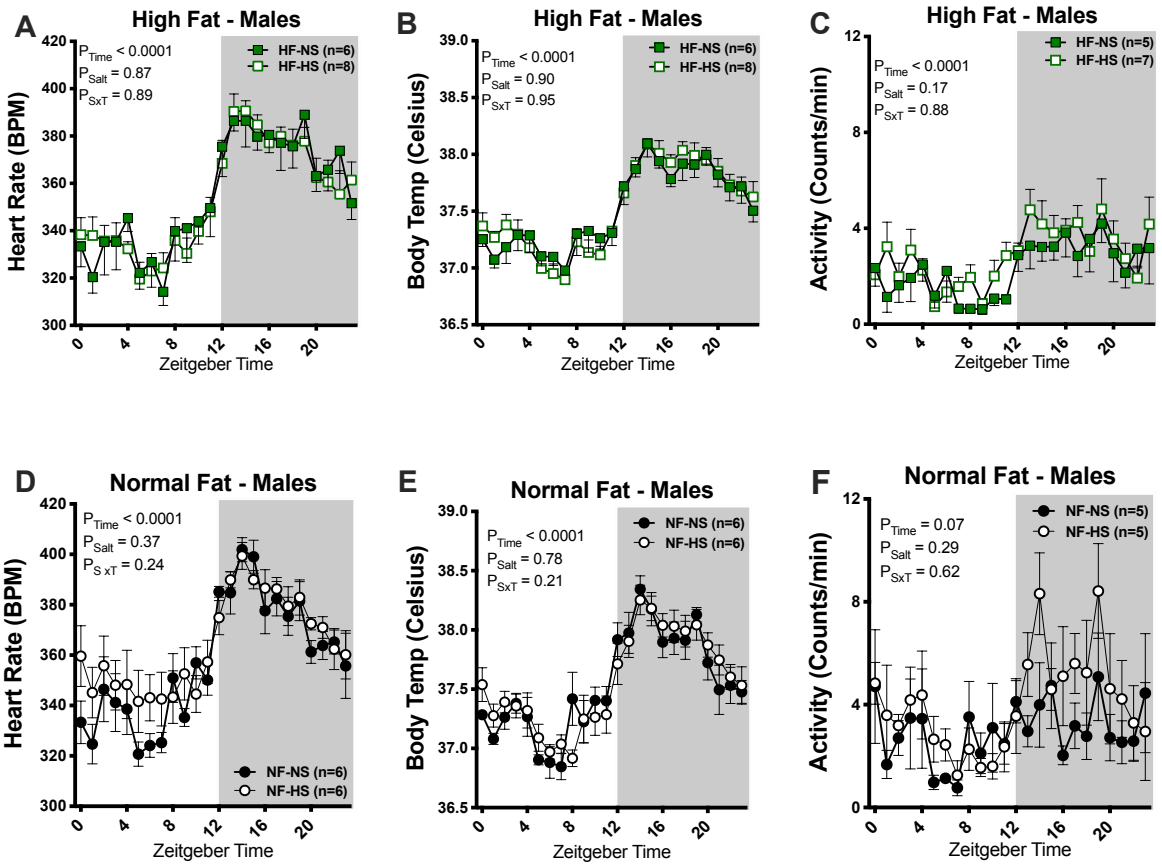

Figure 31: Chronic HS diet had no effect on heart rate (A, D), body temperature (B, E) and activity (C, F) of male Sprague-Dawley rats under either HF or NF diet. Heart rate, body temperature and activity were measured by radiotelemeters after 2 weeks on either NS or HS diets that supplemented the original NF and HF dietary protocol. Data represent 2-day average of 24-hour recordings in both groups ± SEM Repeated measures, 2-way ANOVA.

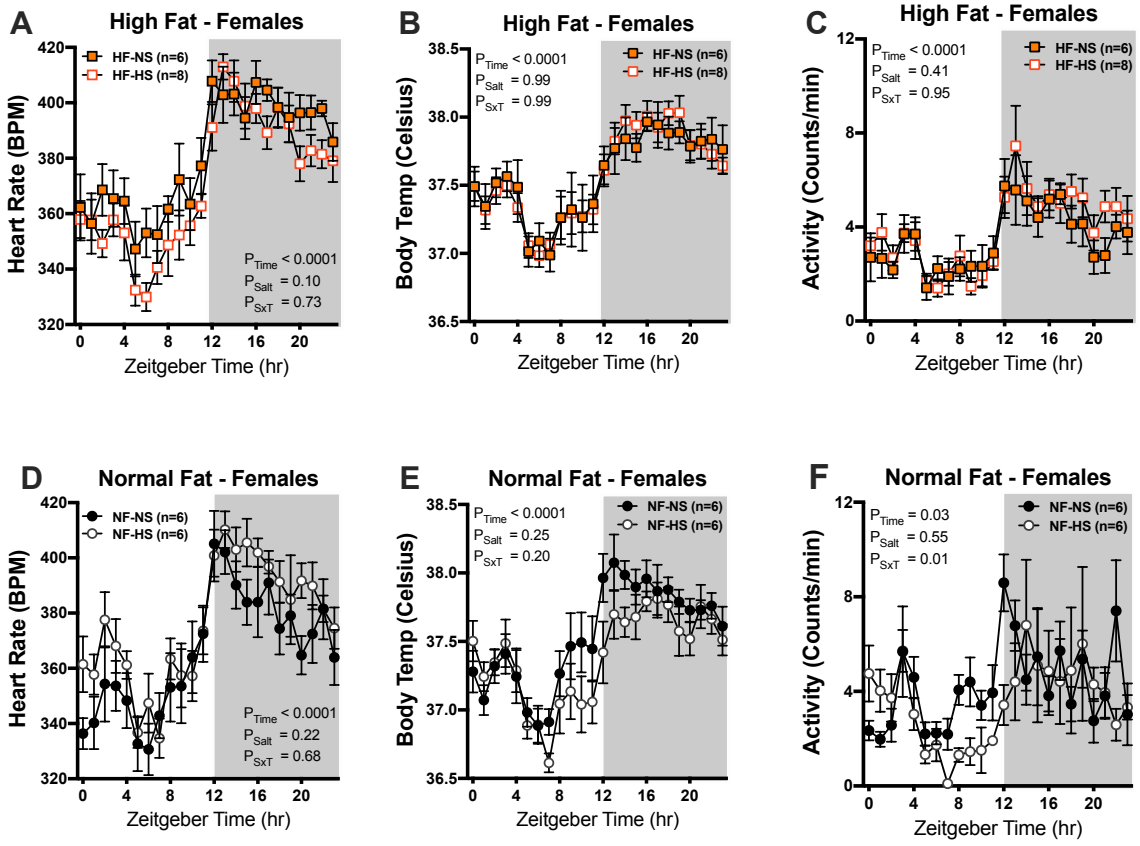

Figure 32: Chronic HS diet had no significant effect on heart rate (A, D), body temperature (B, E) and activity (C, F) of female Sprague-Dawley rats under either HF or NF diet. Heart rate, body temperature and activity were measured by radiotelemeters after 2 weeks on either NS or HS diets that supplemented the original NF and HF dietary protocol. Data represent 2-day average of 24-hour recordings in both groups ± SEM. Repeated measures, 2-way ANOVA.

High Fat Impairs Renal ET-1 Response to High Salt Diet.

Studies showed that renal ET-1 excretion is increased with high salt intake (153). Therefore, we measured urine ET-1 excretion after 2 weeks of HS diet in all groups. HS diet led to significant increase in active period ET-1 excretion in both NF/HS and HF/HS groups compared to their NS controls (Figure 33). However, HS-induced ET-1 excretion was significantly lower in the HF group compared to the NF group (Figure 33B). Similar response was observed in female rats during the active period (Figure 34). While there was no effect of HS on ET-1 excretion during the inactive period in male rats (Figure 33A), females on both NF and HF diets showed increased inactive-period ET-1 with HS (Figure 34A).

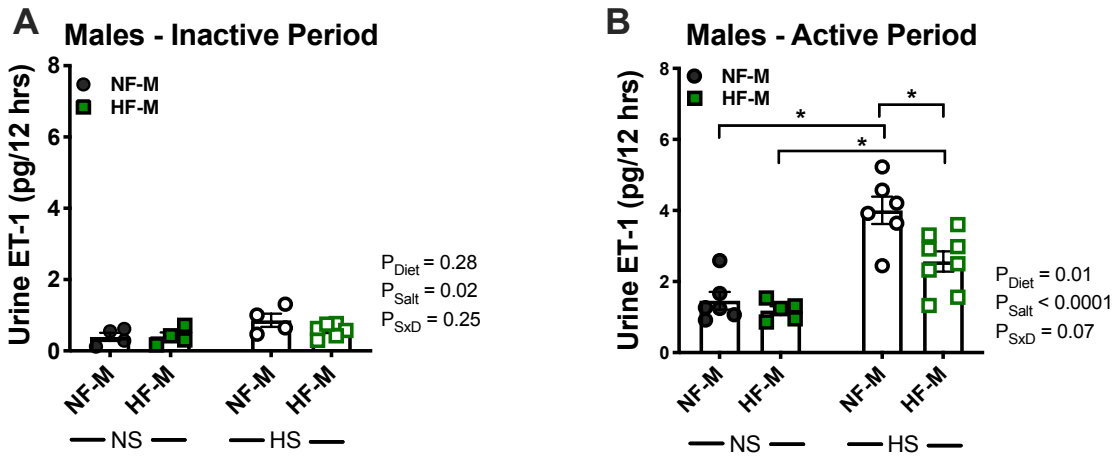

Figure 33: Male Sprague-Dawley rats on HF diet have attenuated active period ET-1 excretion after 2 weeks of HS diet. Data shown represent both inactive (A) and active period excretion rates (B). ET-1 was measured in urine samples collected at either ZT0 or ZT12. Data shown as means ± SEM and were analyzed by 2-way ANOVA, * denotes $p < 0.05$ *vs* corresponding NS control or corresponding NF as determined by Sidak's post-hoc test.

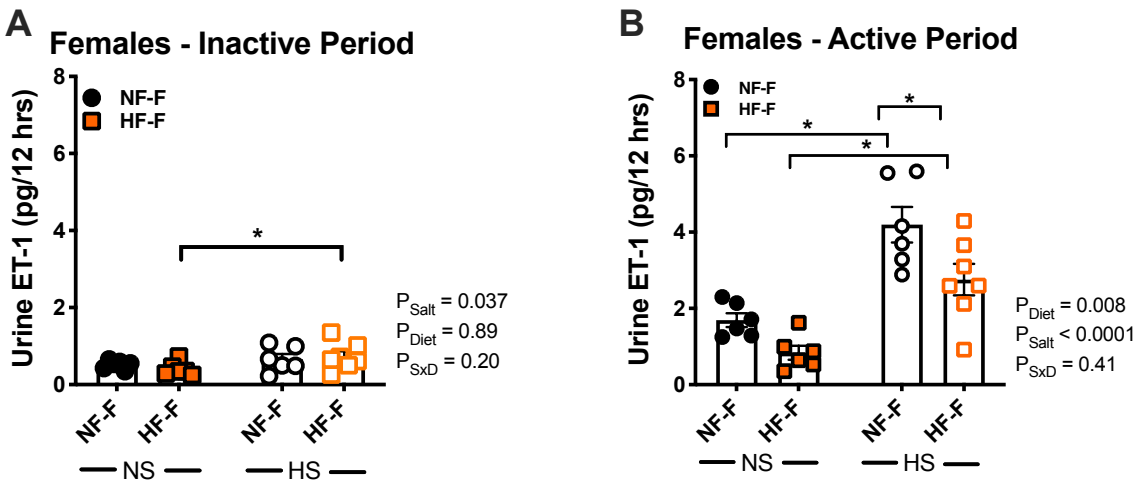

Figure 34: Female Sprague-Dawley rats on HF diet have attenuated active period ET-1 excretion after 2 weeks of HS diet. Data shown represent both inactive (A) and active period excretion rates (B). ET-1 was measured in urine samples collected at either ZT0 or ZT12. Data shown as means ± SEM and were analyzed by 2-way ANOVA, * *denotes* $p < 0.05$ *vs* corresponding NS control or corresponding NF as determined by Sidak's post-hoc test.

AIM 4: TO TEST THE HYPOTHESIS THAT SEX DIFFERENCES IN RENAL SODIUM HANDLING WILL LEAD TO A DIMORPHIC PATTERN IN THE DIURNAL RESPONSE TO PHARMACOLOGICAL INTERVENTION WITH BENZAMIL.

Natriuretic Response to ENaC Blockade is Independent of Time.

First, male and female rats were each divided into two groups, one group was given benzamil (1 mg/kg) and the second was administered an equal volume of vehicle (0.9%

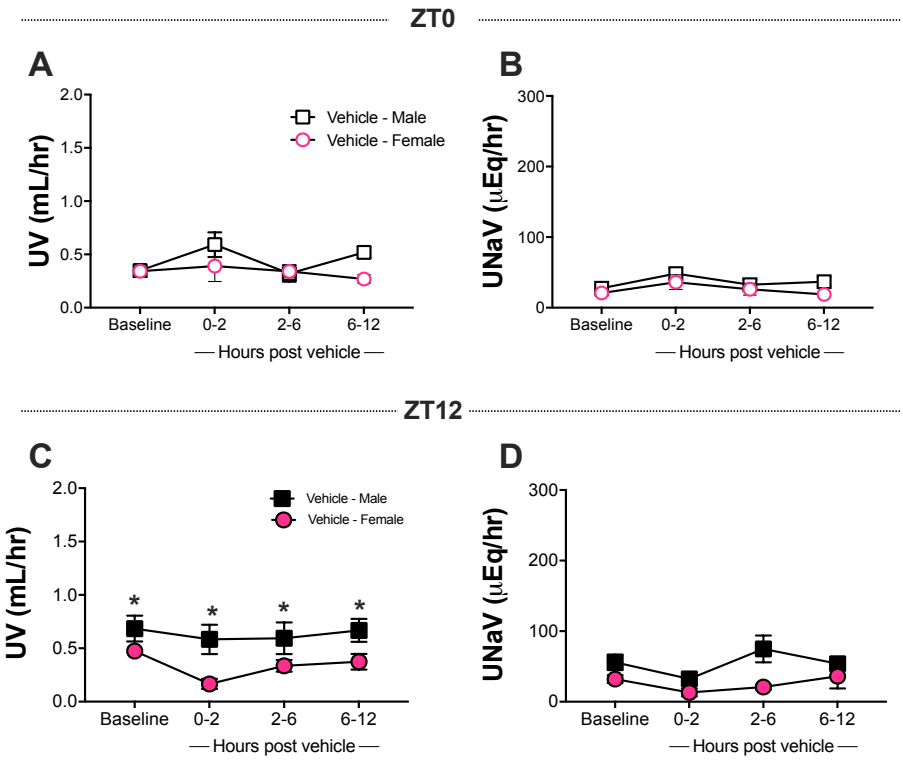

Figure 35: Vehicle injection had no effect on urine flow rate (UV) and urinary sodium excretion (UNaV) as compared with baseline at both Zeitgeber time 0 (ZT0; A and B) and at ZT12 (C and D) in male and female Sprague-Dawley rats. Data shown as means ± SE, repeated-measures 2-way ANOVA, with Sidak's post-hoc test, n = 4–6.

NaCl, 1 ml/kg) to confirm that changes in UV and UNaV were due to the diuretic alone (Figure 35).

Both male and female rats subjected to vehicle injection at ZT0 showed no significant increase in UV or UNaV excretion compared to the corresponding inactive period baseline (Fig.35A, 35B). The diuretic and natriuretic responses observed at ZT12 were similar, as there was no increase in UV or UNaV after vehicle administration (Fig.35C, 35D). Baseline active period UV in male rats was higher compared to the females (Fig.35C), which correlates with higher water intake in the males during the same time frame (Table 3).

Metabolic cage parameters were recorded during both pre- (baseline) as well as post-benzamil i.p. injection (Table 3). Food and water intakes followed a diurnal rhythm in both male and female rats with intake peaking during the dark (active) period (Table 3). However, urine osmolality showed no diurnal or sex difference. There was no difference in urinary potassium excretion (UKV) between sexes during the baseline lights-on (inactive) time period. However, females had lower baseline potassium excretion during the active period (lights-off) compared to males. The sex difference in UKV was abolished after benzamil administration.

Figure 36 depicts observed changes in UV and UNaV in response to benzamil administration at either ZT0 or ZT12 in both male and female rats. Male rats given benzamil at the beginning of their inactive period (ZT0) had a significant increase in UV (from 0.3 ± 0.03 to 1.4 ± 0.2 ml/hr) and UNaV (from 20.4 ± 2.2 to 284.2 ± 79.8 μEq/hr) which peaked after 2 hours of administration. There was a similar pattern of diuresis rising from 0.5 ± 0.1 to 1.4 ± 0.2 ml/hr and natriuresis from 56.9 ± 3.9 to 354.4 ± 30.0 μEq/hr

when the drug was administered at ZT12 with the peak of response after 2 hours of benzamil injection. However, there was no statistically significant difference in UV and UNaV when the drug was administered either at the beginning of the active or inactive periods for all three urine collection time points ($p > 0.05$) (Fig. 36A, 36B).

Table 3

Diurnal parameters from metabolic cage studies in Sprague-Dawley rats.

	Males	***Females***
***Body Weight**, g (n=8)*	355.5 ± 10.9	225.4 ± 3.3*
***Food Intake,** g/day (n=8)*		
Inactive Period	1.5 ± 0.3	2.5 ± 0.4
Active Period	14.7 ± 0.4	9.4 ± 0.8*
***Water Intake**, ml/day (n=8)*		
Inactive Period	4.3 ± 0.7	4.2 ± 0.6
Active Period	21.7 ± 1.1	16.9 ± 1.4*
***Urine Osmolality**, mosm/L (n=8)*		
Inactive Period	1446 ± 140	1205 ± 113
Active Period	1536 ± 119	1099 ± 141
***UKV Inactive** (baseline), µEq/hr (n=8)*	60 ± 4	57 ± 6
0-2 hrs. post ZT0 injection	50 ± 8	71 ± 29
2-6 hrs.	22 ± 3	32 ± 11
6-12 hrs.	43 ± 6	43 ± 5
***UKV Active** (baseline), µEq/hr (n=8)*	144 ± 16	93 ± 8*
0-2 hrs. post ZT12 injection	62 ± 16	25 ± 8
2-6 hrs.	32 ± 2	32 ± 10
6-12 hrs.	73 ± 16	63 ± 14

Data presented as mean ± SEM. *$P < 0.05$ *vs* corresponding timepoint in males, repeated measures, two-way ANOVA. UV: Urine flow rate and UKV: Urinary potassium excretion.

Female Sprague Dawley rats showed a significant increase in UV after benzamil administration from 0.3 ± 0.03 at baseline to 0.7 ± 0.10 ml/hr after 2 hours and a corresponding increase in UNaV from 20.5 ± 2.7 to 104.9 ± 17.6 μEq/hr at ZT0. There was no difference in the diuretic response to benzamil given at ZT0 and ZT12 (Fig. 36A), except for the hours 6-12 post benzamil. On the other hand, UNaV was higher at ZT12 compared to ZT0 for the 2-hour collection time point (Fig. 36B).

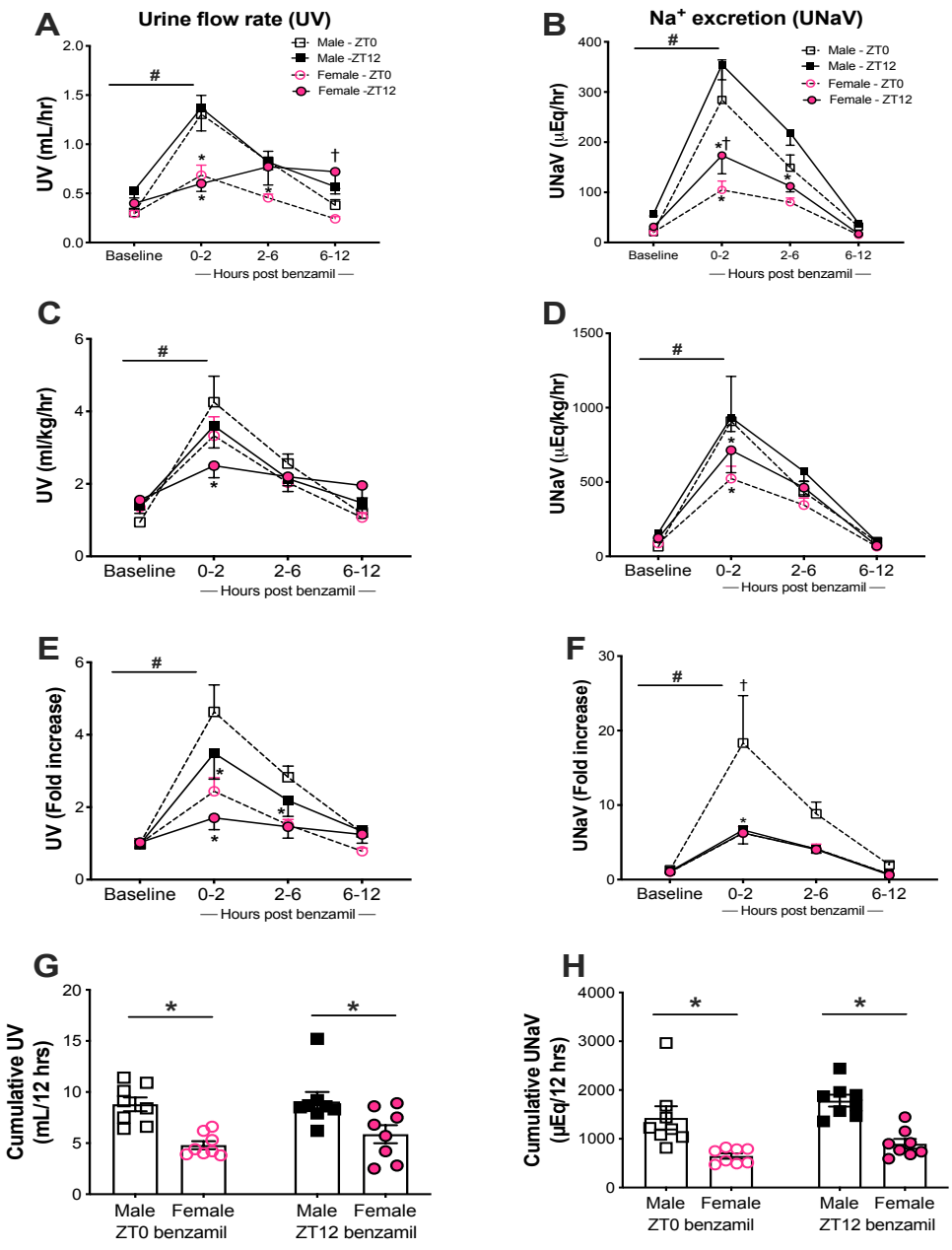

Figure 36: Urine flow rate (UV), and urinary sodium excretion (UNaV) in male and female Sprague-Dawley rats at both pre- (baseline) and post-benzamil administration at either ZT0 or ZT12 (A – F) and the 12-hours cumulative UV and UNaV excretion rates (G, H). **p < 0.05 vs* male at the corresponding time point, *†p < 0.05* vs ZT0 within the same sex and # vs baseline ± SE, repeated measures two-way ANOVA and Sidak's post-hoc test, n= 10-12.

Effect of Sex on Response to Benzamil.

Apart from active period baseline UV being higher in males, the remainder of the UV and UNaV values were not significantly different between male and female rats. Animals were also housed in the same space in the animal house to account for environmental factors as temperature and humidity, so we expect that dissimilarities in the response is not due to different baseline excretion rates across sexes or environmental conditions, but is most likely attributed to ENaC activity and benzamil blockade efficiency. Male rats had higher UV at the 2 and 6-hour marks compared to females when benzamil was given at ZT0 (Fig. 36A). This difference was abolished when excretion rates were normalized to body weights (Fig. 36C), but maintained when data were normalized to baseline excretion rates for both males and females (Fig. 36E). Female rats had blunted UNaV rates when compared to male rats at ZT0, particularly during the peak response to benzamil (Fig. 36B, 36D and 36F). In addition, figure 36 demonstrates male and female responses to benzamil administration at ZT12. Similar to the sex difference observed at ZT0 in UV, male rats had greater diuresis after 2 hours compared to females (Fig. 36A). The difference in the response between sexes was preserved when UV was normalized to body weight or baseline excretion (Fig. 36C, 36E). UNaV was higher in male than female rats in the first 6 hours post injection (Fig. 36B), however, this difference was narrowed down to the first 2 hours and then abolished when normalized to body weights and baseline values respectively (Fig. 36D, 36F).

To account for the difference in water and food intake between both sexes, we further normalized UV to water intake and UNaV to sodium intake at both inactive and active periods at baseline and after benzamil administration (Table 4). UV/water intake

was higher in males in response to ZT12 dose. UNaV/Na^+ intake was significantly higher in male rats at 6 hours after benzamil at ZT12, with an overall significant effect of sex showing higher diuretic and natriuretic responses in males compared to females. Cumulative UV and UNaV in the 12 hours post benzamil were higher in males regardless of time of day (Fig. 36G, 36H).

Table 4

Urine flow rate (UV) and sodium excretion (UNaV) relative to intake

	Males	***Females***	***2-way ANOVA***
UV (mL)/Water intake (mL) inactive (n=12)			P_{Sex}= 0.0005
baseline	1.01 ± 0.14	1.19 ± 0.16	P_{Time}= 0.01
0-2 hrs. post ZT0 injection	1.88 ± 0.29†	0.95 ± 0.14*	$P_{interaction}$= 0.06
2-6 hrs.	2.26 ± 0.23†	1.40 ± 0.19*	
6-12 hrs.	1.57 ± 0.37	0.78 ± 0.24	
UV (mL)/Water intake (mL) active (n=8)			P_{Sex}= 0.04
baseline	0.29 ± 0.03	0.27 ± 0.04	P_{Time}= 0.0005
0-2 hrs. post ZT12 injection	0.57 ± 0.07†	0.39 ± 0.05	$P_{interaction}$= 0.3
2-6 hrs.	0.64 ± 0.09†	0.47 ± 0.11	
6-12 hrs.	0.37 ± 0.04	0.37 ± 0.05	
UNaV (mEq)/sodium intake (mg) inactive (n=12)			P_{Sex}= 0.006
baseline	0.30 ± 0.12	0.14 ± 0.05	P_{Time} < 0.0001
0-2 hrs. post ZT0 injection	1.18 ± 0.59	0.57 ± 0.19	$P_{interaction}$= 0.1
2-6 hrs.	2.37 ± 0.92†	0.97 ± 0.18*	
6-12 hrs.	0.25 ± 0.12	0.07 ± 0.04	
UNaV (mEq)/sodium intake (mg) active (n=8)			P_{Sex}= 0.2
baseline	0.02 ± 0.00†	0.02 ± 0.00†	P_{Time} < 0.0001
0-2 hrs. post injection	0.10 ± 0.01†	0.09 ± 0.02†	$P_{interaction}$= 0.8
2-6 hrs.	0.10 ± 0.02	0.08 ± 0.01	
6-12 hrs.	0.03 ± 0.01	0.02 ± 0.01	

Data presented as mean ± SE. **P <0.05 vs* males, *†P <0.05 vs* baseline, Sidak's multiple comparisons test.

Role of ENaC Blockade on Endothelin-1 Excretion.

The change in ET-1 excretion, which largely reflects tubular secretion, matched UV and UNaV in response to benzamil in both male and female rats regardless of time of day. Following benzamil administration, ET-1 excretion increased in both males and females compared to their corresponding baseline values reaching a maximum excretion rate of 0.28 ± 0.04 pg/hr at ZT0 and 0.23 ± 0.06 pg/hr at ZT12 in males and 0.38 ± 0.14

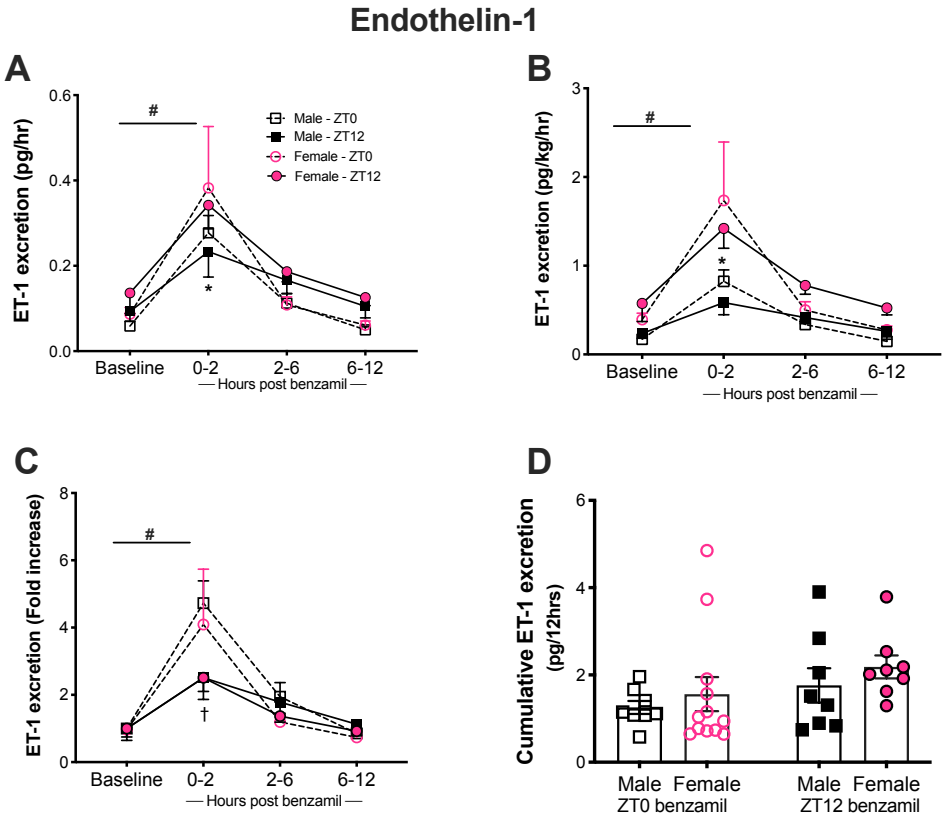

Figure 37: Recordings of urine ET-1 excretion in response to benzamil at ZT0 or ZT12 in male and female Sprague-Dawley rats at baseline and for 12 hours post-benzamil (A, B, C) and 12-hours ET-1 cumulative excretion rate (D). *$p < 0.05$ *vs* male at the corresponding time point, †$p < 0.05$ *vs* ZT0 within the same sex and #$p < 0.05$ *vs* baseline, repeated measures two-way ANOVA and Sidak's post-hoc test.

pg/hr at ZT0 and 0.34 ± 0.06 pg/hr at ZT12 in females after 2 hours of benzamil administration (Fig.37).

Looking into sex differences in urine ET-1 excretion, our data showed no significant difference in excretion rates between males and females at baseline. Following benzamil given at ZT0, the rise in ET-1 excretion was comparable between both sexes. On the other hand, there was a significant sex difference in ET-1 excretion following benzamil at ZT12, which moved in an opposite direction to that observed for UV and UNaV. Here, female rats had higher ET-1 excretion that was evident at the 2-hour time point compared to males (Figure 37A). The observed sex difference was preserved when excretion rate was normalized to body weights, but not when normalized to urinary ET-1 excretion baseline values (Figure 37B, 37C). An observed effect of time at 2 hours post-benzamil was evident in the male group when excretion rates were normalized to baseline excretion (Figure 37C). This could be related to the relatively lower basal ET-1 excretion during inactive time period.

Cortical ENaC Abundance in Male and Female Rats.

To assess whether differences in ENaC protein expression could account for our observed responses to benzamil, we measured abundance of all three ENaC subunits at the beginning of the inactive and active periods in kidneys from male and female Sprague-Dawley rats. Cortical tissues homogenates of kidneys collected at ZT0, showed no significant sex difference in abundance of α and γ subunits, both the full length and the cleaved forms, whereas the β subunit was significantly lower in females (Figure 38A). Protein expression of both the full length and cleaved forms of γENaC was higher in

females at ZT12. Alpha and β subunit expression was similar in kidneys of male and female rats (Figure 38B).

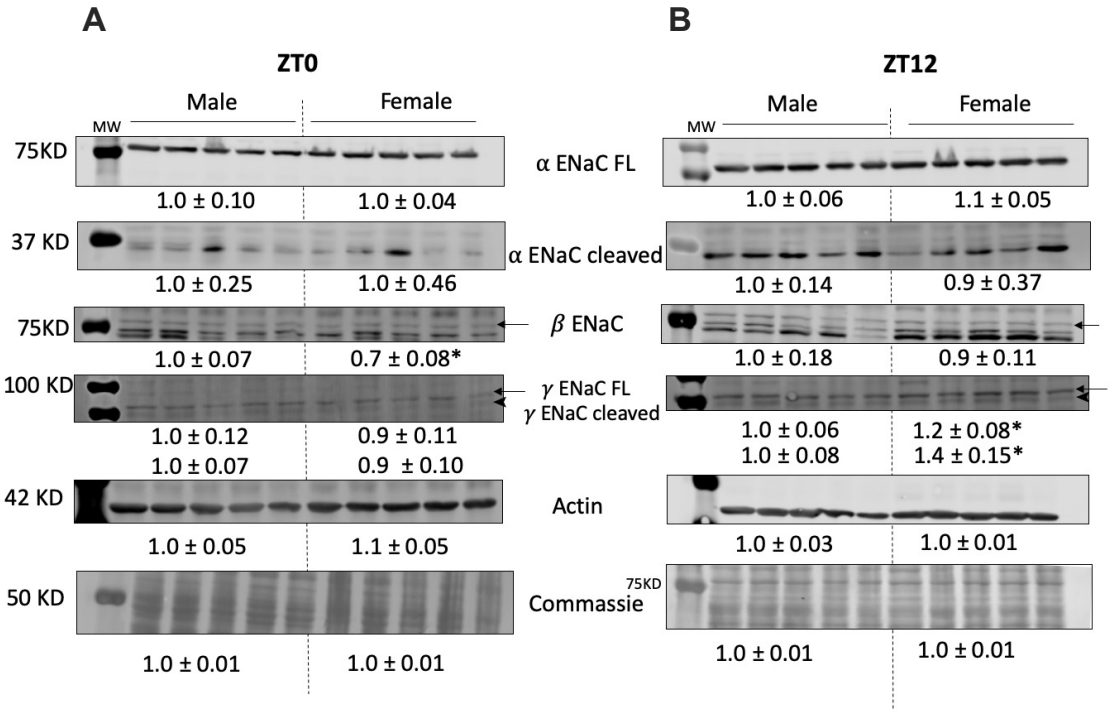

Figure 38: Immunoblots of kidney cortical tissue homogenates demonstrating abundance of α, β and γ- ENaC subunits in both male and female Sprague-Dawley rats. Tissues collected at either ZT0 or ZT12. Representative blots of actin and Coomassie are demonstrated. Densitometry signals were normalized to male rats (set to 1.0) and expressed as mean ± SE. *$p < 0.05$ *vs* male group, unpaired t-test.

Role of Ovarian Hormones.

Ovariectomized (OVx) and sham female Sprague Dawley rats had similar baseline UV and UNaV for their light and dark cycles (Fig. 39). When OVx and sham rats were subjected to a single dose of benzamil at ZT0, both groups showed an increase in UNaV within 2 hours of administration with no effect of ovariectomy. UV increased to 0.8 ± 0.2 ml/hr in OVx and sham controls after light period benzamil injection (Fig. 39A). No diuretic effect was observed after ZT12 benzamil, as evident in the stable urine flow rate for both sham and OVx rats.

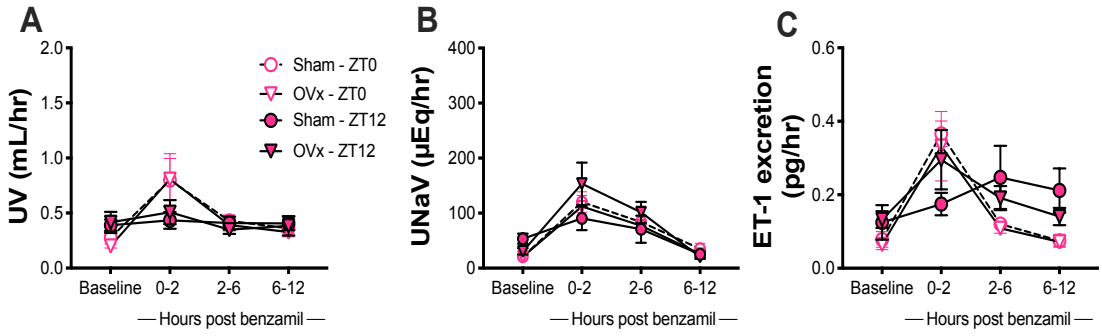

Figure 39: Urine flow rate (UV), urinary sodium excretion (UNaV) and urinary ET-1 as measured in both intact (Sham) and ovariectomized (OVx) female Sprague-Dawley rats at baseline and after i.p. benzamil administration at ZT0 and ZT12. Repeated measures two-way ANOVA, n= 6. $P_{Time} < 0.05$, $P_{OVx} > 0.05$ and $P_{Time*OVx} > 0.05$ and Sidak's post-hoc test, n = 4 – 6/group.

UNaV peaked after the expected 2 hours following benzamil in all groups, although the increase in the sham group was not statistically significant from baseline at ZT12;

UNaV reached 112 ± 20 μEq/hr in OVx and 120 ± 18 μEq/hr in the sham group (Fig. 39B) at the 2-hour time point at ZT0. UNaV increased to 153 ± 39 μEq/hr at ZT12 in OVx females. ET-1 excretion after OVx at both baseline and with benzamil administration remained similar to the sham group regardless of time of day (Fig. 39C). Benzamil administration increased ET-1 excretion in the urine only when it was given at 7 am for both OVx and sham rats. However, no significant increase in urinary ET-1 was observed after ZT12 administration in either group. Overall, ovariectomy only increased the natriuretic effect of benzamil when benzamil was given at ZT12 compared to sham controls. However, sodium excretion values were still similar to Sprague-Dawley females in the original protocol (Fig. 36B).

CHAPTER 5

DISCUSSION

Hypertension is a major pathological sequela of obesity and impaired capacity of the kidney to handle sodium is a major contributor to obesity-related hypertension (16). Obesity is associated with enhanced renal sodium reabsorption due, in part, to activation of the RAAS and sympathetic overactivity. However, our understanding is incomplete especially with the role of endothelin-1 as an important natriuretic factor necessary for eliminating a high salt diet (104, 125). The overall goal of this project was to assess diurnal renal sodium handling capacity with high-fat feeding, and to characterize the status of the renal ET-1 system under these conditions, in addition to its involvement as a potential contributing factor to obesity-related hypertension.

To summarize the main findings of this project, we found that diet-induced obesity impaired diurnal rhythms of sodium excretion, and was indeed associated with diurnal dysfunction in ET-1 expression, production and excretion. Our animal model of diet-induced obesity developed salt sensitivity with high salt diet. In addition, our study found that sex modulated the dietary implications on the kidney, with a dimorphic phenotype in response to high-fat feeding and to pharmacological inhibition of epithelial sodium channel.

Circadian rhythms of blood pressure were maintained in all groups. However, the addition of high salt diet for two weeks led to further increase in blood pressure, only in

male rats, showing that, in our animal model, salt sensitivity is sex specific with high fat feeding. The hypertension phenotype was associated with diurnal alterations in renal ET-1 expression and excretion. ET-1 relative mRNA expression was significantly lower in kidneys collected at ZT12 from male Sprague-Dawley rats under HF diet, which was reflected in a reduction in active period urinary ET-1 excretion of male, but not female rats. Chronic high salt feeding failed to promote ET-1 excretion to levels similar to the NF control group, albeit was higher when compared to normal salt controls. While HF-treated females didn't develop salt sensitivity, their ET-1 response to HS diet was attenuated compared to their lean controls.

We also assessed the functional capacity of kidney sodium handling machinery, with challenging HF and NF groups with an acute sodium load at different times of day. Male rats on HF diet, retained sodium for longer periods when the NaCl load was administered at ZT12, while HF-treated females showed an intact response. Our observation of impaired acute natriuretic response in male, but not female rats, accompanied by evidence showing downregulation of ET-1 expression and excretion only in the male sex, gives credence to our hypothesis that ET-1 dysfunction with high fat diet, is responsible for time-of-day impairment in renal sodium handling. However, the multiple pro-natriuretic pathways that help excrete salt create redundancy in salt handling, and many of these pathways are sex specific. For example, αENaC protein expression is higher in female compared to male rats (196).

We designed experiments to assess channel activity and used pharmacological intervention by benzamil to further investigate sex-specific differences in ENaC inhibition as a downstream ET-1 target under normal dietary conditions. Our results showed that the

natriuretic and diuretic responses to a single dose of benzamil was significantly greater in male compared to female rats whether given at the beginning of the inactive period (ZT0) or active period (ZT12). There was no difference in renal cortical αENaC protein abundance between males and females. ET-1 excretion was significantly increased following benzamil administration in both sexes but it was surprising to find that this increase was significantly greater in females, despite less prominent response to the diuretic. These results suggest that independent of ET-1, ENaC activity is lower in females, in addition to evidence of clear disconnect between ENaC expression and channel activity.

Male rats on HF diet showed a blunted natriuretic response to an acute salt load, that was time-of-day dependent (Figure 14 and 15). It was exciting to find that impaired UNaV was evident in the first 12 hours following salt challenge and only post-ZT12 load. This represents the active phase that mimics most food intake and subsequently excretion. Since sodium excretion follows a diurnal rhythm, with a peak during the dark time in nocturnal animals (21, 44) and during the day in humans (133, 183), we suggest that mechanisms promoting sodium excretion are at maximum capacity during the active period. While rats were able to maintain normal sodium balance at baseline, as evident by similar excretion rates to their lean controls, the extra sodium load imposed with saline injection at ZT12, exceeded renal excretion capacity and they retained more sodium during that part of the day. Circadian dysfunction imposed by the HF diet, as previously described by Kohsaka et al (106), is one of the potential mechanisms contributing to this response. In their study, mice were placed on HF diet for 6 weeks and tissues were collected at 4-hour intervals. Tissues collected from the liver and adipose tissue showed lower expression of *Clock*, *Bmal1 and Per2* mRNA at multiple time points, resulting in an overall attenuated

temporal profile of the core clock transcription factors, with maintained rhythmicity (106). Loss of ET_B receptor impaired acute natriuretic response, that was more evident during the active period (88), suggesting that circadian regulation of renal sodium handling is dependent on ET-system and is time of day dependent. This is consistent with our observation and could explain the impaired acute natriuretic response being restricted to ZT12 challenge. ET-1 expression and excretion follow a circadian rhythm and promotes the rhythmicity of sodium excretion (181), and in that sense, we speculate that impaired active time sodium excretion is ET-1 dependent.

Female rats on HF diet excreted their salt load as efficient as the NF-fed rats (Figure 16 and 17), suggesting that male's renal sodium handling machinery is more susceptible to the adverse effects of obesity. Our sex-specific observation is consistent with Johnston et al finding that impaired acute natriuretic response in ET_B-deficient rats, which is the ET-1 target receptor, is limited to males (88). Female mice while protected from HF-induced circadian disruption, and ovariectomy led to advancement of their liver clock with high fat feeding, along with disruption in eating and activity rhythms (149). Similarly, previously published data showed that ovarian hormones protected female mice from HF-induced metabolic dysfunction, with ovariectomized mice showing higher circulating serum lipids (123) and adipose tissue proinflammatory cytokines (139).

High fat feeding resulted in a 40% reduction of urinary ET-1 excretion (Figure 18), that was accompanied by downregulation of ET-1 mRNA expression in different parts of the kidney (Figure 22). To our knowledge, this is the first report of impaired renal ET-1 system secondary to high fat feeding in rats. We found that HF diet impaired ET-1 excretion during the active period (Figure 18), with corresponding downregulation of ET-

1 mRNA expression in the cortex and outer medullary tissues collected at ZT12 (Figure 22). Previous studies showed peak of urine ET-1 excretion during the active period (181) and its association with the well-described diurnal rhythm of sodium excretion (85). Apart from studies showing lower urinary ET-1 excretion in hypertensive patients (75), studies describing the effect of obesity on renal ET-1 expression and function are lacking. ET-1 through binding to ET_B receptor has been shown to suppress sodium reabsorption in the collecting ducts through NO-mediated ENaC inhibition (18, 28). Patch-clamp studies of rat collecting duct cells showed that ET-1 reduces ENaC activity (18), while the loss of ET-1 promoted sodium retention (3). These data constitute a potential mechanism for the aberrant blood pressure phenotype in our model, secondary to reduced ET-1 secretion and impaired natriuretic response. Johnston et al, reported impaired diurnal rhythm of sodium excretion in ET_B deficient rats that is time of day dependent (88). In contrast to the clear diurnal rhythm in ET-1 secretion, ET-1 mRNA showed no time of day difference similar to previously published data (181).

There is strong evidence that ET-1 is under the control of clock genes. ET-1 suppressed the expression of *Bmal1* in vitro (181). Pharmacological inhibition of *Per1* phosphorylation was shown to suppress its nuclear entry, with subsequent alteration in ET-1 expression, along with downregulation of its downstream target, epithelial sodium channel (ENaC) in the renal cortex (6). *Per1 KO* mice showed increased ET-1 expression in the renal medulla (18). These data, together with the observed downregulation and loss of *Bmal1* rhythmicity in the kidneys of mice under HF diet (71) suggest that time-of-day impairment in the acute natriuretic response as well as ET-1 dysfunction are mediated by HF-induced circadian dysfunction.

Hwang et al, measured urinary ET-1 excretion in human subjects with mild hypertension. In addition to the observed diurnal rhythm of ET-1 excretion, he observed that some hypertensive subjects excreted significantly lower urinary ET-1 after saline infusion, with normal baseline excretion rates (75). This report, in addition to our observed triad of impairment in acute natriuresis, ET-1 excretion and expression allow us to speculate that renal ET-1 system is contributing to the development of hypertension in our animal model.

ET_B-dependent natriuresis was impaired in Dahl SS rats (98). This impairment was attributed to reduced ET_B receptor function in the inner medulla and was evident following intramedullary infusion of the ET_B-agonist serafatoxin (S6C). therefore, it is less likely that the lower expression of ET_B mRNA in the outer medulla of the HF group is contributing to the impaired natriuretic response in our study, since inner medullary ET_B expression was intact (Figure 23). ET_A receptors are mainly expressed on the vascular endothelium of renal medullary vessels, influencing renal hemodynamics (57, 199). ET_A receptors are also expressed on the renomedullary interstitial cells (RMICs) and was characterized as a potential target for ET-1 binding and modulation (73, 128). Recent studies have shown that disruption of ET_A on RMICs lead to enhanced water and sodium excretion under HS diet (73). Expression of the ET_A receptor in our model, was higher in the IM of HF-treated males, with a loss of diurnal rhythm of expression compared to NF controls (Figure 23F). We suggest that the upregulated medullary ET_A receptor in our study could contribute to sodium retention, not only via reduction of renal blood flow, but also through promoting the anti-natriuretic effects of RMICs.

Excess aldosterone in obesity either in association with or independent from the activation of the renin-angiotensin-aldosterone system has been reported in both human and animal models (29, 64, 65). Our data showed persistently elevated urine and plasma aldosterone levels (Figure 26A and 27A), which is consistent with previously published data (33). High aldosterone promotes sodium reabsorption in the collecting ducts of the kidney as well as proinflammatory state and kidney injury in obesity (91, 109). The inappropriately high aldosterone in our animal model further validates the model for the study of obesity-induced hypertension. Failure of acute sodium load to suppress aldosterone secretion is potentially contributing to the blunted natriuretic response in HF male rats. Urine aldosterone excretion after NaCl injection was persistently elevated regardless of the time of bolus injection (Figure 26). This suggests that time-of-day impairment in sodium excretion is mediated mainly through ET-1 dysfunction.

Our animal model showed elevated blood pressure values as early as 6 weeks of the feeding protocol (Figure 10 and 12). Superimposition of chronic high salt diet (4% NaCl) on HF-treated rats, led to a further increase in blood pressure, which is highly indicative of salt sensitivity in our animal model. Both male and female Sprague-Dawley rats on HF diet developed hypertension. This is consistent with previously reported hypertensive phenotype in male Sprague-Dawley rats after 10 weeks of HF diet (32% Kcal fat) (34). However, to our knowledge, this is the first report of blood pressure phenotype in obese female Sprague-Dawley rats.

Studies on animal models of obesity have shown disruption of blood pressure rhythms (187), while weight loss in humans promoted the restoration of night-time dip (26). The development of non-dipping hypertension in humans was directly correlated with

obesity (108). These observations were associated with circadian gene dysfunctions. However, in our study, blood pressure maintained its diurnal rhythm, with preservation of day/night difference. There was no observed phase shift or acrophase changes between groups. The absence of HF-induced circadian misalignment on blood pressure is supported by the observed intact circadian blood pressure pattern in *Bmal1 KO* rats (87), and doesn't exclude circadian dysfunction as a contributing factor our observed time-of-day impaired sodium handling and ET-1 dysfunction. However, these findings call for further studying of strain-specific phenotype differences.

In our approach to investigate ENaC as a potential factor contributing to the sexual dimorphic phenotype in our model of diet-induced obesity, we used a pharmacological model of ENaC inhibition to study sex differences in channel activity under normal dietary conditions. Our study highlighted the effect of sex on the response to benzamil as it belongs to a family of diuretics that are widely used in treatment of hypertension (200). To our knowledge, we showed for the first time that female rats have a lower diuretic and natriuretic response to benzamil compared to their male counterparts. The peak in diuretic and natriuretic responses was achieved within 2 hours of administration in both sexes (Figure 36). This is similar to previously published data on benzamil given the short half-life of the drug (156, 176).

Current hypertension guidelines do not consider sex in the management plans and choice of antihypertension medication, nor do they consider time of day dosing (200). No sufficient data currently exist to evaluate sex differences in response to diuretics and different antihypertension medications. The dosage of benzamil was calculated according

to body weight to eliminate the size difference between both sexes as a confounding variable, which is not considered in regimens targeting human subjects.

Our study shows a sex difference in functional response to ENaC inhibition suggesting a more active transport in males, despite the published data that female rats have higher expression levels of the cleaved forms of α and γ ENaC subunits in the renal cortex (196). This is consistent with our findings of the gamma subunit being higher in females at the beginning of the active period, which corresponds to the time the channel should be most active to handle the increase in filtered sodium during active time food intake. However, there was no statistical difference in the alpha subunit expression between males and females regardless of the time of day. These findings indicate that channel activity is independent of mRNA and protein expression measured in kidney tissue over the course of the day and that other factors including channel localization and gating are more reflective of circadian control of ENaC activity. The skin is a reservoir of osmotically inactive sodium. There are no reported sex differences in osmotically inactive sodium storage under normal salt conditions in rats (192), and under states of balanced intake and excretion, there is no significant sodium mobilization between compartments. The imbalance in this buffering system has been only reported in states of excessive salt intake or under conditions of hypertension and chronic kidney disease (180).

ET-1 is an upstream inhibitor of ENaC through the ET_B receptor (49, 55) that is particularly active in animals on a high salt diet (18, 51, 105). Therefore, lower levels of urinary excretion of ET-1 is typically associated with more ENaC activity. Female rats had higher ET-1 excretion rates compared to males following benzamil administration, suggesting that the weaker natriuretic response is probably due to more active ENaC in

males. The relatively lower response to benzamil in females could also indicate that ENaC has reached maximum inhibition or that ENaC is under a relative state of constant inhibition induced by the relatively, yet not significantly higher ET-1 at baseline conditions, which could explain the less prominent response in female rats.

Urinary ET-1 reflects endothelin that originates from the kidney, which in large part, is produced by the collecting duct (104), the same location where it functions to inhibit ENaC under high salt conditions (51, 84, 104). Kohan and colleagues have shown that ET-1 production in the collecting duct can be stimulated by increases in tubular fluid flow (126). Thus, urinary ET-1 excretion can be increased by not only high salt intake, but also, increased tubular fluid flow, such as that which occurs during diuretic treatment. We observed that the lower diuretic and natriuretic response to benzamil in females compared to male rats was accompanied by higher ET-1 excretion rates. This finding is consistent with previously published data (151) proposing dissociation of the flow-mediated ET-1 response from ENaC channel activity and supports our hypothesis that benzamil function is probably not dependent upon ET-1 effects on ENaC activity. This is further backed up by our findings in male rats having a significant natriuretic response with a significantly lower ET-1 excretory response compared to females. It remains to be determined whether there is a sex difference in the collecting duct to produce ET-1 in response to similar changes in flow.

Differential expression and activity of other sodium channels along the nephron could be contributing to the weaker natriuretic response in females. NCC is reported to have higher activity in females, with higher levels of expression and phosphorylation (120, 162). This channel could be compensating for ENaC blockade and helping to maintain

sodium balance and preventing unnecessary loss of sodium in urine since the animal model in this study is a normotensive model on a normal salt diet. Female mice had a more robust response than males to hydrochlorothiazide intravenous injection (120). This study attributed this difference to higher expression and phosphorylation levels of NCC as well as the angiotensin AT1a receptor status (120). Female rats excrete a salt load more quickly and efficiently than male rats (88, 92, 138, 196). This has been mostly attributed to lower abundance and activity of transporters in the proximal tubules of females leading to lower fractional sodium reabsorption in that area of the nephron that is responsible for about 67% of sodium reabsorption along the nephron (196). However, the greater ability of male kidneys to reabsorb sodium with salt loading could also be attributed to more ENaC activity irrespective of mRNA and protein expression. Distal nephron transporters are in charge of fine-tuning sodium transport and the final steps of maintaining plasma salt homeostasis (50, 122, 148). The ability of female rats to excrete salt more rapidly than males could also reflect lower activity of distal tubule sodium transporters which enhances their ability to unload sodium and contributes to the attenuated response to benzamil. Our study showed that female rats had lower potassium excretion during their active period, which further supports the notion of lower ENaC activity in females and consistent with a previous human study showing failure of amiloride to reduce blood pressure in black individuals, owed to lower ENaC activity as supported by lower potassium excretion and lower plasma aldosterone levels compared to white participants (155).

The kidneys are one of the organs that express highest levels of estrogen receptor-α (ERα). It ranks second to the reproductive organs in expression of ERα mRNA as well as the abundance of ERα-responsive genes (78, 111). Jelinsky et al demonstrated an

estrogen-induced induction of a wide array of genes in rat and mice kidneys (82), which suggests a direct influence of ovarian hormones on renal water and electrolytes homeostasis. ERα is significantly higher in male Sprague-Dawley rat kidneys, while the G protein-coupled estrogen receptor (GPER) has an opposite profile across sexes (74). This suggests differential roles of each estrogen receptor in renal tubular sodium handling that might contribute to the sexual dimorphic pattern of sodium reabsorption. However, we observed that ovarian hormone deprivation by OVx had no effect on the female diuretic and natriuretic responses to benzamil. The lack of response to ovariectomy suggests the presence of non-female sex hormonal factors in the regulation of ENaC activity, at least under our standard diet conditions.

A limited number of studies have shown an improved prognosis for hypertension in patients receiving one or more bed-time antihypertensive medication compared to morning dosing. However, it is not clear if this is due to time-of-day-dependent difference in drug response or merely owed to the control of nocturnal-type hypertension and non-dipping phenotype of the disease that may vary in different populations. Night-time antihypertensive medication is mainly concerned with the control of what is referred to as nocturnal hypertension, which has become more evident with the increased use of ambulatory blood pressure measurements (68, 70). However, there is no clear evidence on the effectiveness of diuretic administration at certain time of day on the control of essential hypertension in the absence of nocturnal blood pressure elevation specifically.

Patients, regardless of sex, receiving either morning or evening dosing of thiazide demonstrated adequate blood pressure control and improvement of left ventricular indices (145). However, participants receiving their dose in the evening showed lower blood

pressure values and reduction of left ventricular mass and posterior wall thickness (145). This highlights the importance of diuretic chronotherapy for better control of hypertension-associated cardiovascular disease risk factors. A number of reviews and clinical trials investigating the treatment of hypertension with chronotherapy have shown that even with comparable reduction in blood pressure indices, evening drug dosing improved cardiovascular risk and overall prognosis (69, 70, 146, 154).

Finally, our results showed that male rats showed no time of day difference in diuretic and natriuretic response to benzamil. However, females given benzamil at the beginning of their active period failed to increase their UV but not UNaV and a more robust diuretic response for inactive time dosage. This suggests that benzamil therapeutic effect is not affected by the diurnal variation of ENaC activity and expression particularly in males. However, since we used a normotensive animal model, cardiovascular disease risk assessment was not feasible.

Animal models used for the study of hypertension, tend to have genetic modifications and/or pharmacological inducers of hypertension with the aim to incite specific-target organ damage related to a specific research aim (117, 118, 124). These models are limited in their poor mimicry to human essential hypertension pathophysiology, which are multifactorial and majorly depend on environmental factors, including high salt and high caloric intakes to manifest clinically. It is difficult to dissociate the complex genetic and environmental factors of hypertension in genetically-induced obesity models. Our choice of the normotensive Sprague-Dawley rats is an attempt to avoid the confounding factors imposed by genetic manipulations and to study dietary risk factors with high fidelity to human cardiovascular disease (115, 124). Kittikulsuth et al showed

that HF Dahl rats have an impaired ability to excrete sodium following acute intramedullary injection of ET_B receptor agonist sarafatoxin (S6C) (98). While this study establishes a direct measure of ET_B receptor function in obesity, the limitation of this study is the fact that Dahl rats have a constitutional dysfunction in the ET-1 system (182). Dahl rats develop hypertension in response to wide variety of stressors (118), which makes it difficult to separate the effect of hypertension from obesity on ET_B function. So, by the use of Sprague-Dawley rats in our study, we avoided the confounding factors of inherit ET-1 system dysfunction and salt sensitivity.

Published studies on diet-induced obesity showed significant effects of diet in mice after 4 - 8 weeks (30, 106), while other studies on Dahl SS rats showed HF-related events as early as 4 weeks of feeding (98). There is a debate on the definition of obesity in animal models, however, many published data identify the state of obesity in rodents with the development of metabolic or functional disturbances in one or more organ system (115). Our HF-treated Sprague-Dawley rats, not only expressed significant body weight differences (Figure 8) and increased total body fat percentage (Figure 9) by the end of the 8-week feeding protocol, they also showed dysfunction of acute sodium handling, salt sensitivity and hypertension.

PERSPECTIVES

Obesity is a major public health adversity that affects most organ systems, leading to increased risk for diabetes, cardiovascular and chronic kidney disease (CKD). It is important to note the linear relationship between increased body weight, as measured by BMI, and the rightward shift of the frequency distribution of blood pressure. Obese individuals have a 75% higher risk of developing hypertension compared to lean individuals and over 40% of hypertensive patients are obese (114, 191). Regulation of blood pressure within physiological levels is strongly dependent upon the kidney's ability to precisely maintain sodium homeostasis, which is disrupted in obesity.

While there are many identified treatment modalities for hypertension, a growing number of patients are showing patterns of resistant and refractory hypertension. This points toward some unidentified mechanistic pathways in the

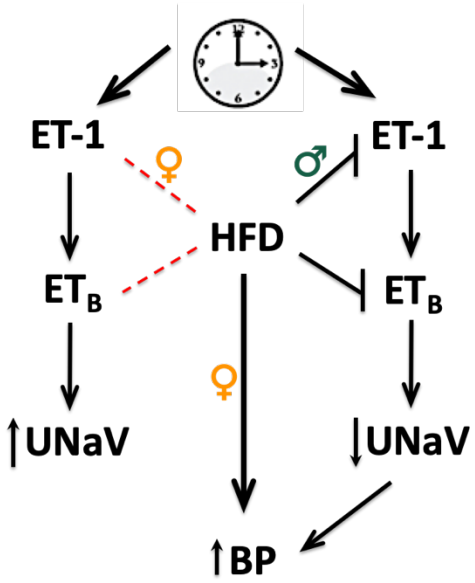

Figure 40: High fat diet (HFD) impairs diurnal regulation of the endothelin system leading to impaired renal sodium excretion (UNaV). This impairment predisposes to elevated blood pressure (BP) in males. Female rats are protected against HF-induced ET-1 impairment.

pathogenesis of hypertension. The renal endothelin system is a very potent natriuretic system in the kidney and an ample number of studies, mainly in animal models, have shown that impaired ET-1 signaling in the renal tubules impairs the excretory capacity of the kidney with the subsequent development of hypertension. However, there is lack of characterization of the renal ET-1 system in obesity or obesity-driven hypertension in the literature.

Our studies showed significant impairment of ET-1 expression and excretion under high-fat feeding, that was associated with the development of hypertension and salt sensitivity. The exact mechanism of HF-induced injury of ET-1 producing tubular cells is still unknown. This opens the door to future studies on mechanisms mediating this injury under conditions of obesity. We speculate that mechanisms related to increased oxidative stress and pro-inflammatory microenvironment is contributing to ET-1 dysfunction in our model. It is of equal importance to characterize the renal ET-1 system in other animal models of hypertension as well as in human subjects with essential hypertension. We speculate that renal ET-1 dysfunction is contributing to the non-dipping pattern and nocturnal hypertension, since ET-1 expression and function follows a diurnal rhythm (181).

Our studies also highlight the importance of time of salt intake as a potential modulator of system response. The growing field of circadian research has brought into spot-light the importance of the timing of food and salt consumption. The majority of physiological functions are under the control of clock genes, such that the body is primed to handle intakes most efficiently if they were in alignment with its clock. Our studies show that renal sodium handling is dependent upon the time of day of salt intake, and that HF-induced dysfunction in renal sodium handling is more evident at certain time windows. It

is critically important to report times of experiments in basic and translational research as underlined by our findings (87, 88, 181) that the response of the kidney to salt load was dependent on time of salt administration. Our study of the diurnal response to benzamil was not dependent on time of day, however further research is needed to determine the epithelial sodium channel activity at different times of day.

Our studies have also reported a clear sex difference in response to high fat diet, suggesting that males are more susceptible to ET-1 dysfunction and salt sensitivity with high fat feeding. Sex differences were also evident in response to benzamil administration. This points up the need for the inclusion of both sexes in animal and clinical studies and to further investigate sex-specific mechanisms that potentially protect against or compensate for a defective molecular pathway as it proposes benefit to the opposite sex.

LITERATURE CITED

1. **Abassi ZA, Pieruzzi F, Nakhoul F, and Keiser HR**. Effects of cyclosporin A on the synthesis, excretion, and metabolism of endothelin in the rat. *Hypertension* 27: 1140-1148, 1996.

2. **Abrams JM, and Osborn JW**. A role for benzamil-sensitive proteins of the central nervous system in the pathogenesis of salt-dependent hypertension. *Clin Exp Pharmacol Physiol* 35: 687-694, 2008.

3. **Ahn D, Ge Y, Stricklett PK, Gill P, Taylor D, Hughes AK, Yanagisawa M, Miller L, Nelson RD, and Kohan DE**. Collecting duct-specific knockout of endothelin-1 causes hypertension and sodium retention. *J Clin Invest* 114: 504-511, 2004.

4. **Al-Qusairi L, Basquin D, Roy A, Rajaram RD, Maillard MP, Subramanya AR, and Staub O**. Renal Tubular Ubiquitin-Protein Ligase NEDD4-2 Is Required for Renal Adaptation during Long-Term Potassium Depletion. *J Am Soc Nephrol* 28: 2431-2442, 2017.

5. **Alexander RT, Dimke H, and Cordat E**. Proximal tubular NHEs: sodium, protons and calcium? *Am J Physiol Renal Physiol* 305: F229-236, 2013.

6. **Alli A, Yu L, Holzworth M, Richards J, Cheng KY, Lynch IJ, Wingo CS, and Gumz ML**. Direct and indirect inhibition of the circadian clock protein Per1: effects on ENaC and blood pressure. *Am J Physiol Renal Physiol* 316: F807-F813, 2019.

7. **Amemiya M, Loffing J, Lotscher M, Kaissling B, Alpern RJ, and Moe OW**. Expression of NHE-3 in the apical membrane of rat renal proximal tubule and thick ascending limb. *Kidney Int* 48: 1206-1215, 1995.

8. **Arinami T, Ishikawa M, Inoue A, Yanagisawa M, Masaki T, Yoshida MC, and Hamaguchi H**. Chromosomal assignments of the human endothelin family genes: the endothelin-1 gene (EDN1) to 6p23-p24, the endothelin-2 gene (EDN2) to 1p34, and the endothelin-3 gene (EDN3) to 20q13.2-q13.3. *Am J Hum Genet* 48: 990-996, 1991.

9. **Armitage JA, Burke SL, Prior LJ, Barzel B, Eikelis N, Lim K, and Head GA**. Rapid onset of renal sympathetic nerve activation in rabbits fed a high-fat diet. *Hypertension* 60: 163-171, 2012.

10. **Bae K, Jin X, Maywood ES, Hastings MH, Reppert SM, and Weaver DR**. Differential functions of mPer1, mPer2, and mPer3 in the SCN circadian clock. *Neuron* 30: 525-536, 2001.

11. **Barton M, and Sorokin A**. Endothelin and the glomerulus in chronic kidney disease. *Semin Nephrol* 35: 156-167, 2015.

12. **Becker BK, Feagans AC, Chen D, Kasztan M, Jin C, Speed JS, Pollock JS, and Pollock DM**. Renal denervation attenuates hypertension but not salt sensitivity in ETB receptor-deficient rats. *Am J Physiol Regul Integr Comp Physiol* 313: R425-R437, 2017.

13. **Becker BK, Zhang D, Soliman R, and Pollock DM**. Autonomic nerves and circadian control of renal function. *Auton Neurosci* 217: 58-65, 2019.

14. **Beutler KT, Masilamani S, Turban S, Nielsen J, Brooks HL, Ageloff S, Fenton RA, Packer RK, and Knepper MA**. Long-term regulation of ENaC expression in kidney by angiotensin II. *Hypertension* 41: 1143-1150, 2003.

15. **Bray GA, Kim KK, Wilding JPH, and World Obesity F**. Obesity: a chronic relapsing progressive disease process. A position statement of the World Obesity Federation. *Obes Rev* 18: 715-723, 2017.

16. **Brooks HL, Allred AJ, Beutler KT, Coffman TM, and Knepper MA**. Targeted proteomic profiling of renal Na(+) transporter and channel abundances in angiotensin II type 1a receptor knockout mice. *Hypertension* 39: 470-473, 2002.

17. **Brooks HL, Sorensen AM, Terris J, Schultheis PJ, Lorenz JN, Shull GE, and Knepper MA**. Profiling of renal tubule Na+ transporter abundances in NHE3 and NCC null mice using targeted proteomics. *J Physiol* 530: 359-366, 2001.

18. **Bugaj V, Pochynyuk O, Mironova E, Vandewalle A, Medina JL, and Stockand JD**. Regulation of the epithelial Na+ channel by endothelin-1 in rat collecting duct. *Am J Physiol Renal Physiol* 295: F1063-1070, 2008.

19. **Butler MJ, Ramnath R, Kadoya H, Desposito D, Riquier-Brison A, Ferguson JK, Onions KL, Ogier AS, ElHegni H, Coward RJ, Welsh GI, Foster RR, Peti-Peterdi J, and Satchell SC**. Aldosterone induces albuminuria via matrix metalloproteinase-dependent damage of the endothelial glycocalyx. *Kidney Int* 95: 94-107, 2019.

20. **Camacho F, Cilio M, Guo Y, Virshup DM, Patel K, Khorkova O, Styren S, Morse B, Yao Z, and Keesler GA**. Human casein kinase Idelta phosphorylation of human circadian clock proteins period 1 and 2. *FEBS Lett* 489: 159-165, 2001.

21. **Cambar J, Toussaint C, Le Moigne F, Cales P, and Crockett R**. [Circadian rhythms in rat and mouse urinary electrolytes and nitrogen derivatives excretion (author's transl)]. *J Physiol (Paris)* 77: 887-890, 1981.

22. **Castagna A, Pizzolo F, Chiecchi L, Morandini F, Channavajjhala SK, Guarini P, Salvagno G, and Olivieri O**. Circadian exosomal expression of renal thiazide-sensitive NaCl cotransporter (NCC) and prostasin in healthy individuals. *Proteomics Clin Appl* 9: 623-629, 2015.

23. **Chaix A, Lin T, Le HD, Chang MW, and Panda S**. Time-Restricted Feeding Prevents Obesity and Metabolic Syndrome in Mice Lacking a Circadian Clock. *Cell Metab* 29: 303-319 e304, 2019.

24. **Collaboration NCDRF**. Worldwide trends in body-mass index, underweight, overweight, and obesity from 1975 to 2016: a pooled analysis of 2416 population-based measurement studies in 128.9 million children, adolescents, and adults. *Lancet* 390: 2627-2642, 2017.

25. **Crowley SD, Gurley SB, Herrera MJ, Ruiz P, Griffiths R, Kumar AP, Kim HS, Smithies O, Le TH, and Coffman TM**. Angiotensin II causes hypertension and cardiac hypertrophy through its receptors in the kidney. *Proc Natl Acad Sci U S A* 103: 17985-17990, 2006.

26. **Czupryniak L, Strzelczyk J, Pawlowski M, and Loba J**. Circadian blood pressure variation in morbidly obese hypertensive patients undergoing gastric bypass surgery. *Am J Hypertens* 18: 446-451, 2005.

27. **Davenport AP, Hyndman KA, Dhaun N, Southan C, Kohan DE, Pollock JS, Pollock DM, Webb DJ, and Maguire JJ**. Endothelin. *Pharmacol Rev* 68: 357-418, 2016.

28. **De Miguel C, Speed JS, Kasztan M, Gohar EY, and Pollock DM**. Endothelin-1 and the kidney: new perspectives and recent findings. *Curr Opin Nephrol Hypertens* 25: 35-41, 2016.

29. **de Paula RB, da Silva AA, and Hall JE**. Aldosterone antagonism attenuates obesity-induced hypertension and glomerular hyperfiltration. *Hypertension* 43: 41-47, 2004.

30. **Della Vedova MC, Munoz MD, Santillan LD, Plateo-Pignatari MG, Germano MJ, Rinaldi Tosi ME, Garcia S, Gomez NN, Fornes MW, Gomez Mejiba SE, and Ramirez DC**. A Mouse Model of Diet-Induced Obesity Resembling Most Features of Human Metabolic Syndrome. *Nutr Metab Insights* 9: 93-102, 2016.

31. **Dhaun N, Moorhouse R, MacIntyre IM, Melville V, Oosthuyzen W, Kimmitt RA, Brown KE, Kennedy ED, Goddard J, and Webb DJ**. Diurnal variation in blood pressure and arterial stiffness in chronic kidney disease: the role of endothelin-1. *Hypertension* 64: 296-304, 2014.

32. **Dhaun N, Webb DJ, and Kluth DC**. Endothelin-1 and the kidney--beyond BP. *Br J Pharmacol* 167: 720-731, 2012.

33. **Dinh Cat AN, Friederich-Persson M, White A, and Touyz RM**. Adipocytes, aldosterone and obesity-related hypertension. *J Mol Endocrinol* 57: F7-F21, 2016.

34. **Dobrian AD, Davies MJ, Prewitt RL, and Lauterio TJ**. Development of hypertension in a rat model of diet-induced obesity. *Hypertension* 35: 1009-1015, 2000.

35. **Doi M, Takahashi Y, Komatsu R, Yamazaki F, Yamada H, Haraguchi S, Emoto N, Okuno Y, Tsujimoto G, Kanematsu A, Ogawa O, Todo T, Tsutsui K, van der Horst GT, and Okamura H**. Salt-sensitive hypertension in circadian clock-deficient Cry-null mice involves dysregulated adrenal Hsd3b6. *Nat Med* 16: 67-74, 2010.

36. **Douma LG, Crislip GR, Cheng KY, Barral D, Masten S, Holzworth M, Roig E, Glasford K, Beguiristain K, Li W, Bratanatawira P, Lynch IJ, Cain BD, Wingo**

CS, and Gumz ML. Knockout of the circadian clock protein PER1 results in sex-dependent alterations of ET-1 production in mice in response to a high-salt diet plus mineralocorticoid treatment. *Can J Physiol Pharmacol* 98: 579-586, 2020.

37. **Douma LG, Holzworth MR, Solocinski K, Masten SH, Miller AH, Cheng KY, Lynch IJ, Cain BD, Wingo CS, and Gumz ML**. Renal Na-handling defect associated with PER1-dependent nondipping hypertension in male mice. *Am J Physiol Renal Physiol* 314: F1138-F1144, 2018.

38. **Ebefors K, Wiener RJ, Yu L, Azeloglu EU, Yi Z, Jia F, Zhang W, Baron MH, He JC, Haraldsson B, and Daehn I**. Endothelin receptor-A mediates degradation of the glomerular endothelial surface layer via pathologic crosstalk between activated podocytes and glomerular endothelial cells. *Kidney Int* 96: 957-970, 2019.

39. **Eckel-Mahan KL, Patel VR, de Mateo S, Orozco-Solis R, Ceglia NJ, Sahar S, Dilag-Penilla SA, Dyar KA, Baldi P, and Sassone-Corsi P**. Reprogramming of the circadian clock by nutritional challenge. *Cell* 155: 1464-1478, 2013.

40. **Eiam-Ong S, Hilden SA, King AJ, Johns CA, and Madias NE**. Endothelin-1 stimulates the Na+/H+ and Na+/HCO3- transporters in rabbit renal cortex. *Kidney Int* 42: 18-24, 1992.

41. **Elisa T, Antonio P, Giuseppe P, Alessandro B, Giuseppe A, Federico C, Marzia D, Ruggero B, Giacomo M, Andrea O, Daniela R, Mariaelisa R, and Claudio L**. Endothelin Receptors Expressed by Immune Cells Are Involved in Modulation of Inflammation and in Fibrosis: Relevance to the Pathogenesis of Systemic Sclerosis. *J Immunol Res* 2015: 147616, 2015.

42. **Fagan KA, McMurtry IF, and Rodman DM**. Role of endothelin-1 in lung disease. *Respir Res* 2: 90-101, 2001.

43. **Fan J, Unoki H, Iwasa S, and Watanabe T**. Role of endothelin-1 in atherosclerosis. *Ann N Y Acad Sci* 902: 84-93; discussion 93-84, 2000.

44. **Firsov D, and Bonny O**. Circadian regulation of renal function. *Kidney Int* 78: 640-645, 2010.

45. **Firsov D, and Bonny O**. Circadian rhythms and the kidney. *Nat Rev Nephrol* 14: 626-635, 2018.

46. **Foster MC, Hwang SJ, Porter SA, Massaro JM, Hoffmann U, and Fox CS**. Fatty kidney, hypertension, and chronic kidney disease: the Framingham Heart Study. *Hypertension* 58: 784-790, 2011.

47. **Froy O**. Circadian rhythms and obesity in mammals. *ISRN Obes* 2012: 437198, 2012.

48. **Froy O**. Metabolism and circadian rhythms--implications for obesity. *Endocr Rev* 31: 1-24, 2010.

49. **Gallego MS, and Ling BN**. Regulation of amiloride-sensitive Na+ channels by endothelin-1 in distal nephron cells. *Am J Physiol* 271: F451-460, 1996.

50. **Gamba G**. Molecular biology of distal nephron sodium transport mechanisms. *Kidney Int* 56: 1606-1622, 1999.

51. **Gariepy CE, Ohuchi T, Williams SC, Richardson JA, and Yanagisawa M**. Salt-sensitive hypertension in endothelin-B receptor-deficient rats. *J Clin Invest* 105: 925-933, 2000.

52. **George Eric Simpson and with the assistance of A. B. Illievitz BPW, and L. F.** DIURNAL VARIATIONS IN THE RATE OF URINE EXCRETION FOR TWO HOUR INTERVALS: SOME ASSOCIATED FACTORS. *The Journal of Biological Chemistry* 59: 107-122, 1924.

53. **Ghezzi C, Loo DDF, and Wright EM**. Physiology of renal glucose handling via SGLT1, SGLT2 and GLUT2. *Diabetologia* 61: 2087-2097, 2018.

54. **Giacchetti G, Faloia E, Mariniello B, Sardu C, Gatti C, Camilloni MA, Guerrieri M, and Mantero F**. Overexpression of the renin-angiotensin system in human visceral adipose tissue in normal and overweight subjects. *Am J Hypertens* 15: 381-388, 2002.

55. **Gilmore ES, Stutts MJ, and Milgram SL**. SRC family kinases mediate epithelial Na+ channel inhibition by endothelin. *J Biol Chem* 276: 42610-42617, 2001.

56. **Gohar EY, Yusuf C, and Pollock DM**. Ovarian hormones modulate endothelin A and B receptor expression. *Life Sci* 159: 148-152, 2016.

57. **Guan Z, and Inscho EW**. Endothelin and the renal vasculature. *Contrib Nephrol* 172: 35-49, 2011.

58. **Gumz ML, Cheng KY, Lynch IJ, Stow LR, Greenlee MM, Cain BD, and Wingo CS**. Regulation of alphaENaC expression by the circadian clock protein Period 1 in mpkCCD(c14) cells. *Biochim Biophys Acta* 1799: 622-629, 2010.

59. **Gumz ML, Popp MP, Wingo CS, and Cain BD**. Early transcriptional effects of aldosterone in a mouse inner medullary collecting duct cell line. *Am J Physiol Renal Physiol* 285: F664-673, 2003.

60. **Gumz ML, Stow LR, Lynch IJ, Greenlee MM, Rudin A, Cain BD, Weaver DR, and Wingo CS**. The circadian clock protein Period 1 regulates expression of the renal epithelial sodium channel in mice. *J Clin Invest* 119: 2423-2434, 2009.

61. **Hager H, Kwon TH, Vinnikova AK, Masilamani S, Brooks HL, Frokiaer J, Knepper MA, and Nielsen S**. Immunocytochemical and immunoelectron microscopic localization of alpha-, beta-, and gamma-ENaC in rat kidney. *Am J Physiol Renal Physiol* 280: F1093-1106, 2001.

62. **Hainault I, Nebout G, Turban S, Ardouin B, Ferre P, and Quignard-Boulange A**. Adipose tissue-specific increase in angiotensinogen expression and secretion in the obese (fa/fa) Zucker rat. *Am J Physiol Endocrinol Metab* 282: E59-66, 2002.

63. **Hales CM, Carroll MD, Fryar CD, and Ogden CL**. Prevalence of Obesity and Severe Obesity Among Adults: United States, 2017-2018. *NCHS Data Brief* 1-8, 2020.

64. **Hall JE, Brands MW, Dixon WN, and Smith MJ, Jr.** Obesity-induced hypertension. Renal function and systemic hemodynamics. *Hypertension* 22: 292-299, 1993.

65. **Hall JE, do Carmo JM, da Silva AA, Wang Z, and Hall ME**. Obesity-induced hypertension: interaction of neurohumoral and renal mechanisms. *Circ Res* 116: 991-1006, 2015.

66. **Hall JE, do Carmo JM, da Silva AA, Wang Z, and Hall ME**. Obesity, kidney dysfunction and hypertension: mechanistic links. *Nat Rev Nephrol* 15: 367-385, 2019.

67. **Hayashi MA, Ligny-Lemaire C, Wollberg Z, Wery M, Galat A, Ogawa T, Muller BH, Lamthanh H, Doljansky Y, Bdolah A, Stocklin R, and Ducancel F**. Long-

sarafotoxins: characterization of a new family of endothelin-like peptides. *Peptides* 25: 1243-1251, 2004.

68. **Hermida RC**. Sleep-time ambulatory blood pressure as a prognostic marker of vascular and other risks and therapeutic target for prevention by hypertension chronotherapy: Rationale and design of the Hygia Project. *Chronobiol Int* 33: 906-936, 2016.

69. **Hermida RC, Ayala DE, and Portaluppi F**. Circadian variation of blood pressure: the basis for the chronotherapy of hypertension. *Adv Drug Deliv Rev* 59: 904-922, 2007.

70. **Hermida RC, Ayala DE, Smolensky MH, Fernandez JR, Mojon A, and Portaluppi F**. Chronotherapy with conventional blood pressure medications improves management of hypertension and reduces cardiovascular and stroke risks. *Hypertens Res* 39: 277-292, 2016.

71. **Hsieh MC, Yang SC, Tseng HL, Hwang LL, Chen CT, and Shieh KR**. Abnormal expressions of circadian-clock and circadian clock-controlled genes in the livers and kidneys of long-term, high-fat-diet-treated mice. *Int J Obes (Lond)* 34: 227-239, 2010.

72. **Hsu CY, McCulloch CE, Iribarren C, Darbinian J, and Go AS**. Body mass index and risk for end-stage renal disease. *Ann Intern Med* 144: 21-28, 2006.

73. **Hu C, Lakshmipathi J, Stuart D, Peti-Peterdi J, Gyarmati G, Hao CM, Hansell P, and Kohan DE**. Renomedullary Interstitial Cell Endothelin A Receptors Regulate BP and Renal Function. *J Am Soc Nephrol* 31: 1555-1568, 2020.

74. **Hutson DD, Gurrala R, Ogola BO, Zimmerman MA, Mostany R, Satou R, and Lindsey SH**. Estrogen receptor profiles across tissues from male and female Rattus norvegicus. *Biol Sex Differ* 10: 4, 2019.

75. **Hwang YS, Hsieh TJ, Lee YJ, and Tsai JH**. Circadian rhythm of urinary endothelin-1 excretion in mild hypertensive patients. *Am J Hypertens* 11: 1344-1351, 1998.

76. **Hyndman KA, Mironova EV, Giani JF, Dugas C, Collins J, McDonough AA, Stockand JD, and Pollock JS**. Collecting Duct Nitric Oxide Synthase 1ss Activation Maintains Sodium Homeostasis During High Sodium Intake Through Suppression of Aldosterone and Renal Angiotensin II Pathways. *J Am Heart Assoc* 6: 2017.

77. **Ingelfinger JR, Zuo WM, Fon EA, Ellison KE, and Dzau VJ**. In situ hybridization evidence for angiotensinogen messenger RNA in the rat proximal tubule. An hypothesis for the intrarenal renin angiotensin system. *J Clin Invest* 85: 417-423, 1990.

78. **Irsik DL, Carmines PK, and Lane PH**. Classical estrogen receptors and ERalpha splice variants in the mouse. *PLoS One* 8: e70926, 2013.

79. **Isobe S, Ohashi N, Fujikura T, Tsuji T, Sakao Y, Yasuda H, Kato A, Miyajima H, and Fujigaki Y**. Disturbed circadian rhythm of the intrarenal renin-angiotensin system: relevant to nocturnal hypertension and renal damage. *Clin Exp Nephrol* 19: 231-239, 2015.

80. **Ivy JR, Jones NK, Costello HM, Mansley MK, Peltz TS, Flatman PW, and Bailey MA**. Glucocorticoid receptor activation stimulates the sodium-chloride cotransporter and influences the diurnal rhythm of its phosphorylation. *Am J Physiol Renal Physiol* 317: F1536-F1548, 2019.

81. **Ivy JR, Oosthuyzen W, Peltz TS, Howarth AR, Hunter RW, Dhaun N, Al-Dujaili EA, Webb DJ, Dear JW, Flatman PW, and Bailey MA**. Glucocorticoids Induce Nondipping Blood Pressure by Activating the Thiazide-Sensitive Cotransporter. *Hypertension* 67: 1029-1037, 2016.

82. **Jelinsky SA, Harris HA, Brown EL, Flanagan K, Zhang X, Tunkey C, Lai K, Lane MV, Simcoe DK, and Evans MJ**. Global transcription profiling of estrogen activity: estrogen receptor alpha regulates gene expression in the kidney. *Endocrinology* 144: 701-710, 2003.

83. **Jernigan NL, and Drummond HA**. Myogenic vasoconstriction in mouse renal interlobar arteries: role of endogenous beta and gammaENaC. *Am J Physiol Renal Physiol* 291: F1184-1191, 2006.

84. **Jin C, Speed JS, and Pollock DM**. High salt intake increases endothelin B receptor function in the renal medulla of rats. *Life Sci* 159: 144-147, 2016.

85. **Johnston JG, and Pollock DM**. Circadian regulation of renal function. *Free Radic Biol Med* 2018.

86. **Johnston JG, and Pollock DM**. Circadian regulation of renal function. *Free Radic Biol Med* 119: 93-107, 2018.

87. **Johnston JG, Speed JS, Becker BK, Kasztan M, Soliman RH, Rhoads MK, Tao B, Jin C, Geurts AM, Hyndman KA, Pollock JS, and Pollock DM**. Diurnal Control of Blood Pressure Is Uncoupled From Sodium Excretion. *Hypertension* 75: 1624-1634, 2020.

88. **Johnston JG, Speed JS, Jin C, and Pollock DM**. Loss of endothelin B receptor function impairs sodium excretion in a time- and sex-dependent manner. *Am J Physiol Renal Physiol* 311: F991-F998, 2016.

89. **Karet FE, and Davenport AP**. Localization of endothelin peptides in human kidney. *Kidney Int* 49: 382-387, 1996.

90. **Kashlan OB, and Kleyman TR**. ENaC structure and function in the wake of a resolved structure of a family member. *Am J Physiol Renal Physiol* 301: F684-696, 2011.

91. **Kawarazaki W, and Fujita T**. The Role of Aldosterone in Obesity-Related Hypertension. *Am J Hypertens* 29: 415-423, 2016.

92. **Khraibi AA, Liang M, and Berndt TJ**. Role of gender on renal interstitial hydrostatic pressure and sodium excretion in rats. *Am J Hypertens* 14: 893-896, 2001.

93. **Kimura G, Dohi Y, and Fukuda M**. Salt sensitivity and circadian rhythm of blood pressure: the keys to connect CKD with cardiovascular events. *Hypertens Res* 33: 515-520, 2010.

94. **Kimura S, Kasuya Y, Sawamura T, Shinimi O, Sugita Y, Yanagisawa M, Goto K, and Masaki T**. Conversion of big endothelin-1 to 21-residue endothelin-1 is essential for expression of full vasoconstrictor activity: structure-activity relationships of big endothelin-1. *J Cardiovasc Pharmacol* 13 Suppl 5: S5-7; discussion S18, 1989.

95. **Kitamura K, Tanaka T, Kato J, Eto T, and Tanaka K**. Regional distribution of immunoreactive endothelin in porcine tissue: abundance in inner medulla of kidney. *Biochem Biophys Res Commun* 161: 348-352, 1989.

96. **Kitamura K, Tanaka T, Kato J, Ogawa T, Eto T, and Tanaka K**. Immunoreactive endothelin in rat kidney inner medulla: marked decrease in spontaneously hypertensive rats. *Biochem Biophys Res Commun* 162: 38-44, 1989.

97. **Kittikulsuth W, Hyndman KA, Pollock JS, and Pollock DM**. Natriuretic response to renal medullary endothelin B receptor activation is impaired in Dahl-salt sensitive rats on a high-fat diet. *Physiol Res* 67: S149-S154, 2018.

98. **Kittikulsuth W, Hyndman KA, Pollock JS, and Pollock DM**. Natriuretic response to renal medullary endothelin B receptor activation is impaired in Dahl-salt sensitive rats on a high-fat diet. *Physiol Res* 67: S149-S154, 2018.

99. **Kittikulsuth W, Looney SW, and Pollock DM**. Endothelin ET(B) receptors contribute to sex differences in blood pressure elevation in angiotensin II hypertensive rats on a high-salt diet. *Clin Exp Pharmacol Physiol* 40: 362-370, 2013.

100. **Kittikulsuth W, Sullivan JC, and Pollock DM**. ET-1 actions in the kidney: evidence for sex differences. *Br J Pharmacol* 168: 318-326, 2013.

101. **Kobori H, Alper AB, Jr., Shenava R, Katsurada A, Saito T, Ohashi N, Urushihara M, Miyata K, Satou R, Hamm LL, and Navar LG**. Urinary angiotensinogen as a novel biomarker of the intrarenal renin-angiotensin system status in hypertensive patients. *Hypertension* 53: 344-350, 2009.

102. **Kobori H, Nangaku M, Navar LG, and Nishiyama A**. The intrarenal renin-angiotensin system: from physiology to the pathobiology of hypertension and kidney disease. *Pharmacol Rev* 59: 251-287, 2007.

103. **Kohan DE**. Introduction: basic biology of the renal endothelin system. *Semin Nephrol* 35: 121-124, 2015.

104. **Kohan DE, Inscho EW, Wesson D, and Pollock DM**. Physiology of endothelin and the kidney. *Compr Physiol* 1: 883-919, 2011.

105. **Kohan DE, Rossi NF, Inscho EW, and Pollock DM**. Regulation of blood pressure and salt homeostasis by endothelin. *Physiol Rev* 91: 1-77, 2011.

106. **Kohsaka A, Laposky AD, Ramsey KM, Estrada C, Joshu C, Kobayashi Y, Turek FW, and Bass J**. High-fat diet disrupts behavioral and molecular circadian rhythms in mice. *Cell Metab* 6: 414-421, 2007.

107. **Kotelevtsev Y, and Webb DJ**. Endothelin as a natriuretic hormone: the case for a paracrine action mediated by nitric oxide. *Cardiovasc Res* 51: 481-488, 2001.

108. **Kotsis V, Stabouli S, Bouldin M, Low A, Toumanidis S, and Zakopoulos N**. Impact of obesity on 24-hour ambulatory blood pressure and hypertension. *Hypertension* 45: 602-607, 2005.

109. **Kotsis V, Stabouli S, Papakatsika S, Rizos Z, and Parati G**. Mechanisms of obesity-induced hypertension. *Hypertens Res* 33: 386-393, 2010.

110. **Krid H, Dorison A, Salhi A, Cheval L, and Crambert G**. Expression profile of nuclear receptors along male mouse nephron segments reveals a link between ERRbeta and thick ascending limb function. *PLoS One* 7: e34223, 2012.

111. **Kuiper GG, Carlsson B, Grandien K, Enmark E, Haggblad J, Nilsson S, and Gustafsson JA**. Comparison of the ligand binding specificity and transcript tissue distribution of estrogen receptors alpha and beta. *Endocrinology* 138: 863-870, 1997.

112. **Kuruppu S, and Smith AI**. Endothelin Converting Enzyme-1 phosphorylation and trafficking. *FEBS Lett* 586: 2212-2217, 2012.

113. **Kushner RF, and Roth JL**. Assessment of the obese patient. *Endocrinol Metab Clin North Am* 32: 915-933, 2003.

114. **Landi F, Calvani R, Picca A, Tosato M, Martone AM, Ortolani E, Sisto A, D'Angelo E, Serafini E, Desideri G, Fuga MT, and Marzetti E**. Body Mass Index is

Strongly Associated with Hypertension: Results from the Longevity Check-up 7+ Study. *Nutrients* 10: 2018.

115. **Lang P, Hasselwander S, Li H, and Xia N**. Effects of different diets used in diet-induced obesity models on insulin resistance and vascular dysfunction in C57BL/6 mice. *Sci Rep* 9: 19556, 2019.

116. **Lenoir O, Milon M, Virsolvy A, Henique C, Schmitt A, Masse JM, Kotelevtsev Y, Yanagisawa M, Webb DJ, Richard S, and Tharaux PL**. Direct action of endothelin-1 on podocytes promotes diabetic glomerulosclerosis. *J Am Soc Nephrol* 25: 1050-1062, 2014.

117. **Leong XF, Ng CY, and Jaarin K**. Animal Models in Cardiovascular Research: Hypertension and Atherosclerosis. *Biomed Res Int* 2015: 528757, 2015.

118. **Lerman LO, Kurtz TW, Touyz RM, Ellison DH, Chade AR, Crowley SD, Mattson DL, Mullins JJ, Osborn J, Eirin A, Reckelhoff JF, Iadecola C, and Coffman TM**. Animal Models of Hypertension: A Scientific Statement From the American Heart Association. *Hypertension* 73: e87-e120, 2019.

119. **Li HC, Du Z, Barone S, Rubera I, McDonough AA, Tauc M, Zahedi K, Wang T, and Soleimani M**. Proximal tubule specific knockout of the Na(+)/H(+) exchanger NHE3: effects on bicarbonate absorption and ammonium excretion. *J Mol Med (Berl)* 91: 951-963, 2013.

120. **Li J, Hatano R, Xu S, Wan L, Yang L, Weinstein AM, Palmer L, and Wang T**. Gender difference in kidney electrolyte transport. I. Role of AT1a receptor in thiazide-sensitive Na(+)-Cl(-) cotransporter activity and expression in male and female mice. *Am J Physiol Renal Physiol* 313: F505-F513, 2017.

121. **Li XC, Zheng X, Chen X, Zhao C, Zhu D, Zhang J, and Zhuo JL**. Genetic and genomic evidence for an important role of the Na(+)/H(+) exchanger 3 in blood pressure regulation and angiotensin II-induced hypertension. *Physiol Genomics* 51: 97-108, 2019.

122. **Loffing J, Loffing-Cueni D, Valderrabano V, Klausli L, Hebert SC, Rossier BC, Hoenderop JG, Bindels RJ, and Kaissling B**. Distribution of transcellular calcium and sodium transport pathways along mouse distal nephron. *Am J Physiol Renal Physiol* 281: F1021-1027, 2001.

123. **Ludgero-Correia A, Jr., Aguila MB, Mandarim-de-Lacerda CA, and Faria TS**. Effects of high-fat diet on plasma lipids, adiposity, and inflammatory markers in ovariectomized C57BL/6 mice. *Nutrition* 28: 316-323, 2012.

124. **Lutz TA, and Woods SC**. Overview of animal models of obesity. *Curr Protoc Pharmacol* Chapter 5: Unit5 61, 2012.

125. **Lynch IJ, Welch AK, Kohan DE, Cain BD, and Wingo CS**. Endothelin-1 inhibits sodium reabsorption by ET(A) and ET(B) receptors in the mouse cortical collecting duct. *Am J Physiol Renal Physiol* 305: F568-573, 2013.

126. **Lyon-Roberts B, Strait KA, van Peursem E, Kittikulsuth W, Pollock JS, Pollock DM, and Kohan DE**. Flow regulation of collecting duct endothelin-1 production. *Am J Physiol Renal Physiol* 300: F650-656, 2011.

127. **Manolopoulou J, Bielohuby M, Caton SJ, Gomez-Sanchez CE, Renner-Mueller I, Wolf E, Lichtenauer UD, Beuschlein F, Hoeflich A, and Bidlingmaier M**. A highly sensitive immunofluorometric assay for the measurement of aldosterone in small sample volumes: validation in mouse serum. *J Endocrinol* 196: 215-224, 2008.

128. **Maric C, Aldred GP, Antoine AM, Eitle E, Dean RG, Williams DA, Harris PJ, and Alcorn D**. Actions of endothelin-1 on cultured rat renomedullary interstitial cells are modulated by nitric oxide. *Clin Exp Pharmacol Physiol* 26: 392-398, 1999.

129. **Masilamani S, Kim GH, Mitchell C, Wade JB, and Knepper MA**. Aldosterone-mediated regulation of ENaC alpha, beta, and gamma subunit proteins in rat kidney. *J Clin Invest* 104: R19-23, 1999.

130. **Maury E**. Off the Clock: From Circadian Disruption to Metabolic Disease. *Int J Mol Sci* 20: 2019.

131. **Maury E, Ramsey KM, and Bass J**. Circadian rhythms and metabolic syndrome: from experimental genetics to human disease. *Circ Res* 106: 447-462, 2010.

132. **Mills JN**. Diurnal rhythm in urine flow. *J Physiol* 113: 528-536, 1951.

133. **Mills JN, and Stanbury SW**. Persistent 24-hour renal excretory rhythm on a 12-hour cycle of activity. *J Physiol* 117: 22-37, 1952.

134. **Mojon A, Ayala DE, Pineiro L, Otero A, Crespo JJ, Moya A, Boveda J, de Lis JP, Fernandez JR, Hermida RC, and Hygia Project I**. Comparison of ambulatory blood pressure parameters of hypertensive patients with and without chronic kidney disease. *Chronobiol Int* 30: 145-158, 2013.

135. **Moniwa N, Varagic J, Ahmad S, VonCannon JL, and Ferrario CM**. Restoration of the blood pressure circadian rhythm by direct renin inhibition and blockade of angiotensin II receptors in mRen2.Lewis hypertensive rats. *Ther Adv Cardiovasc Dis* 6: 15-29, 2012.

136. **Morita S, Kitamura K, Yamamoto Y, Eto T, Osada Y, Sumiyoshi A, Koono M, and Tanaka K**. Immunoreactive endothelin in human kidney. *Ann Clin Biochem* 28 (Pt 3): 267-271, 1991.

137. **Muller MJ, and Geisler C**. Defining obesity as a disease. *Eur J Clin Nutr* 71: 1256-1258, 2017.

138. **Nakano D, and Pollock DM**. Contribution of endothelin A receptors in endothelin 1-dependent natriuresis in female rats. *Hypertension* 53: 324-330, 2009.

139. **Neto NI, Rodrigues ME, Hachul AC, Moreno MF, Boldarine VT, Ribeiro EB, Oyama LM, and Oller do Nascimento CM**. A Hyperlipidic Diet Combined with Short-Term Ovariectomy Increases Adiposity and Hyperleptinemia and Decreases Cytokine Content in Mesenteric Adipose Tissue. *Mediators Inflamm* 2015: 923248, 2015.

140. **Nikolaeva S, Pradervand S, Centeno G, Zavadova V, Tokonami N, Maillard M, Bonny O, and Firsov D**. The circadian clock modulates renal sodium handling. *J Am Soc Nephrol* 23: 1019-1026, 2012.

141. **Nishijima Y, Kobori H, Kaifu K, Mizushige T, Hara T, Nishiyama A, and Kohno M**. Circadian rhythm of plasma and urinary angiotensinogen in healthy volunteers and in patients with chronic kidney disease. *J Renin Angiotensin Aldosterone Syst* 15: 505-508, 2014.

142. **Nishinaga H, Komatsu R, Doi M, Fustin JM, Yamada H, Okura R, Yamaguchi Y, Matsuo M, Emoto N, and Okamura H**. Circadian expression of the Na+/H+ exchanger NHE3 in the mouse renal medulla. *Biomed Res* 30: 87-93, 2009.

143. **Nugrahaningsih DA, Emoto N, Vignon-Zellweger N, Purnomo E, Yagi K, Nakayama K, Doi M, Okamura H, and Hirata K**. Chronic hyperaldosteronism in

cryptochrome-null mice induces high-salt- and blood pressure-independent kidney damage in mice. *Hypertens Res* 37: 202-209, 2014.

144. **Ohashi N, Isobe S, Ishigaki S, and Yasuda H**. Circadian rhythm of blood pressure and the renin-angiotensin system in the kidney. *Hypertens Res* 40: 413-422, 2017.

145. **Okeahialam BN, Ohihoin EN, and Ajuluchukwu JN**. Diuretic drugs benefit patients with hypertension more with night-time dosing. *Ther Adv Drug Saf* 3: 273-278, 2012.

146. **Orias M, and Correa-Rotter R**. Chronotherapy in hypertension: a pill at night makes things right? *J Am Soc Nephrol* 22: 2152-2155, 2011.

147. **Ortmann J, Amann K, Brandes RP, Kretzler M, Munter K, Parekh N, Traupe T, Lange M, Lattmann T, and Barton M**. Role of podocytes for reversal of glomerulosclerosis and proteinuria in the aging kidney after endothelin inhibition. *Hypertension* 44: 974-981, 2004.

148. **Palmer LG, and Schnermann J**. Integrated control of Na transport along the nephron. *Clin J Am Soc Nephrol* 10: 676-687, 2015.

149. **Palmisano BT, Stafford JM, and Pendergast JS**. High-Fat Feeding Does Not Disrupt Daily Rhythms in Female Mice because of Protection by Ovarian Hormones. *Front Endocrinol (Lausanne)* 8: 44, 2017.

150. **Pan X, and Hussain MM**. Clock is important for food and circadian regulation of macronutrient absorption in mice. *J Lipid Res* 50: 1800-1813, 2009.

151. **Pandit MM, Inscho EW, Zhang S, Seki T, Rohatgi R, Gusella L, Kishore B, and Kohan DE**. Flow regulation of endothelin-1 production in the inner medullary collecting duct. *Am J Physiol Renal Physiol* 308: F541-552, 2015.

152. **Pizarro A, Hayer K, Lahens NF, and Hogenesch JB**. CircaDB: a database of mammalian circadian gene expression profiles. *Nucleic Acids Res* 41: D1009-1013, 2013.

153. **Pollock DM, and Pollock JS**. Evidence for endothelin involvement in the response to high salt. *Am J Physiol Renal Physiol* 281: F144-150, 2001.

154. **Portaluppi F, and Smolensky MH**. Perspectives on the chronotherapy of hypertension based on the results of the MAPEC study. *Chronobiol Int* 27: 1652-1667, 2010.

155. **Pratt JH**. Central role for ENaC in development of hypertension. *J Am Soc Nephrol* 16: 3154-3159, 2005.

156. **Riazi S, Madala-Halagappa VK, Hu X, and Ecelbarger CA**. Sex and body-type interactions in the regulation of renal sodium transporter levels, urinary excretion, and activity in lean and obese Zucker rats. *Gend Med* 3: 309-327, 2006.

157. **Richards J, All S, Skopis G, Cheng KY, Compton B, Srialluri N, Stow L, Jeffers LA, and Gumz ML**. Opposing actions of Per1 and Cry2 in the regulation of Per1 target gene expression in the liver and kidney. *Am J Physiol Regul Integr Comp Physiol* 305: R735-747, 2013.

158. **Richards J, Cheng KY, All S, Skopis G, Jeffers L, Lynch IJ, Wingo CS, and Gumz ML**. A role for the circadian clock protein Per1 in the regulation of aldosterone levels and renal Na+ retention. *Am J Physiol Renal Physiol* 305: F1697-1704, 2013.

159. **Richards J, and Gumz ML**. Mechanism of the circadian clock in physiology. *Am J Physiol Regul Integr Comp Physiol* 304: R1053-1064, 2013.

160. **Richards J, Welch AK, Barilovits SJ, All S, Cheng KY, Wingo CS, Cain BD, and Gumz ML**. Tissue-specific and time-dependent regulation of the endothelin axis by the circadian clock protein Per1. *Life Sci* 118: 255-262, 2014.

161. **Rittig S, Matthiesen TB, Pedersen EB, and Djurhuus JC**. Circadian variation of angiotensin II and aldosterone in nocturnal enuresis: relationship to arterial blood pressure and urine output. *J Urol* 176: 774-780, 2006.

162. **Rojas-Vega L, Reyes-Castro LA, Ramirez V, Bautista-Perez R, Rafael C, Castaneda-Bueno M, Meade P, de Los Heros P, Arroyo-Garza I, Bernard V, Binart N, Bobadilla NA, Hadchouel J, Zambrano E, and Gamba G**. Ovarian hormones and prolactin increase renal NaCl cotransporter phosphorylation. *Am J Physiol Renal Physiol* 308: F799-808, 2015.

163. **Saifur Rohman M, Emoto N, Nonaka H, Okura R, Nishimura M, Yagita K, van der Horst GT, Matsuo M, Okamura H, and Yokoyama M**. Circadian clock genes directly regulate expression of the Na(+)/H(+) exchanger NHE3 in the kidney. *Kidney Int* 67: 1410-1419, 2005.

164. **Santos RAS, Oudit GY, Verano-Braga T, Canta G, Steckelings UM, and Bader M**. The renin-angiotensin system: going beyond the classical paradigms. *Am J Physiol Heart Circ Physiol* 316: H958-H970, 2019.

165. **Schultheis PJ, Lorenz JN, Meneton P, Nieman ML, Riddle TM, Flagella M, Duffy JJ, Doetschman T, Miller ML, and Shull GE**. Phenotype resembling Gitelman's syndrome in mice lacking the apical Na+-Cl- cotransporter of the distal convoluted tubule. *J Biol Chem* 273: 29150-29155, 1998.

166. **Schutten MT, Houben AJ, de Leeuw PW, and Stehouwer CD**. The Link Between Adipose Tissue Renin-Angiotensin-Aldosterone System Signaling and Obesity-Associated Hypertension. *Physiology (Bethesda)* 32: 197-209, 2017.

167. **Shi SQ, Ansari TS, McGuinness OP, Wasserman DH, and Johnson CH**. Circadian disruption leads to insulin resistance and obesity. *Curr Biol* 23: 372-381, 2013.

168. **Shi-Wen X, Rodriguez-Pascual F, Lamas S, Holmes A, Howat S, Pearson JD, Dashwood MR, du Bois RM, Denton CP, Black CM, Abraham DJ, and Leask A**. Constitutive ALK5-independent c-Jun N-terminal kinase activation contributes to endothelin-1 overexpression in pulmonary fibrosis: evidence of an autocrine endothelin loop operating through the endothelin A and B receptors. *Mol Cell Biol* 26: 5518-5527, 2006.

169. **Shinagawa S, Okazaki T, Ikeda M, Yudoh K, Kisanuki YY, Yanagisawa M, Kawahata K, and Ozaki S**. T cells upon activation promote endothelin 1 production in monocytes via IFN-gamma and TNF-alpha. *Sci Rep* 7: 14500, 2017.

170. **Skrapari I, Tentolouris N, Perrea D, Bakoyiannis C, Papazafiropoulou A, and Katsilambros N**. Baroreflex sensitivity in obesity: relationship with cardiac autonomic nervous system activity. *Obesity (Silver Spring)* 15: 1685-1693, 2007.

171. **Sodhi K, Wu CC, Cheng J, Gotlinger K, Inoue K, Goli M, Falck JR, Abraham NG, and Schwartzman ML**. CYP4A2-induced hypertension is 20-hydroxyeicosatetraenoic acid- and angiotensin II-dependent. *Hypertension* 56: 871-878, 2010.

172. **Soliman RH, Johnston JG, Gohar EY, Taylor CM, and Pollock DM**. Greater natriuretic response to ENaC inhibition in male versus female Sprague-Dawley rats. *Am J Physiol Regul Integr Comp Physiol* 318: R418-R427, 2020.

173. **Solocinski K, and Gumz ML**. The Circadian Clock in the Regulation of Renal Rhythms. *J Biol Rhythms* 30: 470-486, 2015.

174. **Solocinski K, Holzworth M, Wen X, Cheng KY, Lynch IJ, Cain BD, Wingo CS, and Gumz ML**. Desoxycorticosterone pivalate-salt treatment leads to non-dipping hypertension in Per1 knockout mice. *Acta Physiol (Oxf)* 220: 72-82, 2017.

175. **Solocinski K, Richards J, All S, Cheng KY, Khundmiri SJ, and Gumz ML**. Transcriptional regulation of NHE3 and SGLT1 by the circadian clock protein Per1 in proximal tubule cells. *Am J Physiol Renal Physiol* 309: F933-942, 2015.

176. **Song J, Hu X, Riazi S, Tiwari S, Wade JB, and Ecelbarger CA**. Regulation of blood pressure, the epithelial sodium channel (ENaC), and other key renal sodium transporters by chronic insulin infusion in rats. *Am J Physiol Renal Physiol* 290: F1055-1064, 2006.

177. **Song P, Huang W, Onishi A, Patel R, Kim YC, van Ginkel C, Fu Y, Freeman B, Koepsell H, Thomson S, Liu R, and Vallon V**. Knockout of Na(+)-glucose cotransporter SGLT1 mitigates diabetes-induced upregulation of nitric oxide synthase NOS1 in the macula densa and glomerular hyperfiltration. *Am J Physiol Renal Physiol* 317: F207-F217, 2019.

178. **Sparks MA, Crowley SD, Gurley SB, Mirotsou M, and Coffman TM**. Classical Renin-Angiotensin system in kidney physiology. *Compr Physiol* 4: 1201-1228, 2014.

179. **Speed JS, Fox BM, Johnston JG, and Pollock DM**. Endothelin and renal ion and water transport. *Semin Nephrol* 35: 137-144, 2015.

180. **Speed JS, Hyndman KA, Kasztan M, Johnston JG, Roth KJ, Titze JM, and Pollock DM**. Diurnal pattern in skin Na(+) and water content is associated with salt-sensitive hypertension in ETB receptor-deficient rats. *Am J Physiol Regul Integr Comp Physiol* 314: R544-R551, 2018.

181. **Speed JS, Hyndman KA, Roth K, Heimlich JB, Kasztan M, Fox BM, Johnston JG, Becker BK, Jin C, Gamble KL, Young ME, Pollock JS, and Pollock DM**. High dietary sodium causes dyssynchrony of the renal molecular clock in rats. *Am J Physiol Renal Physiol* 314: F89-F98, 2018.

182. **Speed JS, LaMarca B, Berry H, Cockrell K, George EM, and Granger JP**. Renal medullary endothelin-1 is decreased in Dahl salt-sensitive rats. *Am J Physiol Regul Integr Comp Physiol* 301: R519-523, 2011.

183. **Stow LR, and Gumz ML**. The circadian clock in the kidney. *J Am Soc Nephrol* 22: 598-604, 2011.

184. **Stow LR, Gumz ML, Lynch IJ, Greenlee MM, Rudin A, Cain BD, and Wingo CS**. Aldosterone modulates steroid receptor binding to the endothelin-1 gene (edn1). *J Biol Chem* 284: 30087-30096, 2009.

185. **Stow LR, Jacobs ME, Wingo CS, and Cain BD**. Endothelin-1 gene regulation. *FASEB J* 25: 16-28, 2011.

186. **Stow LR, Richards J, Cheng KY, Lynch IJ, Jeffers LA, Greenlee MM, Cain BD, Wingo CS, and Gumz ML**. The circadian protein period 1 contributes to blood

pressure control and coordinately regulates renal sodium transport genes. *Hypertension* 59: 1151-1156, 2012.

187. **Su W, Guo Z, Randall DC, Cassis L, Brown DR, and Gong MC**. Hypertension and disrupted blood pressure circadian rhythm in type 2 diabetic db/db mice. *Am J Physiol Heart Circ Physiol* 295: H1634-1641, 2008.

188. **Susa K, Sohara E, Isobe K, Chiga M, Rai T, Sasaki S, and Uchida S**. WNK-OSR1/SPAK-NCC signal cascade has circadian rhythm dependent on aldosterone. *Biochem Biophys Res Commun* 427: 743-747, 2012.

189. **Sussman W, Stevenson M, Mowdawalla C, Mota S, Ragolia L, and Pan X**. BMAL1 controls glucose uptake through paired-homeodomain transcription factor 4 in differentiated Caco-2 cells. *Am J Physiol Cell Physiol* 317: C492-C501, 2019.

190. **Tamaki S, Nakamura Y, Yoshino T, Matsumoto Y, Tarutani Y, Okabayashi T, Kawashima T, and Horie M**. The association between morning hypertension and metabolic syndrome in hypertensive patients. *Hypertens Res* 29: 783-788, 2006.

191. **Tesfaye F, Nawi NG, Van Minh H, Byass P, Berhane Y, Bonita R, and Wall S**. Association between body mass index and blood pressure across three populations in Africa and Asia. *J Hum Hypertens* 21: 28-37, 2007.

192. **Titze J, Lang R, Ilies C, Schwind KH, Kirsch KA, Dietsch P, Luft FC, and Hilgers KF**. Osmotically inactive skin Na+ storage in rats. *Am J Physiol Renal Physiol* 285: F1108-1117, 2003.

193. **Turek FW, Joshu C, Kohsaka A, Lin E, Ivanova G, McDearmon E, Laposky A, Losee-Olson S, Easton A, Jensen DR, Eckel RH, Takahashi JS, and Bass J**. Obesity and metabolic syndrome in circadian Clock mutant mice. *Science* 308: 1043-1045, 2005.

194. **Vallender TW, and Lahn BT**. Localized methylation in the key regulator gene endothelin-1 is associated with cell type-specific transcriptional silencing. *FEBS Lett* 580: 4560-4566, 2006.

195. **Van Harmelen V, Ariapart P, Hoffstedt J, Lundkvist I, Bringman S, and Arner P**. Increased adipose angiotensinogen gene expression in human obesity. *Obes Res* 8: 337-341, 2000.

196. **Veiras LC, Girardi ACC, Curry J, Pei L, Ralph DL, Tran A, Castelo-Branco RC, Pastor-Soler N, Arranz CT, Yu ASL, and McDonough AA**. Sexual Dimorphic Pattern of Renal Transporters and Electrolyte Homeostasis. *J Am Soc Nephrol* 28: 3504-3517, 2017.

197. **Velasquez MT, Beddhu S, Nobakht E, Rahman M, and Raj DS**. Ambulatory Blood Pressure in Chronic Kidney Disease: Ready for Prime Time? *Kidney Int Rep* 1: 94-104, 2016.

198. **Wei N, Gumz ML, and Layton AT**. Predicted effect of circadian clock modulation of NHE3 of a proximal tubule cell on sodium transport. *Am J Physiol Renal Physiol* 315: F665-F676, 2018.

199. **Wendel M, Knels L, Kummer W, and Koch T**. Distribution of endothelin receptor subtypes ETA and ETB in the rat kidney. *J Histochem Cytochem* 54: 1193-1203, 2006.

200. **Whelton PK, Carey RM, Aronow WS, Casey DE, Jr., Collins KJ, Dennison Himmelfarb C, DePalma SM, Gidding S, Jamerson KA, Jones DW, MacLaughlin EJ, Muntner P, Ovbiagele B, Smith SC, Jr., Spencer CC, Stafford RS, Taler SJ, Thomas RJ, Williams KA, Sr., Williamson JD, and Wright JT, Jr.** 2017

ACC/AHA/AAPA/ABC/ACPM/AGS/APhA/ASH/ASPC/NMA/PCNA Guideline for the Prevention, Detection, Evaluation, and Management of High Blood Pressure in Adults: Executive Summary: A Report of the American College of Cardiology/American Heart Association Task Force on Clinical Practice Guidelines. *J Am Soc Hypertens* 12: 579 e571-579 e573, 2018.

201. **Wofford MR, Anderson DC, Jr., Brown CA, Jones DW, Miller ME, and Hall JE**. Antihypertensive effect of alpha- and beta-adrenergic blockade in obese and lean hypertensive subjects. *Am J Hypertens* 14: 694-698, 2001.

202. **Wort SJ, Ito M, Chou PC, Mc Master SK, Badiger R, Jazrawi E, de Souza P, Evans TW, Mitchell JA, Pinhu L, Ito K, and Adcock IM**. Synergistic induction of endothelin-1 by tumor necrosis factor alpha and interferon gamma is due to enhanced NF-kappaB binding and histone acetylation at specific kappaB sites. *J Biol Chem* 284: 24297-24305, 2009.

203. **Wu CC, Gupta T, Garcia V, Ding Y, and Schwartzman ML**. 20-HETE and blood pressure regulation: clinical implications. *Cardiol Rev* 22: 1-12, 2014.

204. **Xie JX, Li X, and Xie Z**. Regulation of renal function and structure by the signaling Na/K-ATPase. *IUBMB Life* 65: 991-998, 2013.

205. **Yan B, Yan H, Sun L, Yan X, Peng L, Wang Y, and Wang G**. Novel Association Between the Reverse-Dipper Pattern of Ambulatory Blood Pressure Monitoring and Metabolic Syndrome in Men But Not in Women. *Medicine (Baltimore)* 94: e2115, 2015.

206. **Yanagisawa M, Kurihara H, Kimura S, Tomobe Y, Kobayashi M, Mitsui Y, Yazaki Y, Goto K, and Masaki T**. A novel potent vasoconstrictor peptide produced by vascular endothelial cells. *Nature* 332: 411-415, 1988.

207. **Yasue S, Masuzaki H, Okada S, Ishii T, Kozuka C, Tanaka T, Fujikura J, Ebihara K, Hosoda K, Katsurada A, Ohashi N, Urushihara M, Kobori H, Morimoto N, Kawazoe T, Naitoh M, Okada M, Sakaue H, Suzuki S, and Nakao K**. Adipose tissue-specific regulation of angiotensinogen in obese humans and mice: impact of nutritional status and adipocyte hypertrophy. *Am J Hypertens* 23: 425-431, 2010.

208. **Yu M, Lopez B, Dos Santos EA, Falck JR, and Roman RJ**. Effects of 20-HETE on Na+ transport and Na+ -K+ -ATPase activity in the thick ascending loop of Henle. *Am J Physiol Regul Integr Comp Physiol* 292: R2400-2405, 2007.

209. **Zaika O, Mamenko M, Staruschenko A, and Pochynyuk O**. Direct activation of ENaC by angiotensin II: recent advances and new insights. *Curr Hypertens Rep* 15: 17-24, 2013.

210. **Zhang R, Lahens NF, Ballance HI, Hughes ME, and Hogenesch JB**. A circadian gene expression atlas in mammals: implications for biology and medicine. *Proc Natl Acad Sci U S A* 111: 16219-16224, 2014.

211. **Zuber AM, Centeno G, Pradervand S, Nikolaeva S, Maquelin L, Cardinaux L, Bonny O, and Firsov D**. Molecular clock is involved in predictive circadian adjustment of renal function. *Proc Natl Acad Sci U S A* 106: 16523-16528, 2009.

APPENDIX A

IACUC APPOVAL FORM

THE UNIVERSITY OF ALABAMA AT BIRMINGHAM
Institutional Animal Care and Use Committee (IACUC)

MEMORANDUM

DATE: 11-Jan-2017

TO: Pollock, David

FROM:

Robert A. Kesterson, Ph.D., Chair

Institutional Animal Care and Use Committee (IACUC)

SUBJECT: **NOTICE OF APPROVAL**

The following application was approved by the University of Alabama at Birmingham Institutional Animal Care and Use Committee (IACUC) on 11-Jan-2017.

Protocol PI: Pollock, David

Title: Integrating Novel Mechanisms Controlling Sodium Excretion and Blood Pressure: Project 1- Circadian Control of Sodium Excretion

Sponsor: National Heart, Lung, and Blood Institute/NIH/DHHS

Animal Project Number (APN): IACUC-20721

This institution has an Animal Welfare Assurance on file with the Office of Laboratory Animal Welfare (OLAW), is registered as a Research Facility with the USDA, and is accredited by the Association for Assessment and Accreditation of Laboratory Animal Care International (AAALAC).

Institutional Animal Care and Use Committee (IACUC)
CH19 Suite 403
933 19th Street South
(205) 934-7692
FAX (205) 934-1188

Mailing Address:
CH19 Suite 403
1530 3rd Ave S
Birmingham, AL 35294-0019